

**Synthesis of zeolites from South African coal fly ash:
Investigation of scale-up conditions**

By

Dakalo Mainganye

Thesis submitted in fulfilment of requirements for the degree

Magister Technologiae: Chemical Engineering

In the FACULTY OF ENGINEERING

At the CAPE PENINSULA UNIVERSITY OF TECHNOLOGY

Supervisor: Prof. Tunde V. Ojumu

Co-supervisor: Prof. Leslie F Petrik

Cape Town Campus

November 2012

CPUT copyright information

The dissertation/thesis may not be published either in part (in scholarly, scientific or technical journals), or as a whole (as a monograph), unless permission has been obtained from the University.

DECLARATION

I, Dakalo Mainganye, declare that the contents of this thesis represent my own unaided work, and that the thesis has not previously been submitted for academic examination towards any qualification. Furthermore, it represents my own opinions and not necessarily those of the Cape Peninsula University of Technology.

.....

Signed

.....

Date

ABSTRACT

The generation of electricity from coal in South Africa results in millions of tons of fly ash being produced each year. Less than 10 % of the fly ash generated is being used constructively and the remaining unused ash is currently inducing disposal and environmental problems. Intensive research on the utilisation of fly ash has been conducted either to reduce the cost of disposal or to minimise its impact on the environment. It has been shown that South African fly ash can be used as a feedstock for zeolite synthesis due to its compositional dominance of aluminosilicate and silicate phases.

Most of the studies conducted on zeolite synthesis using South African fly ash are performed on small laboratory scale. Therefore, production of zeolites on an industrial/pilot plant scale would, in addition to producing a valuable product, help abate the pollution caused by the disposal of fly ash in the country. This research focuses on the investigation of the scale-up opportunity of zeolite synthesis from South African fly ashes with the view of understanding the effects of some reactor and operational parameters on the quality of the zeolite produced. Two types of zeolites (zeolite Na-P1 and zeolite A) were synthesised via two different routes in this study: (1) a two stage hydrothermal synthesis method (zeolite Na-P1) and (2) alkaline fusion prior to hydrothermal synthesis (zeolite A). The synthesis variables evaluated in this study were; the effect of impeller design and agitation rates during the aging step (zeolite Na-P1) using three different impellers (anchor, 4-flat-blade and Archimedes screw impeller) at three agitation speeds (150, 200 and 300 rpm), the effect of fly ash composition and solvents (water sources) on the phase purity of both zeolite Na-P1 and zeolite A, and the effect of the hydrothermal reaction time during the synthesis of zeolite Na-P1 using low amorphous phase fly ash i.e. aging time (12-48 hours) and hydrothermal treatment time (12-48 hours).

The raw materials (fly ashes from Arnot, Hendrina, Tutuka, Lethabo and Matla power stations) and the synthesised zeolite product were characterised chemically, mineralogically and morphologically by X-ray fluorescence spectrometry, X-ray powder diffraction and scanning electron microscopy. Other characterisation techniques used in the study were 1) Fourier transform infrared spectroscopy to provide structural information and also monitor the evolution of the zeolite crystals during synthesis and 2) inductively coupled plasma atomic emission (ICP-AES) and mass spectrometry for multi-elemental analysis of the synthesis solution and the solvents used in this study.

The experimental results demonstrated that the phase purity of zeolite Na-P1 was strongly affected by agitation and the type of impeller used during the aging step of the synthesis

process. A high crystalline zeolite Na-P1 was obtained with a 4-flat-blade impeller at a low agitation rate of 200 rpm. Although a pure phase of zeolite Na-P1 was obtained at low agitation rates, the variation in the mineralogy of the fly ash was found to affect the quality of the zeolite produced significantly. The results suggested that each batch of fly ash would require a separate optimisation process of the synthesis conditions. Therefore, there is a need to develop a database of the synthesis conditions for zeolite Na-P1 based on the fly ash composition. As a consequence, the scale-up synthesis of zeolite Na-P1 would require step-by-step optimisation of the synthesis conditions, since this zeolite was sensitive to the $\text{SiO}_2/\text{Al}_2\text{O}_3$ ratio, agitation and the mineralogy of the fly ash.

On the other hand, zeolite A synthesis had several advantages over zeolite Na-P1. The results suggested that a pure phase of zeolite A can be produced at very low reaction temperature (i.e. below 100 °C, compared to 140 °C for zeolite Na-P1), shorter reaction times (i.e. less than 8 hours compared to 4 days for zeolite Na-P1), with complete dissolution of fly ash phases and more importantly less sensitive to the $\text{SiO}_2/\text{Al}_2\text{O}_3$ ratio of the raw materials. The zeolite A synthesis process was found to be more robust and as a result, it would be less rigorous to scale-up despite the energy requirements for fusion.

This study showed for the first time that different impeller designs and agitation during the aging step can have a profound impact on the quality of the zeolite produced. Therefore, it is not only the hydrothermal synthesis conditions and the molar regime but also the dissolution kinetics of the feedstock that influence the outcome of the zeolite synthesis process. This study has also shown for the first time that a pure phase of zeolite A can be synthesised from various sources of South African fly ash containing different mineralogical and chemical compositions via the alkali fusion method under the same synthesis conditions. Therefore, the effective zeolitisation of fly ash on a large scale would assist to mitigate the depletion of resources and environmental problems caused by the disposal of fly ash.

DEDICATION

This thesis is dedicated to my parents:

Mashudu Phaniel Mainganye

and

Nndwayamato Joyce Mainganye

ACKNOWLEDGEMENTS

First and foremost, I would like to thank the Almighty God for giving me the strength, ability and courage to carry out this project successfully.

I would also like to thank;

- My supervisor, Associate Professor T.V. Ojumu and co-supervisor, Associate Professor L.F. Petrik (UWC) for their guidance, advice, criticism and insight throughout the research as well as providing me with the opportunity to work in the Environmental and Nano Sciences research group (ENS). I would also like to thank them for their patience, care and for all the things I have learnt from them over the duration of this project, as well as for the freedom granted during the research.
- H. Small and A. Bester for their technical assistance throughout this project. This project wouldn't be a success without your intervention.
- Nicholas Musyoka for his constructive comments and suggestions and for always having answers to my questions.
- Wynand Du Plessis and Ncumisa Hardy for their assistance with lab work and analytical data acquisition.
- All my postgraduate colleagues from the Chemical Engineering Department (CPUT) for the support and assistance.
- The entire ENS group for their warm welcome and assistance whenever I needed it. I am very grateful to Averil Abbot and Vanessa Kellerman for their administrative support and Ilse Wells for her assistance with ICP data acquisition.
- My parents, Mashudu Phanel Mainganye and Nndwayamato Joyce Mainganye for their love, moral and financial support throughout my studies and for all that they have sacrificed to give me an opportunity to get educated. I am what I am because of them. Thank you.
- My sister Phathutshedzo Thabane and my brother-in-law, Kekeletso Joseph Thabane for their financial support and encouragement throughout my studies, you are the best.
- My entire family for their love and support and their trust in me.

- My girlfriend Dineo Kadi for her patience, understanding, encouragement, emotional and financial support and for always believing in me throughout the duration of this research. Thank you for being you.
- ESKOM and Cape Peninsula University of Technology for funding this project.

LIST OF PUBLICATIONS AND PRESENTATIONS

Oral presentations

1. Mainganye, D., Ojumu, T.V., & Petrik, L.F. 2012. Development of scale-up conditions for the synthesis of zeolites from South African coal fly ash: effect of fly ash composition and synthesis time. *62nd Canadian Chemical Engineering Conference*, Vancouver, British Columbia, Canada, 14-17 October 2012.
2. Mainganye, D., Du Plessis, P.W., Ojumu, T.V. & Petrik, L.F. 2011. Scale-up synthesis of zeolites from South African coal fly ash: Effect of impeller design and agitation on the aging step. *10th Annual Nigerian Materials Congress*, Akure, Nigeria, 21-24 November 2011.
3. Mainganye, D., Hardy N., Ojumu, T.V. & Petrik, L.F. 2011. Synthesis of zeolites from South African coal fly ash using different water sources. *10th Annual Nigerian Materials Congress*, Akure, Nigeria, 21-24 November 2011.

Poster Presentations

1. Mainganye, D., Du Plessis, P.W., Ojumu T.V and Petrik L.F. 2012. Development of scale-up conditions for the synthesis of zeolites from South African coal fly ash: effect of impeller design and agitation. *62nd Canadian Chemical Engineering Conference*, Vancouver, British Columbia, Canada, 14-17 October 2012.
2. Mainganye, D., Ojumu, T.V. & Petrik, L.F. 2012. Synthesis of zeolite Na-P1 from South African coal fly ash: investigation of scale-up conditions. *SAIChE Conference*, Champagne Sport Resort, Kwazulu Natal, South Africa, 16-19 September 2012.
3. Mainganye, D., Ojumu, T.V., Petrik, L.F. & Musyoka, N.M. 2012. Synthesis of zeolite A from coal fly ashes obtained from different South African power stations. *SAIChE Conference*, Champagne Sport Resort, Kwazulu Natal, South Africa, 16-19 September 2012.

Journal publications

1. Mainganye, D., Du Plessis, P.W, Ojumu, T.V. & Petrik, L.F. 2012. Development of scale-up conditions for the synthesis of zeolites from South African coal fly ash: effect of impeller design and agitation. (Submitted to *Materials* 2012).

TABLE OF CONTENTS

DECLARATION	ii
ABSTRACT	iii
DEDICATION	v
ACKNOWLEDGEMENTS	vi
LIST OF PUBLICATIONS AND PRESENTATIONS	viii
LIST OF FIGURES	xiv
LIST OF TABLES	xvii
LIST OF ABBREVIATIONS	xviii
CHAPTER 1	1
1. INTRODUCTION	1
1.1. Background.....	1
1.2. Problem statement.....	3
1.3. Research objectives and questions.....	4
1.4. Significance of the study.....	5
1.5. Scope and limitations of the thesis.....	5
1.6. Thesis outline.....	6
CHAPTER 2	7
2. LITERATURE REVIEW	7
2.1. FLY ASH.....	7
2.1.1. General introduction.....	7
2.1.2. Properties of fly ash.....	8
2.1.3. Chemical properties.....	8
2.1.4. Physical properties.....	9
2.1.5. Classification of fly ash.....	9
2.1.6. Utilisation of fly ash.....	10
2.1.6.1. Fly ash as a cement and concrete additive.....	10
2.1.6.2. The use of fly ash in the treatment of acid mine drainage.....	11
2.1.6.3. Zeolite synthesis from fly ash.....	11
2.1.7. Environmental impacts of fly ash.....	12
2.2. ZEOLITES.....	12
2.2.1. General introduction to zeolites.....	12

2.2.2.	Zeolite framework structure	13
2.2.3.	Properties and Applications of zeolites	15
2.2.3.1.	Properties	15
2.2.3.2.	Zeolite Applications	16
2.2.3.2.1.	Ion-exchange properties of zeolites	17
2.2.3.2.2.	Adsorption capacity for zeolites	17
2.2.3.2.3.	Catalysis/catalytic applications of zeolites.....	18
2.2.4.	Classification of zeolites	18
2.2.5.	Synthetic zeolites.....	19
2.2.6.	Zeolite synthesis from fly ash.....	20
2.2.7.	Methods of zeolite synthesis.....	21
2.2.7.1.	Synthesis methods used in this study	22
2.2.7.1.1.	Aging stage.....	23
2.2.7.1.2.	Hydrothermal treatment stage.....	23
2.2.8.	Zeolite formation mechanism	23
2.2.9.	Factors influencing zeolite formation.....	26
2.2.9.1.	SiO ₂ /Al ₂ O ₃ ratio of the starting material	26
2.2.9.2.	Type of the charge balancing cations	27
2.2.9.3.	NaOH concentration	27
2.2.9.4.	Effect of synthesis time.....	28
2.2.9.5.	Effect of temperature	28
2.2.9.6.	Water concentration.....	29
2.2.9.7.	Effect of agitation on zeolites synthesis	29
2.2.10.	Characterisation of zeolites.....	30
2.2.10.1.	Mineralogy by X-Ray powder diffraction.....	30
2.2.10.2.	Scanning electron microscopy	31
2.2.10.3.	Chemical analysis by X-ray Fluorescence	31
2.2.10.4.	Structural configuration by infra-red spectroscopy	32
2.2.11.	Gaps in the literature with respect to zeolites synthesis	32
2.3.	Chapter summary	33
CHAPTER 3	34
3. EXPERIMENTAL AND ANALYTICAL TECHNIQUES	34
3.1.	SECTION A: Synthesis of Zeolite Na-P1	34
3.1.1.	Materials.....	34
3.1.2.	Sample storage	35
3.1.3.	Synthesis equipment	35

3.1.4.	Synthesis procedure	37
3.1.4.1.	Aging step	37
3.1.4.2.	Hydrothermal treatment	38
3.1.4.3.	Recovery of zeolites	38
3.1.5.	Experiments.....	38
3.1.5.1.	Synthesis of a pure phase of zeolite Na-P1	38
3.1.5.2.	Effects of impeller design and agitation during the aging step.....	38
3.1.5.3.	Effect of fly ash composition as a feedstock	39
3.1.5.4.	Effects of water chemistry on the quality of zeolite Na-P1.....	39
3.1.5.5.	Effects of hydrothermal reaction time.....	40
3.2.	SECTION B: Synthesis of zeolite A	41
3.2.1.	Materials.....	41
3.2.2.	Synthesis Procedure and conditions.....	42
3.2.2.1.	Fusion	42
3.2.2.2.	Extraction step.....	42
3.2.2.3.	Preparation and addition of the aluminate solution	42
3.2.2.4.	Crystallization step	43
3.2.2.5.	Recovery of zeolites	43
3.2.3.	Experiments.....	43
3.2.3.1.	Synthesis of a pure phase zeolite A.....	44
3.2.3.2.	Synthesis of zeolite A using South African fly ash from different sources.....	44
3.3.	SECTION C: Techniques of characterisation	44
3.3.1.	X-ray Fluorescence spectrometry	45
3.3.1.1.	Sample preparation and procedure.....	45
3.3.2.	Inductively Coupled Plasma (Atomic Emission and Mass) Spectroscopy.....	45
3.3.3.	Ion chromatography.....	46
3.3.4.	X-ray Diffraction Spectroscopy	46
3.3.4.1.	Qualitative XRD analysis	46
3.3.4.1.1.	Sample preparation and procedure.....	46
3.3.4.1.2.	Determination of percentage crystallinity.....	47
3.3.4.1.3.	Quantification of the zeolite phase	47
3.3.4.2.	Quantitative XRD analysis	47
3.3.4.2.1.	Sample preparation and procedure.....	47
3.3.5.	Fourier Transform Infrared Spectroscopy	48
3.3.6.	Scanning Electron Microscopy.....	48
3.4.	Summary	48
CHAPTER 4		49

4. CHARACTERISATION OF RAW MATERIALS	49
4.1. Introduction.....	49
4.2. Chemical composition of the fly ashes.....	49
4.3. Mineralogical composition of the fly ashes.....	53
4.3.1. Qualitative X-ray diffraction analysis.....	53
4.3.2. Quantitative X-ray diffraction analysis.....	54
4.4. Morphology of fly ash particles.....	57
4.5. Particle size distribution.....	58
4.6. Conclusions.....	59
CHAPTER 5	60
5. SYNTHESIS OF ZEOLITE NA-P1 FROM SOUTH AFRICAN COAL FLY ASH: investigation of scale-up conditions	60
5.1. Introduction.....	60
5.2. Materials and Method.....	61
5.2.1. Experimental procedure.....	61
5.2.2. Analytical Techniques.....	61
5.3. Results and discussion.....	61
5.3.1. Effect of impeller design and agitation during the aging step.....	62
5.3.1.1. Mineralogical analysis of the synthesised zeolites.....	62
5.3.1.2. Structural analysis of the synthesised zeolites.....	66
5.3.1.3. Morphological characterisation by SEM.....	69
5.3.1.4. Summary.....	69
5.3.2. Effect of fly ash composition on the synthesis of zeolite Na-P1.....	70
5.3.2.1. Mineralogical and physical characterization.....	70
5.3.2.2. Synthesis of zeolite Na-P1 from other South African coal fly ashes.....	74
5.3.2.3. Summary.....	76
5.3.3. The use of different water sources for synthesis of zeolite Na-P1.....	77
5.3.3.1. Characterisation of the AMD.....	77
5.3.3.2. Characterisation of tap and distilled water.....	79
5.3.3.3. Mineralogical and physical analysis of the synthesis products.....	80
5.3.3.4. Summary.....	83
5.3.4. Effects of hydrothermal reaction time.....	83
5.3.4.1. Variation of aging time.....	83
5.3.4.1.1. Mineralogical analysis by XRD.....	84
5.3.4.1.2. Crystallinity.....	85
5.3.4.1.3. Si/Al ratio of the synthesis solution.....	86

5.3.4.1.4. Crystallinity of mullite and zeolite Na-P1	86
5.3.4.2. Variation of Hydrothermal treatment (HT) time.....	87
5.3.4.2.1. Zeolite synthesis at 12 hours of aging with a variation of HT time	87
5.3.4.2.2. Zeolite synthesis at 24 hours of aging with a variation of HT time	88
5.3.4.2.3. Zeolite synthesis at 36 hours of aging with a variation of HT time	89
5.3.4.2.4. Zeolite synthesis at 48 hours of aging with a variation of HT time	91
5.3.4.2.5. Summary	94
5.4. Conclusions to Chapter 5.....	94
CHAPTER 6	97
6. SYNTHESIS OF ZEOLITE A.....	97
6.1. Introduction.....	97
6.2. Materials and Methods	97
6.2.1. Experimental procedure.....	97
6.2.2. Analytical techniques	97
6.3. Results and discussion	98
6.3.1. Alkaline fusion of fly ash	98
6.3.2. Effect of water sources on the synthesis of a zeolite A	99
6.3.2.1. Characterisation of the circumneutral mine water	99
6.3.2.2. Mineralogical analysis.....	100
6.3.2.3. Morphological analysis	102
6.3.3. Effect of fly ash composition on the synthesis of zeolite A	102
6.3.3.1. Mineralogical analysis.....	103
6.3.3.2. Crystallinity	103
6.3.3.3. Elemental composition of the synthesised product	106
6.3.3.4. Morphological analysis	107
6.4. Conclusion to Chapter 6	109
CHAPTER 7	110
7. CONCLUSIONS AND RECOMMENDATIONS.....	110
7.1. General conclusions	110
7.2. Recommendations and future work	113
REFERENCES	115

LIST OF FIGURES

Figure 2-1: Illustration of SiO_4 and AlO_4 tetrahedral and the orientation of the tetrahedra to form framework structures	14
Figure 2-2: Illustration of Na ions inside the voids of zeolite A.....	17
Figure 2-3: Illustration of reaction mechanism for the batch hydrothermal conversion of fly ash to zeolites.....	25
Figure 3-1: Experimental set-up of the aging process	36
Figure 3-2: Three types of impellers used in this study i.e. A). Archimedes Screw B). Anchor C). 4 flat-blade impeller.....	36
Figure 3-3: Parr bomb and Teflon lining used as small scale reactors in the hydrothermal treatment process	37
Figure 3-4: Flowchart illustrating the synthesis process of zeolite A from fly ash.....	43
Figure 4-1: XRD spectra of Arnot (Batch 1 and 2) and Hendrina fly ash.....	53
Figure 4-2: XRD spectra of Lethabo, Matla and Tutuka fly ash	54
Figure 4-3: Quantification of the fly ash phases	55
Figure 4-4: SEM images of fly ash morphology. (a) Typical view of the FA particles with a predominantly spherical morphology. (b) Smaller particles attached to the surface of a larger particle. (c) Hollow spheres (cenospheres). (d) Hollow sphere containing smaller spheres (plerospheres).....	57
Figure 4-5: Particle size distribution of coal fly ashes. A) Tutuka, B) Matla, C) Hendrina, D) Lethabo and E) Arnot (batch 1) fly ash.....	58
Figure 5-1: XRD spectra of the products synthesised using Magnetic stirrer, 4 flat-blade, Anchor and Archimedes screw impeller at different stirring speeds.....	63
Figure 5-2: FTIR spectra of the zeolitic products synthesised using different impellers with variation of stirring speed	67
Figure 5-3: SEM images of zeolite Na-P1 synthesised with the 4 flat-blade impeller at 200 rpm. a) and b) both show zeolite Na-P1	69

Figure 5-4: XRD spectra of the zeolites synthesised with the use of two batches of Arnot FA. Product 1 and 2-zeolites synthesised using Arnot batch 1 and batch 2 fly ashes respectively.	71
Figure 5-5: FTIR spectra of FA and the zeolitic products. Product 1 and 2-zeolites synthesised using Arnot batch 1 and batch 2 fly ashes respectively.	73
Figure 5-6: SEM images of fly ash and the synthesis products. (a) Pure phase of Na-P1. (b) Na-P1 and Analcime.	74
Figure 5-7: Zeolitic products synthesised using Arnot batch 2 and Hendrina fly ashes.	75
Figure 5-8: XRD patterns of the synthesis products obtained when different waters were used as solvents	80
Figure 5-9: SEM images showing morphological aspects in the zeolitic products obtained when waters from different sources were used as solvents. a) UP b) TW c) DW d) AMD	82
Figure 5-10: XRD patterns and SEM images of the synthesis products obtained after 12 hours of hydrothermal treatment at 140 °C and variation of aging period. a) 12 b) 24 c) 36 and d) 48 hours of aging.	84
Figure 5-11: Percentage crystallinity of mullite and zeolite Na-P1 together with the Si/Al ratio of the synthesis solution as a function of the aging time.	85
Figure 5-12: XRD patterns of the synthesis products obtained after 12 hours aging followed by variation of hydrothermal treatment time. a) XRD spectra and b) percentage crystallinity of different phases.	87
Figure 5-13: XRD patterns of the synthesis products obtained after 24 hours aging with variation of hydrothermal treatment time. a) XRD spectra and b) percentage crystallinity of different phases.	89
Figure 5-14: XRD patterns of the synthesis products obtained after 36 hours aging with variation of hydrothermal treatment time. a) XRD spectra and b) percentage crystallinity of different phases.	90
Figure 5-15: XRD patterns of the synthesis products obtained after 48 hours aging with variation of hydrothermal treatment time. a) XRD spectra and b) percentage crystallinity of different phases.	91
Figure 5-16: XRD patterns and SEM image of the zeolite products synthesised at 36 hours of aging and 48 hours of HT.	92

Figure 5-17: XRD spectra of zeolite Na-P1. (Product 1 (red) and 2 (black) are zeolite Na-P1 synthesised using batch 1 and batch 2 of Arnot fly ash respectively). 93

Figure 6-1: XRD patterns and SEM images of the original FA and fused FA. a) XRD patterns of the original FA. b) SEM image revealing the morphology of the original FA. c) XRD patterns of fused FA. d) SEM image of fused FA. 98

Figure 6-2: XRD patterns of zeolite A synthesised using Arnot FA, ultrapure and mine waters as the starting materials. 101

Figure 6-3: SEM images of zeolite A synthesised from Arnot fly ash using different solvents. a) Ultrapure water b) CMW. 102

Figure 6-4: XRD patterns of zeolite A synthesised from Arnot, Hendrina and Matla fly ashes 104

Figure 6-5: XRD patterns of zeolite A synthesised from Tutuka and Lethabo fly ashes..... 105

Figure 6-6: SEM images illustrating the transformation of fused fly ash into zeolite A using different fly ashes. a) fused fly ash b) Arnot c) Hendrina d) Matla e) Lethabo and f) Tutuka 108

LIST OF TABLES

Table 2-1: Classification of Fly ash based on chemical composition (ASTM C618-95)	10
Table 2-2: Physio-chemical properties of zeolites and molecular sieves.....	16
Table 2-3: Physical Properties of four well known zeolites	16
Table 2-4: Examples of the three letter coding system used by International Zeolite Association	19
Table 2-5: Zeolites and other neomorphic phases synthesised from fly ash	21
Table 3-1: List of chemicals used in this study.....	35
Table 3-2: Experimental conditions for the investigation of effect of the impeller design and agitation during the aging step	39
Table 3-3: Experimental conditions for the investigation of effect of aging time using a 4 flat-blade impeller at 200 rpm.	41
Table 3-4: XRD operating parameters.....	46
Table 4-1: Major elemental composition of coal fly ashes used in this study	50
Table 4-2: Trace elements in the coal fly ashes used in this study	51
Table 4-3: Quantification of the fly ash phases	56
Table 5-1: Percentage crystallinity of zeolite Na-P1	65
Table 5-2: Overview of mid-infrared vibrations of zeolites (cm^{-1})	66
Table 5-3: Composition of the AMD.....	78
Table 5-4: Composition of tap and distilled water	79
Table 6-1: Composition of the CMW.....	100
Table 6-2: Crystallinity of the synthesis product.....	103
Table 6-3: Chemical composition (major oxides) of the representative zeolite A products synthesised from different fly ashes.	106

LIST OF ABBREVIATIONS

Abbreviation	Meaning
A	Zeolite A
Al	Aluminium
AMD	Acid Mine Drainage
ANA	Analcime
CCP	Coal combustion product
CEC	Cation exchange capacity
cm	Centimetre
CMW	Circumneutral mine water
DW	Distilled water
EC	Electrical conductivity
FA	Fly ash
FTIR	Fourier transform infrared spectroscopy
H	Hematite
hrs	Hours
HS	Hydroxysodalite
HT	Hydrothermal treatment
ICP-AES	Inductively coupled plasma atomic emission spectroscopy
ICP-MS	Inductively coupled plasma mass spectroscopy
IR	Infrared
IZA	International zeolite association
JCPDS	Joint Committee on Powder Diffraction Standards
KOH	Potassium hydroxide
LOI	Loss on ignition
M	Mullite
Mag	Magnetite
NaOH	Sodium hydroxide
NO _x	Nitrogen oxides
O	Oxygen
P	Zeolite Na-P1
PBU	Primary building units
ppm	Parts per million
Q	Quartz
rpm	Revolutions per minute

SBU	Secondary building units
SEM	Scanning electron microscope
Si	Silicon
SO _x	Sulphur oxides
SR	Solid residues
Std	Standard
TW	Tap water
UP	Ultrapure water
wt	weight
XRD	X-ray diffraction spectroscopy
XRF	X-ray Fluorescent Spectroscopy

CHAPTER 1

1. INTRODUCTION

1.1. Background

Coal is the most abundant source of energy in South Africa. About 90 % of the electricity generated in South Africa is largely from coal-fired power stations. Eskom used approximately 124.7 million tons of pulverised coal for electricity generation in the year 2011 (Eskom, 2011). Combustion of coal produces residues known as coal combustion by-products (CCPs). One of the principal components of CCPs from the coal-powered utilities is fly ash (FA). FA is a fine-grained inorganic powder residue which is composed of spherical glassy particles which are derived from minerals formed during coal combustion. It has been found that most of the coal in South Africa is of low quality with a low calorimetric heat value and high ash content (Eskom, 2009). Vast quantities of ash are being produced each year due to power generation. It was reported that approximately 36.22 million tons of coal ash were produced at Eskom's power stations in 2011. However, only 5.5 % of this ash was used in the production of cement (Eskom, 2011). This presents a huge environmental problem since the remaining ash is disposed in ash dams and dumps, both of which can be regarded as unsightly, environmentally undesirable and/or results in non-productive use of land resources. The maintenance of these dumps and dams also poses an on-going financial burden on Eskom. In South Africa, fly ash has found limited applications in the cement and concrete industry and in land reclamation and restoration. Therefore, it is necessary to find alternative usages for FA.

Numerous approaches have been made for the utilisation of fly ash either to reduce the cost of disposal or to minimise its impact on the environment. FA has found uses in the cement and concrete industry as an additive, treatment of acid mine drainage as well as in land reclamation and restoration (Ahmaruzzaman, 2010; Gitari *et al.*, 2008; Vadapalli *et al.*, 2008; Landman, 2003; Scheetz and Earle, 1998; Taylor, 1998). However, it was found that one approach to reduce the pollution from FA is to convert the waste FA into high value zeolites (Querol *et al.*, 2001). Zeolites are crystalline hydrated aluminosilicates of alkali and alkaline earth cations with three-dimensional silicate structures (Pfenninger, 1999). Numerous varieties of zeolites occur in nature, however, in the middle of the last century it was found that zeolites could be synthesised in the laboratory (Pfenninger, 1999). The earliest studies on the synthesis of zeolites were conducted by Richard Barrer and Robert Milton in the late

1940`s (Cundy and Cox, 2005; Breck, 1974). According to Cundy (2005), Barrer began his studies by investigating the conversion of known mineral phases under the action of a strong salt solution at fairly high temperatures i.e. about 170 to 270 °C. However, Milton pioneered the use of more reactive alkali-metal aluminosilicate gel at low temperatures (≈ 100 °C) and autogenous pressure (Ibrahim, 2007; Cundy and Cox, 2005; Pfenninger, 1999). The principal starting materials used to synthesise zeolites are silica and alumina which are hydrothermally treated with a metal cation solution. Zeolite synthesis was conventionally developed by hydrothermal crystallisation under alkaline conditions, which has been reported by several patents and technical articles (Hollman *et al.*, 1999; Amrhein *et al.*, 1996; Shigemoto, 1996; Singer and Berggaut, 1995; Kolousek *et al.*, 1993; Shigemoto *et al.*, 1993; Mondragon *et al.*, 1990). Recently, the classic alkaline hydrothermal synthesis has been improved by using more sophisticated treatments, which include an alkaline fusion step followed by hydrothermal treatment, the application of microwave-assisted zeolite synthesis and a method for synthesising zeolites under molten conditions without any addition of water (Reyes, 2008; Querol *et al.*, 2002).

Synthetic zeolites have found applications in ion-exchange, as molecular sieves, catalysts and adsorbents (Pfenninger, 1999; Breck, 1974). The wide variety of applications includes separation and recovery of normal paraffin hydrocarbons, catalysis of hydrocarbon reactions, drying of refrigerants, separation of air components, carrying catalysts in the curing of plastics and rubber, recovering radioactive ions from radioactive waste solutions and as an adsorbent for the removal toxic elements during the wastewater treatment (Musyoka, 2009; Pfenninger, 1999; Breck, 1974). Their application has led to the establishment of intensive research on targeted zeolites products for specific application. It has been reported that zeolites can also be produced from coal fly ash due to the compositional similarity of fly ash to some volcanic material, which is a precursor of natural zeolites (Querol *et al.*, 2007; Somerset *et al.*, 2005; Somerset *et al.*, 2005; Querol *et al.*, 2002; Querol *et al.*, 2001; Hollman *et al.*, 1999; Querol *et al.*, 1996; Holler and Wirsching, 1985).

It has been shown that zeolite Na-P1 and zeolite A can be produced from South African coal fly ash (Musyoka *et al.*, 2011; Musyoka, 2009). According to the author, the optimum conditions to obtain a pure phase of zeolite Na-P1 from South African fly ash were: aging at 47 °C for 48 hours followed by hydrothermal treatment at 140 °C maintained for 48 hours. Under these conditions a Zeolite Na-P1 having 4.11 meq/g cation exchange capacity was produced in a static Parr bomb (Musyoka, 2009). According to Musyoka *et al.* (2011), the optimum conditions to synthesise a pure phase of zeolite A from South African coal fly ash are; via the alkali fusion method, fusion step at 550 °C for 1.5 hours, dissolution step at room temperature for 2 hours under vigorous stirring (± 1400 rpm) and hydrothermal treatment step

at 100 °C for 2 hours under static conditions. However, the above studies were conducted on a small lab scale.

Given that South Africa generates about 36.22 million tons of fly ash per annum as waste of which only 5.5 % is used, exploring the use of fly ash to produce zeolites on an industrial scale would be of immense benefit for the nation. Therefore, this study investigated the scale-up opportunities for both zeolite Na-P1 and zeolite A synthesis. Large scale production of zeolites must be imperatively conducted in an agitated reactor (Caschi, 2005; Marrot *et al.*, 2001). This is because, the reaction mixture produces a viscous gel and if mixing is inadequate or absent, an inhomogeneous reaction mixture may result with pockets of gel having different compositions and consistency. According to Caschi (2005) each “pocket” behaves like a mini reactor and generates phases corresponding to the composition in that mini reactor. Therefore, it is essential to investigate the effects of physical and chemical parameters on the scale-up process for the synthesis of these zeolites. Parameters such as the reactor size, impeller design, type and position of the impeller, the effect of agitation and the order of mixing, composition of the starting materials, type of solvent used as well as the effect of temperature and pressure, will have a significant effect on the phase and quality of the zeolite being produced (Musyoka, 2009; Caschi, 2005; Bebon *et al.*, 2002; Marrot *et al.*, 2001; Querol *et al.*, 2001; Pfenninger, 1999).

Querol and co-workers have shown that it is possible to scale-up the synthesis of zeolite and that the products obtained from scaled experiments were similar to those obtained from the laboratory (Querol *et al.*, 2001). However, most of the studies that were conducted concentrated on the synthesis of zeolites from Class C fly ash. South African fly ash belongs to Class F and very few studies have reported the use of South African fly ash as a feedstock (Musyoka, 2009). Thus, it is important to investigate the scalability of the processes designed for zeolite synthesis from South African fly ashes with the view of understanding the effects of some reactor and operational parameters on the quality of the product produced. This study would be carried out with reference to previous work by Musyoka (2009) and Musyoka *et al.* (2011).

1.2. Problem statement

As aforementioned, South Africa produces a large quantity of coal FA each year due to its power generation activities. Currently, there are low-end strategies for the utilisation of this abundant FA. Ash presents a huge environmental problem as the unused ash is disposed in ash dams and dumps. It has been shown in the literature that zeolites can be produced using FA as a raw material; however, the zeolites were synthesised on a micro-scale. Therefore, the use of this waste fly ash (FA) to produce zeolites on an industrial scale, in addition to

creating value-added products and technology, will contribute to the mitigation of environmental problems caused by the FA disposal in South Africa. However, it is important to investigate the effects of parameters such as temperature, pressure, agitation and also the compositional variability of the feedstock on the quality of the zeolites produced. Therefore, there is a need to explore the possibility of synthesising zeolites on a large/industrial scale.

1.3. Research objectives and questions

In general, the objective of this study was to investigate the effects of scale-up conditions on the synthesis of zeolite Na-P1 and zeolite A from South African coal fly ashes with the view to understand the effects of reactor configuration and operational conditions on the quality of the product. In specific terms, this study focused on the following objectives:

- To demonstrate the reproducibility of previous results achieved by Musyoka *et al.* (2012) - a base case for this study (Musyoka *et al.*, 2012).
- To investigate the effect of impeller design and agitation during the aging step of zeolite Na-P1 synthesis on the quality and purity of the product using the optimum condition obtained by Musyoka *et al.* (2012).
- To investigate the effect of variability in the composition of the fly ash used as the starting material during the synthesis of zeolite Na-P1.
- To assess the possibility of synthesising zeolite Na-P1 using different water sources as a substitute for ultrapure water.
- To investigate the optimum reaction time needed during the synthesis of zeolite Na-P1 and monitor the evolution of the zeolite phase.
- To assess the possibility of synthesising zeolite A from five different sources of South African coal fly ash.

This investigation will provide understanding for the following questions:

- What effects does impeller design and agitation have on the quality of zeolite Na-P1?
- Is it possible to synthesise zeolite Na-P1 and zeolite A from different sources of South African coal fly ash?
- Is it possible to synthesise zeolite Na-P1 using other solvent sources instead of ultrapure water?

- What is the optimum of reaction time for achieving the highest quality and purity of zeolite Na-P1 under the applied conditions?

1.4. Significance of the study

According to Ahmaruzzaman (2010), the disposal of FA will soon be too costly if not forbidden. Despite the positive uses of FA, its production outweighs its consumption and its production rate is expected to increase due to increasing electricity demand and the construction of new coal-fired power stations in South Africa. Due to the shortage of landfill sites and stricter environmental regulations, effective zeolitisation of FA on a large scale would contribute to the mitigation of this by-product and reduce its environmental impact. The zeolite produced from FA can be used in the decontamination of waste-waters (such as brines and acid mine drainage). A possibility of selling the high-valued zeolites to other countries may also exist. This project can assist the power generation utility, Eskom, to reduce the cost of FA disposal as well as minimise its impact on the environment.

1.5. Scope and limitations of the thesis

There are a number of zeolites types that have been successfully synthesised from fly ash (Querol *et al.*, 2002). Studies have shown that zeolite phases other than the expected phase may appear during the synthesis process depending on the reaction conditions. However, this study focused prominently on the synthesis of zeolite Na-P1 and zeolite A. The choice of the zeolite types was motivated by their potential industrial applications. The scope of this work was to conduct the synthesis and characterisation of the zeolites using different characterisation techniques; however, the application of the synthesised zeolites was not covered in this study.

There are a number of factors that affect the synthesis of zeolite Na-P1 as well as the scale-up process. However, in this study only four synthesis parameters that have been found to significantly influence the synthesis and the scale-up process were investigated i.e. impeller design and agitation, FA composition, chemistry of the water and reaction time. The choice of the synthesis parameters was motivated by the results obtained by Musyoka (2009) and from other relevant literature (Casci, 2005; Inada *et al.*, 2005; Marrot *et al.*, 2001).

There are over 10 coal-fired power stations in South Africa. In this study, only fly ash from five power stations (namely; Arnot, Hendrina, Matla, Lethabo and Tutuka power stations) were used to synthesise zeolites.

1.6. Thesis outline

This thesis is divided into seven chapters, including this chapter (Chapter 1). In this thesis, Chapter 1 is the introductory chapter and it presents a brief overview of the background aspects of the proposed study, problem statement, the objectives as well as the significance of this study. Chapter 2 presents the literature survey on FA and zeolites. This included the genesis, properties, classification and environmental problems associated with the disposal of FA. The literature on zeolites covers the historical background of zeolites, the structures, properties and applications, synthesis of zeolites from FA as well as their characterisation.

Chapter 3 presents the materials and the experimental methods used in this work. Its purpose was to provide background information on the raw materials used in the synthesis process and the experimental methods of the investigation. The fundamental techniques of characterisation are also discussed in this chapter.

Chapter 4 examines the characterisation of the fly ash used in this study, providing useful information on their mineralogical and chemical composition for their application in zeolite synthesis, taking into account that the chemical composition has a direct influence on both the potential application of the FA and the environmental impact of its subsequent use.

Chapters 5 and 6 discuss the results of the synthesis and characterisation of zeolite Na-P1 and zeolite A respectively. The results are summarised, followed by a discussion of the main trends, and then both are connected with the literature surveyed and any correlations that have emerged in the data are highlighted.

Chapter 7 summarises the important conclusions that can be drawn from the results presented in this thesis and suggests directions for future research.

CHAPTER 2

2. LITERATURE REVIEW

This chapter gives a detailed description of the origin, physical and chemical properties, classification, and applications of fly ash, since it is the main raw material for zeolite synthesis in this study.

2.1. FLY ASH

2.1.1. General introduction

Coal is a vital part of energy production in South Africa. South African coal reserves are estimated to be about 53 Billion tonnes with a projected availability of 200 years. About 90 % of this coal is being used for electricity generation. The need to produce electric power has resulted in the construction of a large number of coal-fired power plants. Over 12 coal-fired power stations exist in South Africa to date (Catalfamo *et al.*, 1993). Increasing demand for electricity has resulted in the burning of large quantities of coal to produce electricity. The conversion of coal into electricity results in the generation of solid coal combustion by-products. These solid by-products include bottom ash, boiler slag, economiser ash and fly ash (Scheetz and Earle, 1998). Within these by-products, fly ash is the principal component (up to 80 % of the coal ash) of coal combustion from coal-fired power stations.

Fly ash is a fine-grained inorganic powder residue which is composed of spherical glassy particles which are derived from minerals produced during the combustion of coal. It appears grey in colour, abrasive, mostly alkaline and refractory in nature (Ahmaruzzaman, 2010). It consists of inorganic, incombustible matter present in the coal that has been fused during combustion into a glassy, amorphous structure. According to Scheetz & Earle (1998), fly ash particle size normally ranges from 0.5 to 200 μm and is mainly composed of amorphous aluminosilicate glass, crystalline phases (such as quartz, mullite, hematite, lime and magnetite) together with varying amounts of iron, sodium, potassium, calcium, titanium, sulphur, carbon and magnesium (Wang and Wu, 2006; Scheetz and Earle, 1998; Querol *et al.*, 1995).

Fly ash is carried off in the flue gas as it leaves the combustion chamber and is usually collected from the flue gas by means of electrostatic precipitators and in some cases by bag houses, or mechanical collection devices such as cyclones (Scheetz and Earle, 1998). The formation of fly ash during combustion of coal consists of a series of complex mechanisms to

form each constituent of the ash and is determined by a vast amount of factors (Musyoka, 2009; Koukouzas *et al.*, 2007; Goodarzi, 2006).

Eskom, South Africa's primary power utility, is the biggest producer of fly ash in South Africa. According to Eskom's 2009 annual report, South African coal is of low quality, with a low calorimetric heat value and high ash content. About 122.7 Million tonnes of coal were burnt by Eskom during the generation of electricity in South Africa for the year 2010. This resulted in about 36.01 Million tonnes of ash being produced in the country. South African fly ash contains a relatively high concentration of SiO_2 , Al_2O_3 and CaO .

2.1.2. Properties of fly ash

Knowledge of the physical characteristics, chemical composition and properties of fly ash is essential to understanding any possible environmental impacts. Chemical and physical properties of fly ash vary greatly (.i.e. from one sample to the next) as a function of the coal source, type of coal burnt, the boiler used and its operating conditions and the process undergone by coal before combustion (Vassilev and Vassileva, 2007; Kutchko and Kim, 2006; Scheetz and Earle, 1998; Kruger, 1997). Although fly ash varies from sample to sample, some generalisations can be made in terms of the physical, chemical and mineralogical characteristics.

2.1.3. Chemical properties

Fly ash is a complex heterogeneous material which consists of amorphous and crystalline phases. X-ray Diffraction (XRD) analysis has been used to establish the mineralogy of the fly ash and it was found that the dominant mineral phases are quartz, kaolite, illite, mullite and sideraete with trace amounts of magnetite and hematite (Ahmaruzzaman, 2010; Musyoka, 2009; Iyer and Scott, 2001; Querol *et al.*, 2001). An amorphous glass phase has also been found to be one of the major constituents of most fly ashes and is responsible for the pozzolanic properties of fly ash (Goodarzi, 2006). In addition, Ahmaruzzaman (2010) stated that quartz and mullite are the major crystalline phases in low-calcium fly ash, whereas high-calcium fly ash consists of quartz (SiO_2), tricalcium aluminate ($\text{Ca}_3\text{Al}_2\text{O}_6$) and Calcium silicate (Ca_2SiO_4).

The primary components of fly ash are silica (SiO_2), alumina (Al_2O_3) and iron oxides (Fe_2O_3) with varying amounts of carbon, calcium (as lime or gypsum), magnesium and sulphur (sulphides or sulphates) (Ahmaruzzaman, 2010; Iyer and Scott, 2001). Fly ash can also be regarded as a ferro-aluminosilicate mineral with Al, Si, Fe, Ca, K and Na being the predominant elements. It was also found that a number of trace and minor elements such as Ba, Ce, Cl, Cr, Cu, F, La, Mn, P, Nb, Pb, Sb, Sr, Th, Ti, U, Y, W, Zn, Zr and probably Ag, As,

Ga, Ge, Hf, Mo, Sn, and V occur, or may occur, as proper accessory minerals and phases in fly ash (Vassilev and Vassileva, 2007; Iyer and Scott, 2001).

Fly ashes are also considered as pozzolans (substances containing silica and alumina) and together with water and calcium hydroxide form cementitious products at ambient temperatures (Ahmaruzzaman, 2010; Iyer and Scott, 2001). This means that fly ash hardens when reacted with Ca(OH)_2 and water. According to Iyer and Scott (2001), the pozzolanic property of fly ash arises when the silicate phases have an amorphous structure rather than crystalline. In addition to the chemical properties, fly ashes exhibit some common physical properties and are discussed below.

2.1.4. Physical properties

Numerous studies have been undertaken in order to get a clear and better understanding of the physical nature of fly ash. As aforementioned, fly ash varies from sample to sample; however, researchers have established some generalisations in terms of its physical properties. Fly ash is generally composed predominantly of small, glassy, hollow particles with particle sizes ranging from 0.01 to 200 μm (Ahmaruzzaman, 2010; Scheetz and Earle, 1998). According to Ahmaruzzaman (2010), the particle distribution of most bituminous fly ash is generally less than 0.075 mm. The specific gravity of fly ash usually ranges from 2.1 to 3.0 with a specific surface area ranging from 170 to a 1000 m^2/kg (Ahmaruzzaman, 2010). The colour of fly ash can vary from tan to grey to black, depending on the amount of unburned carbon in the ash (Scheetz and Earle, 1998). Tan and light colours of fly ash are typically associated with high lime content. The transparent appearance of fly ash indicates the melting of silicate minerals during coal combustion (Adriano *et al.*, 1980).

2.1.5. Classification of fly ash

The fly ash produced during coal combustion can be classified (by American Society for Testing and Materials (ASTM) standard C618-95) into two groups (i.e. class C and class F) based on the content of its major elements (Si, Al, Fe and Ca)- see Table 2.1 (Musyoka, 2009; Vassilev and Vassileva, 2007; Scheetz and Earle, 1998). The class of fly ash is also dependent on the coal from which it was derived. The classification is as follows;

Class C: This type of fly ash is normally produced by the combustion of lignite or sub-bituminous coal (Alonso and Wesche, 1991). Class C fly ash may contain lime contents in excess of 10 %. These fly ashes have both cementitious (self-hardening when reacted with water) and pozzolanic properties (Vassilev and Vassileva, 2007).

Class F: This type of fly ash results from the burning of the harder, older anthracite and bituminous coal (Vassilev and Vassileva, 2007; Alonso and Wesche, 1991). Class F fly

ashes have been reported to contain low content of calcium (less than 10 %). These fly ashes are pozzolanic in nature (hardening when reacted with $\text{Ca}(\text{OH})_2$ and water) (Vassilev and Vassileva, 2007). This type of fly ash has $\text{SiO}_2 + \text{Al}_2\text{O}_3 + \text{Fe}_2\text{O}_3$ content that is greater than 70 % whereas the class C has a sum in the range 50-70 % (Vassilev and Vassileva, 2007).

Table 2-1: Classification of Fly ash based on chemical composition (ASTM C618-95) (Scheetz and Earle, 1998)

Properties	Fly Ash Class	
	Class F	Class C
Silicon dioxide (SiO_2) + aluminium oxide (Al_2O_3) + Iron oxide (Fe_2O_3), min. (%)	70	50
Sulphur trioxide (SO_3), max. (%)	5	5
Moisture Content, max. (%)	3	3
Loss on ignition, max. (%)	6	6
Available Alkalis (as NaOH) max. (%)	1.5	1.5

2.1.6. Utilisation of fly ash

According to Ahmaruzzaman (2010), the disposal of fly ash will soon be too costly, if not forbidden. Although fly ash is regarded as a waste product, it has been confirmed to be a valuable by-product in a number of environmental and commercial applications due to its pozzolanic, cementitious and alkaline properties. Numerous studies have been performed on the utilisation of fly ash to reduce the cost of disposal, reduce the amount of land used for disposal and/or minimise its impacts on the environment. In South Africa, fly ash has found limited applications in the cement and concrete industry and in land reclamation and restoration. Therefore, this section briefly outlines some of the uses of fly ash.

2.1.6.1. Fly ash as a cement and concrete additive

Exhaustive research has been devoted to the topic of fly ash admixtures in concrete and the properties it exhibits. Due to the overwhelming information that is available in literature on this topic, this section only outlines some of the findings on this aspect, since further exposition of this topic was beyond the scope of this research. According to Ahmaruzzaman (2010), the cement and concrete industry is the major consumer of fly ash. Fly ash is used as an additive in cement and concrete. Due to the small size of particles of fly ash in comparison to the aggregate, fly ash decreases air entrainment in the concrete. The addition

of fly ash to Portland cement material results in a decrease in the water demand of the mix (water:cement ratio) and decreases the overall production cost (Scheetz and Earle, 1998). In addition, when used in correct proportions, addition of fly ash results in greater strength concrete than straight Portland cement, because the glass phase in the fly ash is believed to react with lime released from cement. It is this pozzolanic reaction that adds strength to the cement (Landman, 2003). Fly ash further increases resistance to corrosion and ingress of corrosive liquids by reacting with calcium hydroxide in the cement to form stable cementitious calcium silicate hydrate gel. The less soluble calcium silicate hydrate reduces the possibility of calcium hydroxide leaching from the concrete. The reaction products also lead to the filling of capillary voids in the concrete mixture, thereby reducing the permeability of the concrete (Taylor, 1998).

2.1.6.2. The use of fly ash in the treatment of acid mine drainage

Recent studies have reported that the major problem faced in coal mining areas is acid mine drainage (AMD). AMD is highly acidic water, usually containing high concentrations of metals, sulphides and salts, as a consequence of mining activity. Acid mine drainage is a result of the reactions that occur between pyritic minerals associated with coal, oxygen and water. These reactions result in the formation of sulphuric acid which, during rainy weather, is carried away with the water streams, which in turn results in detrimental effects on the environment and downstream water sources. Due to its high alkalinity (presence of lime) and availability, FA has been used to treat acid mine drainage. Fly ash is mixed with the AMD at various solid/liquid ratios and as a result of the neutralisation, sulphates are removed from the water, the pH is corrected and metals precipitate out as hydroxides (Gitari *et al.*, 2008). The problem associated with treating AMD with fly ash is the generation of solid residues (SR) which in turn requires disposal (Vadapalli *et al.*, 2008). In 2008, Vadapalli *et al.* successfully neutralised AMD by using AMD to fly ash mass ratio of 3 to 1. Their study also addressed the suitability of the SR as a backfill material. The study reported that the addition of 3 % pozzolanic binder to the SR increased its strength by 300 %. The ability of toxins to leach from the SR was also proved to be insignificant in their study, illustrating that SR is a viable backfill material (Vadapalli *et al.*, 2008).

2.1.6.3. Zeolite synthesis from fly ash

Fly ash can be used as a raw material in the production of high value zeolite products due to the compositional similarity of fly ash to some volcanic material-a precursor of natural zeolites (Querol *et al.*, 2007; Somerset *et al.*, 2005; Somerset *et al.*, 2005; Querol *et al.*, 2002; Querol *et al.*, 2001; Hollman *et al.*, 1999; Querol *et al.*, 1996; Holler and Wirsching, 1985). This topic will be further discussed in detail in this study, since it is the main focus of the current study-see section 2.2.

2.1.7. Environmental impacts of fly ash

Although a percentage of fly ash is being utilised constructively, there is still a significant amount that is disposed of in ash dams and dumps. The disposal of fly ash has presented a significant environmental problem, due to its potential impacts on the terrestrial and aquatic ecosystems (Carlson and Adriano, 1993). This is because fly ash contains toxic metals such as selenium, chromium, boron, and in some instances, mercury and barium, which have a potential for leaching out from fly ash into ponds or landfills. The impacts of fly ash on terrestrial ecosystems include (Carlson and Adriano, 1993);

- Leaching of potentially toxic elements into soils and groundwater.
- Reduction of plant establishment and growth due to adverse chemical characteristics of the ash.
- Increased mobility and accumulation of potentially toxic elements throughout the food chain.

The disposal of fly ash in ash dumps and dams influences the aquatic ecosystems directly through groundwater contamination. According to Carlson and Adriano (1993), the major impacts associated with changes in water chemistry include changes in pH and concentrations of potentially toxic elements present in the water. Studies have also shown that fly ash has the potential to be used for soil amendment in order to improve soil texture and water holding capacity, as well as soil fertility. However, this may result in excessive soluble salt concentrations, increased concentrations of other toxic trace substances, elemental imbalances due to excessively high pH and cementation or compaction of soil (Carlson and Adriano, 1993). There are a number of environmental aspects associated with fly ash disposal. However, for the purpose of this study, only a few aspects have been discussed above.

2.2. ZEOLITES

2.2.1. General introduction to zeolites

The roots of zeolites go back to 1756, when a Swedish mineralogist by the name of Axel F. Cronstedt first discovered intriguing well-formed crystals in nature. Upon heating, Cronstedt observed that these crystals seemed to boil or froth. Based on this, he named the materials “zeolites” derived from Greek words “zeos” meaning “to boil” and “lithos” meaning “a stone”. Since then, zeolites have been recognised as a separate group of minerals, one of the most abundant on earth. Numerous varieties of zeolites occur in nature, however, in the middle of the last century it was found that zeolites could be synthesised in the laboratory (Pfenninger, 1999).

The earliest studies on the synthesis of zeolites were conducted by Richard Barrer and Robert Milton in the late 1940s (Cundy and Cox, 2005; Breck, 1974). According to Cundy and Cox (2005), Barrer began his studies by investigating the conversion of known mineral phases under the action of a strong salt solution at fairly high temperatures, i.e. about 170-270 °C. Using this approach, Barrer synthesised the first non-naturally occurring zeolites, as two variants, species P and Q (Cundy and Cox, 2005).

In 1949, Milton pioneered the use of more reactive alkali-metal aluminosilicate gel at low temperatures (≈ 100 °C) and autogenous pressure (Ibrahim, 2007; Cundy and Cox, 2005; Pfenninger, 1999). By the end of the year (1949), Milton had successfully prepared zeolite A, B (now known as Na-P) and C (hydroxysodalite), together with a crystalline impurity designated X. By 1953, Milton *et al.* had synthesised 20 zeolites, including 14 unknown as natural minerals (Cundy and Cox, 2005). The principal starting materials used to synthesise zeolites are silica and alumina, which are hydrothermally treated with a metallic cation solution. Since synthetic zeolites became available, they have become very attractive materials as catalysts, adsorbents, and ion-exchangers in most fields of the chemical industry.

2.2.2. Zeolite framework structure

By definition, zeolites are crystalline, hydrated aluminosilicates of alkali and alkaline earth cations, having three dimensional silicate structures (Pfenninger, 1999). Structurally, zeolites are made up of a framework of aluminosilicates that are based on an infinite extension of a three dimensional network of AlO_4 and SiO_4 tetrahedra linked to each other by sharing all oxygen atoms (Breck, 1974). A zeolite structure contains two types of building units, namely, primary and secondary units. A primary building unit (PBU) is made up of SiO_4 and AlO_4 units which are arranged such that the four corners of the tetrahedron are occupied by oxygen atoms surrounding a central ion of either silicon (Si^{4+}) or aluminium (Al^{3+}), as shown in Figure 2.1. These PBUs are linked together to form more complicated secondary building units (SBUs) (Figure 2.1). These SBUs join to form structurally and chemically important zeolite pores or channels, which are known as oxygen windows, which pass through the zeolite. Different combinations of the same secondary building unit (SBU) may give numerous distinctive structural polyhedra formed from smaller ring units-see Figure 2.1.

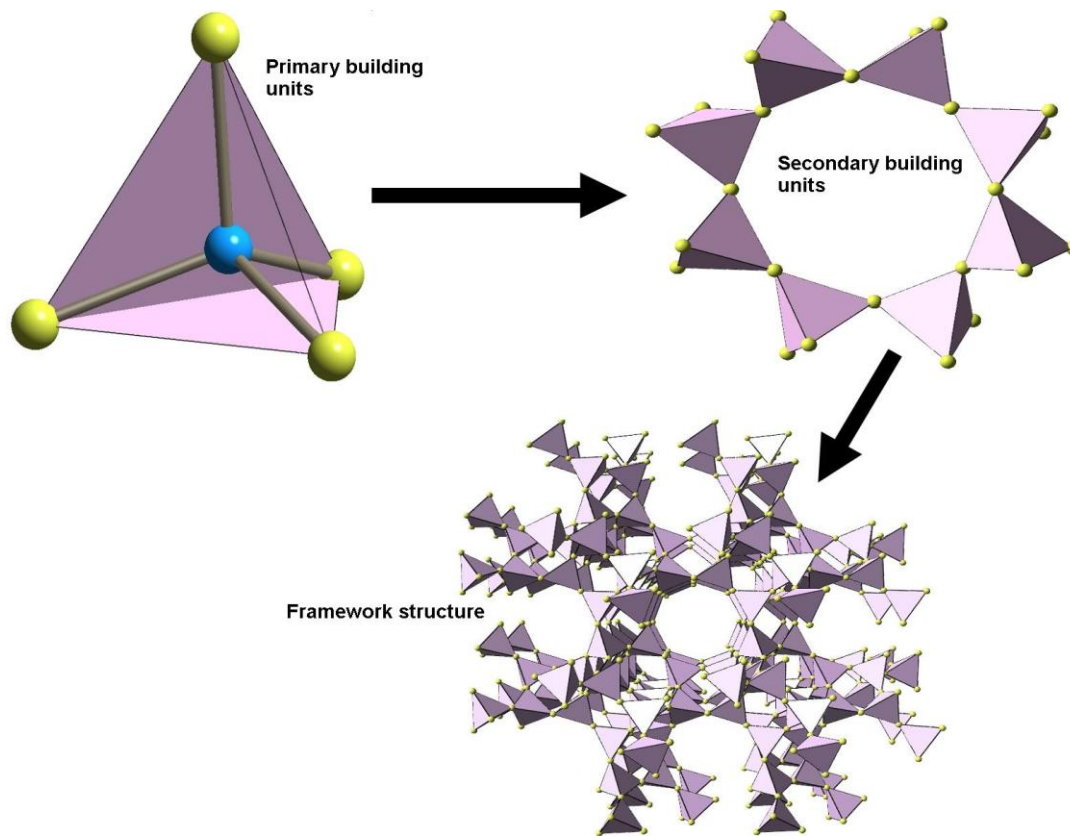
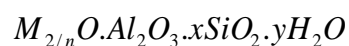


Figure 2-1: Illustration of SiO_4 and AlO_4 tetrahedral and the orientation of the tetrahedra to form framework structures (Elliot, 2006)

However, the crystal structure of each member of the zeolite group is unique, as shown by X-ray diffraction patterns. Nonetheless, all of them are characterised by networks of channels or pores leading to sizeable central cavities at the Angstrom level. In a hydrated form, the cavities are filled with alkali or alkaline earth cations which are surrounded by water molecules (Pfenninger, 1999). Cations are introduced as extra framework species into the voids, acting as charge compensating ions to preserve the electronic neutrality of the zeolite, since the replacement of the tetravalent silicon (Si^{4+}) atoms by the trivalent aluminium (Al^{3+}) atoms results in the formation of ionic sites in the vicinity of the aluminium atoms. It is also possible for other elements to take the place of silicon or aluminium tetrahedra in the framework. These elements are typically Phosphorous, Gallium and Germanium. This class of materials is referred to as *zeotypes* (Taylor, 2007)

Zeolites are also characterised by the ability to lose and gain water reversibly and to exchange constituent cations without major changes in the structure. A representative empirical formula for zeolites is (Breck, 1974);



In this formula, M represents the exchangeable cation of valence n . M is generally an alkali or alkaline earth cation, although other metal, non-metal and organic cations may also balance the negative charge created by the presence of Al in the structure.

Zeolites exhibit the following unique properties (Pfenninger, 1999): micro-porosity with uniform pore dimensions, ion-exchange properties, ability to possess acidity, high thermal stability, reversible hydration ability.

The pore size, generally between 3 and 10 Å in diameter, can allow certain molecules to pass through, while others are rejected. This gives zeolites a selective adsorption property (Pfenninger, 1999).

2.2.3. Properties and Applications of zeolites

2.2.3.1. Properties

Zeolite properties such as uniform pore sizes and exchangeable cation capacity have resulted in zeolites becoming attractive materials in a wide range of applications (Pfenninger, 1999). Zeolites are thermally stable over a wide range of temperatures. The decomposition temperature of low silica zeolites is about 700 °C while the high silica zeolites is about 1300 °C (Auerbach *et al.*, 2003). Cation concentration and exchange selectivity vary considerably with the Si/Al ratios and play an important role in adsorption, catalysis and ion-exchange applications. Lowry-Bronsted acid sites have been found in zeolites thus its application in catalysis (Auerbach *et al.*, 2003).

According to Byrappa and Yashimura (2001), the channel system in various zeolites is formed by different combinations of linked rings in the tetrahedra. The size of the cation that can be introduced into the zeolite structure is dependent on the size of the channels (Byrappa and Yoshimura, 2001). The zeolites are microporous solids with a broad range of general physio-chemical properties-see Table 2.2.

Table 2-2: Physio-chemical properties of zeolites and molecular sieves (Byrappa & Yoshimura, 2001)

Property	Range
Pore size	4-13 Å
Pore shape	Circular, elliptical
Dimensionality of pore system	1-D,2-D,3-D
Pore configuration	Channels, Cages
Surface Properties	Hydrophilic, hydrophobic (high silica)
Void Volume	Less than 50 %
Framework oxide composition	Si, Al, P, Ge, B, Be, Zn :minor Ti, Fe, Co, Cr, V, Mg, Mn: minor

Specific physical properties of some well-known zeolites have also been reported. They are listed in Table 2.3.

Table 2-3: Physical Properties of four well known zeolites (Chen *et al.*, 2002)

Type	Isotope	Pore Window (free diameter)	Si/Al ratio	Pores/Channels
LTA	A Zeolite	8-ring : 0.41 nm	1	3D Spherical 1.14 nm cavities
FAU	X Zeolite	12-ring : 0.74 nm	1-1.5 (X)	3D Spherical 1.18 nm cavities
	Y Zeolite		1.5-3 (Y)	
MOR	Mordenite	12-ring : 0.70 nm	5-20	2D Straight 0.70 nm channels
MFI	ZMS-5	10-ring : 0.60 nm	30 (ZMS-5)	3D Straight 0.60 nm channels with 0.90 nm intersection cavities
	Silicate-1			

2.2.3.2. Zeolite Applications

Zeolites have found widespread industrial applications, which are gaining new research interests mainly due to one or more of these three properties: adsorption, ion-exchange and catalytic properties. Major uses of zeolitic materials include petrochemical cracking, ion-exchange (water softening and purification), gas and solvent separations and removal, agriculture, mining, paper products, animal husbandry and construction, among others

(Pfenninger, 1999; Breck, 1974). The regular network of channels and cavities provide an excellent means of separating species (hence their other name “molecular sieves”).

2.2.3.2.1. Ion-exchange properties of zeolites

Zeolite structures can be considered as solid electrolytes. The charge-stabilising cations incorporated into the voids of the zeolites can be easily exchanged with other ions, as they do not form part of the zeolite network structure (Pfenninger, 1999). Figure 2.2 illustrates the location of sodium ions in the voids of zeolite A.

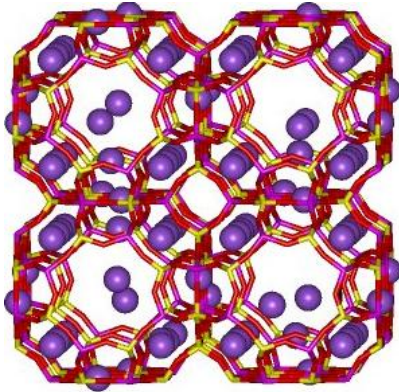


Figure 2-2: Illustration of Na ions inside the voids of zeolite A

The cations are loosely exchanged when the zeolites are in contact with solutions of saturating or indexing ions (Hedström, 2001; Kitsopoulos, 1999). The major use of zeolites as ion-exchange agents is for water-softening applications in the detergent industry and substitute use of phosphates (Endres *et al.*, 2001).

Querol *et al.* (2001) studied the utilisation of zeolites derived from fly ash in the wastewater and flue gas decontamination. Their study revealed that zeolites have a high affinity to NH_4^+ ions in the wastewater, but the efficiency of the NH_4^+ uptake was affected by the presence of other impurities and ions in the wastewater. Heavy metal uptake of zeolites from acid mine water was also tested in the study by Moreno *et al.* (2001). The results indicated that the trivalent cations in acid mine water have a higher affinity for the cation exchange position in the zeolites with respect to the divalent heavy metals. The order of the sorption potential was reported as follows (Querol *et al.*, 2001):



2.2.3.2.2. Adsorption capacity for zeolites

Zeolites are microporous materials with uniform pore dimensions. Certain molecules may enter the pores, while others are rejected, thereby leading to selective adsorption by the zeolites (Pfenninger, 1999). The adsorption applications include drying and purification of

natural gas and petrochemical streams (Pfenninger, 1999). Zeolites are also used in bulk separations of normal paraffins and in air separations to produce oxygen using Pressure Swing Adsorption (PSA) (Pfenninger, 1999).

2.2.3.2.3. Catalysis/catalytic applications of zeolites

The structure of zeolites enables them to act as selective catalysts in which the reactions take place inside the cavities of the zeolites (Auerbach *et al.*, 2003). The acidic properties of the zeolites promoted by ion-exchange are the main reasons for this application (Pfenninger, 1999). Bronsted acid sites in zeolites are able to transfer a proton from the solid to the adsorbed molecule, whereas Lewis sites transfer an electron pair from the adsorbed molecule to the solid surface (Nagy *et al.*, 1998). Generally both types of acid sites are simultaneously present in zeolites.

The first industrial application of zeolites in catalysis was in the petroleum industry for alkaline cracking due to their thermal and mechanical properties (Auerbach *et al.*, 2003). The most striking feature of the zeolite catalysts is shape selectivity. The zeolites' selectivity is as a result of; (1) the differences in diffusivity of reactants and products; (2) the difference in adsorption of reactants in zeolitic cavities of different sizes and shapes and (3) transition state selectivity (Auerbach *et al.*, 2003).

2.2.4. Classification of zeolites

Zeolites are often classified on the basis of their framework structures. The topology of zeolite frameworks is given by a code consisting of three capital letters assigned by the 'Structure Commission of the International Zeolite Association' (IZA). The codes are generally derived from the names of the type material, which is the species first used to establish the structure type. The IZA Structure Commission provides up-to-date classification by framework type, which is available on the website of the IZA (<http://www.iza-online.org>) or in the Atlas of Zeolite Framework Types (Baerlocher *et al.*, 2007). The table below gives examples of the three letter coding system (the entire alphabetic list can be found in "Atlas of zeolite framework types" by Baerlocher *et al.* (2007) and also on the IZA website as mentioned above.

Table 2-4: Examples of the three letter coding system used by International Zeolite Association

Code	Zeolite Name
FAU	Faujasite
GIS	Gismondine
GME	Gmelinite
BOG	Boggsite
MOR	Mordenite

Currently, three classification schemes are widely used for zeolite structures, i.e. classification based on the framework density (FD), secondary building units (SBU's) and pore structure. These classification schemes are well described in literature (Musyoka, 2009; Baerlocher *et al.*, 2007; Auerbach *et al.*, 2003).

2.2.5. Synthetic zeolites

Zeolites may be grouped as; natural and synthetic zeolites. Natural zeolites may originate from volcanic ash (Nagy *et al.*, 1998). The chemical reaction of glassy volcanic ash (source of aluminosilicate) with pervading pore water changes the glass fraction into various zeolite crystalline mineral phases over geological time scales under suitable conditions. Many pure zeolite types can also be prepared via hydrothermal synthetic routes. The hydrothermal synthesis of aluminosilicate zeolites corresponds to the conversion of a mixture of silicon and aluminium compounds, alkali metal cations, organic molecules (in some cases) and water, via an alkaline supersaturated solution into a microporous crystalline aluminosilicate.

Since the pioneering work of Barrer and Milton in the late 1940's, the zeolite synthesis conditions have changed and this has led to the synthesis of numerous types of zeolites. All the synthetic zeolites are distinguishable from each other and from natural zeolites on the basis of their composition, crystal structure, and sorption properties. Zeolite synthesis has been extensively reviewed in several books and literature on this subject is abundant (Cundy and Cox, 2005; Auerbach *et al.*, 2003; Byrappa and Yoshimura, 2001; Nagy *et al.*, 1998; Occelli and Robson, 1989; Szostak, 1989; Breck, 1974). Synthetic zeolites play a major role on an industrial scale, in terms of catalysis, molecular sieving and environmental protection (Breck, 1974). The wide variety of applications includes separation and recovery of normal paraffin hydrocarbons, catalysis of hydrocarbon reactions, drying of refrigerants, separation of air components, carrying catalysts in the curing of plastics and rubber, recovering radioactive ions from radioactive waste solutions and as an adsorbent for the removal of toxic elements in wastewater treatment operations (Musyoka, 2009; Pfenninger, 1999; Breck,

1974). Their application has led to the establishment of intensive research on targeted zeolite products for specific applications.

Zeolite A, X and Y were the first commercially significant zeolites to be synthesised in the 1950's. In 1954, zeolites were commercialised as a new class of industrial materials for separation and purification (Pfenninger, 1999). Pfenninger (1999) stated that their earliest application included the drying of refrigerants and natural gas. Zeolites have been synthesised using various starting materials and are reviewed in Pfenninger (1999). Nonetheless, the current study focuses on the synthesis of zeolites using coal fly ash as a starting material.

Since this work is concerned with synthesis of zeolite Na-P1 and zeolite A from fly ash, the following discussion will first concentrate on the general properties of synthetic zeolites and then narrow down to the zeolites of interest, i.e. Na-P1 and A.

2.2.6. Zeolite synthesis from fly ash

The compositional similarity of fly ash to some volcanic material has led to the synthesis of zeolites using fly ash as a raw material. The initial study on the synthesis of zeolites from coal fly ash was conducted by Holler and Wirshing in 1985. Since then, many patents and technical reports have proposed different hydrothermal activation methods to synthesise different types of zeolites (Querol *et al.*, 2002; Hollman *et al.*, 1999; Amrhein *et al.*, 1996; Shigemoto, 1996; Singer and Berggaut, 1995; Kolousek *et al.*, 1993; Shigemoto *et al.*, 1993; Mondragon *et al.*, 1990). However, all these methods were based on the dissolution of fly ash phases with alkaline solutions (mainly sodium hydroxide (NaOH) and potassium hydroxide (KOH)) followed by the hydrothermal crystallisation of the zeolite material (Querol *et al.*, 2002). These methods have been briefly described below. Through these methods, a number of zeolites were synthesised. Table 2.5 illustrates some zeolites that were successfully synthesised from fly ash. However, it should be noted that most of these zeolites were synthesised from Class C fly ashes-see Table 2.5.

Table 2-5: Zeolites and other neomorphic phases synthesised from fly ash (Querol *et al.*, 2002)

Zeolitic product	
Na-P1 zeolite	$\text{Na}_6\text{Al}_6\text{Si}_{10}\text{O}_{32}\cdot 12\text{H}_2\text{O}$
Phillipsite	$\text{K}_2\text{Al}_2\text{Si}_3\text{O}_{10}\cdot \text{H}_2\text{O}$
K-chabazite	$\text{K}_2\text{Al}_2\text{SiO}_6\cdot \text{H}_2\text{O}$
Zeolite F linde	$\text{KAISiO}_4\cdot 1.5\text{H}_2\text{O}$
Herschelite	$\text{Na}_{1.08}\text{Al}_2\text{Si}_{1.68}\text{O}_{7.44}\cdot 1.8\text{H}_2\text{O}$
Faujasite	$\text{Na}_2\text{Al}_2\text{Si}_{3.3}\text{O}_{8.8}\cdot 6.7\text{H}_2\text{O}$
Zeolite A	$\text{NaAlSi}_{1.1}\text{O}_{4.2}\cdot 2.25\text{H}_2\text{O}$
Zeolite X	$\text{NaAlSi}_{1.23}\text{O}_{4.46}\cdot 3.07\text{H}_2\text{O}$
Zeolite Y	$\text{NaAlSi}_{2.43}\text{O}_{6.86}\cdot 4.46\text{H}_2\text{O}$
Perlielite	$\text{K}_9\text{NaCaAl}_{12}\text{Si}_{24}\text{O}_{72}\cdot 15\text{H}_2\text{O}$
Analcime	$\text{NaAlSi}_2\text{O}_6\cdot \text{H}_2\text{O}$
Hydroxy-sodalite	$\text{Na}_{1.08}\text{Al}_2\text{Si}_{1.68}\text{O}_{7.44}\cdot 1.8\text{H}_2\text{O}$
Hydroxy-cancrinite	$\text{Na}_{14}\text{Al}_{12}\text{Si}_{13}\text{O}_{51}\cdot 6\text{H}_2\text{O}$
Kalsilite	KAISiO_4
Tobermorite	$\text{Ca}_5(\text{OH})_2\text{Si}_6\text{O}_{16}\cdot 4\text{H}_2\text{O}$

Major potential applications of zeolites synthesised from fly ash are based on their use as high capacity ion-exchangers in industrial wastewater treatment, which is also coupled with their excellence as sorbents, due to their large pore volumes (Querol *et al.*, 1996; Flanigien, 1991; Holler and Wirsching, 1985). These zeolites have also proven to be good candidates for use in soil decontamination (Singer and Berggaut, 1995) and have shown great potential for use in the removal of post-combustion gases, such as SO_x and NO_x (Querol *et al.*, 2002).

2.2.7. Methods of zeolite synthesis

The synthesis of zeolites from fly ash was first done using the conventional synthesis method. This method consisted of a single step involving direct hydrothermal conversion of a mixture of fly ash and alkaline solution (mainly NaOH and KOH) to zeolites. Even though this was the simplest method to produce zeolites, this approach was not adequate because of the low percentage conversion (around 50 %) of the fly ash to a zeolite phase, as pointed out by Berggaut and Singer in 1996. Due to this, more sophisticated procedures have been recently developed to improve this method. These developments include:

- The introduction of the alkaline fusion step prior to hydrothermal treatment. In this method, the fly ash is mixed with NaOH or Na₂CO₃ as fusion chemicals and the product of the mixture is fused at temperatures above 500°C. The fusion results in the conversion of fly ash into soluble sodium aluminate or sodium silicate, which is further dissolved in water. The dissolved mixture is then reacted under hydrothermal conditions. Introduction of this fusion step is characterised by high fly ash conversion and a high energy demand because of the fusion temperatures (Musyoka, 2009; Molina and Poole, 2004; Berggaut and Singer, 1996; Querol *et al.*, 1996).
- Hollman *et al.* (1999) developed a two stage procedure for the synthesis of pure zeolite products from high-Si solutions by light alkaline attack of fly ash. The procedure was estimated to produce >99 % pure zeolites products from the fly ash. This method involves the extraction of silicon from fly ash, followed by hydrothermal reaction of the extracted silica with the addition of an aluminate solution in varying ratios to synthesise high purity zeolitic materials.
- A dry or molten-salt conversion technique has also been developed. This method uses salt mixtures instead of alkaline solutions as the reaction medium (Querol *et al.*, 2002). Furthermore, this method appears to be environmentally friendly as no waste water is generated during synthesis. However, the high operating temperatures could limit its application.

All these different processes resulted in the synthesis of low-silica sodium and potassium zeolitic materials. Variation of the synthesis parameters such as solution/fly ash ratios, reaction temperature, time and pressure has resulted in the synthesis of different types of zeolites.

Recent studies have shown that the application of microwaves to the conventional synthesis method results in a drastic reduction of the synthesis time (Koukouzas *et al.*, 2007; Inada *et al.*, 2005; Querol *et al.*, 2002; Querol *et al.*, 1996). Microwaves are absorbed directly into water as solvent and enable rapid heating when compared to a conventional heating process. The electromagnetic waves cause dipole rotation of the water molecules resulting in the activation of the molecules by the breaking of its hydrogen bonds.

2.2.7.1. Synthesis methods used in this study

The synthesis methods used in this study were the alkaline fusion method and the two stage procedure developed by Hollman *et al.* (1999). These synthesis methods have been described above. The two stage method consisted of aging and hydrothermal treatment of the reaction mixture.

2.2.7.1.1. Aging stage

This step involves mixing of the starting materials using the desired molar ratio ($\text{Al}+\text{Si}+\text{Na}+\text{OH}+\text{H}_2\text{O}$) in order to make up the reaction mixture. The aging period is important in the synthesis of a desired zeolite. This step is normally conducted at room temperature and atmospheric pressure with stirring. During this step, dissolution or depolymerisation of the silicon and aluminium sources occurs. This dissolution process is facilitated and promoted by the alkaline conditions for zeolite synthesis (Byrappa and Yoshimura, 2001). Subsequently, the aluminosilicate species are liberated from the solid phase into the solution (Rees *et al.*, 2007). As a result, an XRD amorphous aluminosilicate gel is formed. This aluminosilicate gel may partially dissolve and rearrange to form nuclei, which are the building blocks of the final zeolite crystals (Taylor, 2007). This step is then followed by the hydrothermal treatment stage.

2.2.7.1.2. Hydrothermal treatment stage

After the aging step, the subsequent step is the hydrothermal treatment or the crystallisation step at elevated temperatures, which is usually conducted in a stirred or static reactor under autogenous pressure. In this step, the synthesis gel formed during aging is said to completely dissolve and rearrange to form a well-structured material. During this step, the nuclei formed during the aging step grow into observable crystals upon heating (Byrappa and Yoshimura, 2001).

2.2.8. Zeolite formation mechanism

The mechanism of zeolite formation has been a subject of research for decades. Although various mechanisms have been proposed based on a variety of experimental observations, the zeolite formation mechanism is still poorly understood. However, progress is being made towards fuller understanding, since zeolite nanoparticles have received much attention due to their various potential applications. A summary of proposed zeolite crystallisation mechanisms can be found in a review by Cundy and Cox (2005). The mechanisms of zeolite formation are complex due to the diversity of chemical reactions, equilibriums, and solubility variations that occur throughout the heterogeneous synthesis mixture during the crystallisation process (Davis and Raul, 1992).

Since this study is concerned with the synthesis of zeolites from fly ash, the zeolite formation mechanism described focuses on fly ash as the raw material. Zeolite synthesis occurs during a hydrothermal process with reagents being a silica source, an alumina source and a mineralising agent such as OH^- . Zeolite formation from fly ash has been studied by many researchers through spectroscopic evaluation and microscopic observations of the solid product (Inada *et al.*, 2005; Murayama *et al.*, 2002). It is said to occur in three steps, (see

Figure 2.3, adopted from (Elliot, 2006)) which are (Paniias *et al.*, 2007; Rees *et al.*, 2007; Inada *et al.*, 2005):

- The dissolution of the alumina (Al_2O_3) and silica (SiO_2) precursors from the fly ash (especially from the glass phase) in a strongly alkaline solution,
- The deposition of the initial aluminosilicate gel, and
- The crystallisation of zeolites.

Rees *et al.* (2007) explained the formation of the aluminosilicate gel as a result of an alkali-metal hydroxide attack on the fly ash particles. Furthermore, he stated that initially the surface of the solid particle (fly ash) contacts the activating solution and hydrolysis reactions begin to occur, depolymerising the particles and thus liberating the network species into the solution (Rees *et al.*, 2007). Criado *et al.* (2010) explained this phenomenon (gel formation) as a result of the inter-reactions of monomeric aluminates and silicates to form dimers, which in turn react with other monomers to form trimers and tetramers. These inter-reactions result in the precipitation of the aluminosilicate gel once the solution becomes saturated. As the synthesis proceeds, the aluminosilicate gel rearranges and forms more organised structures by equilibrium reactions such as polymerisation and de-polymerisation. This newly formed slurry is referred to as the secondary gel and acts as the zeolite precursor. In the secondary gel, the structures developed already contain sites in which nucleation and crystal growth can occur (Cundy and Cox, 2005).

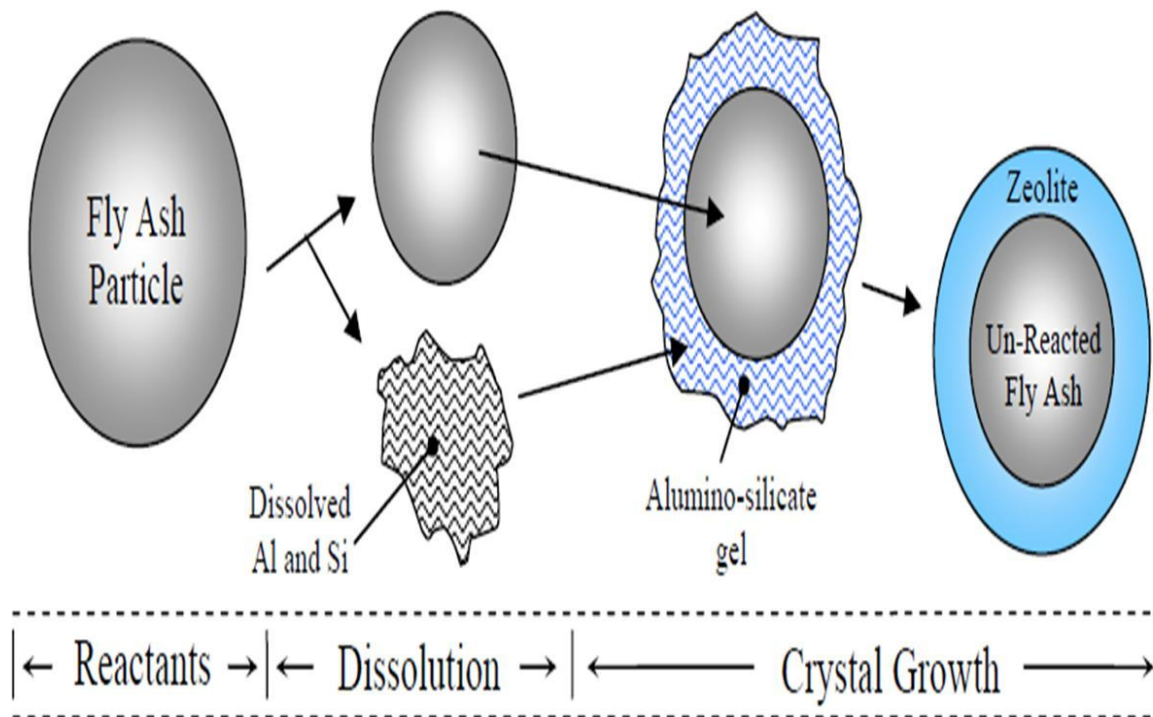


Figure 2-3: Illustration of reaction mechanism for the batch hydrothermal conversion of fly ash to zeolites (Elliot, 2006; Murayama *et al.*, 2002).

Over the years, this aluminosilicate gel has been difficult to characterise since it is amorphous to X-ray diffraction. Nonetheless, with increasing powerful techniques now developed, the understanding of its structure and composition is growing steadily and more precise (Criado *et al.*, 2007). Studies by Palomo *et al.* (2004) reported that this gel does however exhibit a short-range order, with a three dimensional structure in which silicon is found in a variety of environments. On this basis the gel could be regarded as a zeolite precursor (Palomo *et al.*, 2004).

As the synthesis proceeds at elevated temperatures (hydrothermal treatment), zeolite crystals are formed by the nucleation step and the zeolite nuclei then grow larger by assimilation of aluminosilicate material from the solution phase. Simultaneously, the amorphous gel phase dissolves to replenish the solution with aluminosilicate species.

As stated earlier in this section, the mechanism of zeolite synthesis is very complex. Thus, the mechanism illustrated by Figure 2.3 may not be valid for all zeolite synthesis methods. For example, during the synthesis of zeolite A from FA using the alkali fusion method two synthesis routes may be followed; (1) after the dissolution of fused ash in water the solids may be filtered and the clear solution obtained after the filtration process may be used for the crystallisation of zeolites, or (2) after the dissolution of fused ash in water, the slurry may be used for zeolite crystallisation. When the former (Route 1) is followed, new zeolite crystals are formed in the absence of FA particles, meaning that the proposed mechanism does not

apply. However, when Route 2 is followed the mechanism illustrated by Figure 2.3 may apply.

2.2.9. Factors influencing zeolite formation

There are a number of factors that influence the zeolitisation of FA. These factors include, but are not limited to, FA properties, temperature, time, cations, agitation and water concentration.

2.2.9.1. $\text{SiO}_2/\text{Al}_2\text{O}_3$ ratio of the starting material

In this study, FA was the main raw material used during zeolite synthesis. FA serves as a source of both silicon and aluminium, which build-up the zeolite framework. Zeolites are made up of building blocks consisting of SiO_4 and AlO_4 . This makes the $\text{SiO}_2/\text{Al}_2\text{O}_3$ ratio of the FA imperative in zeolite synthesis. This ratio plays an important role in determining the zeolite type that crystallises during zeolite synthesis. It places constraints on the framework composition of the zeolite produced (Szostak, 1989). Changing this ratio may result in a change of the final structure obtained (Szostak, 1989) and may also lead to the crystallisation of unwanted phases. Querol *et al.* (1995) reported that the formation of a particular zeolite species depends on the Si/Al ratio in the raw material. Furthermore, the study also mentioned that high silica content in FA will result in a high silica (SiO_2) zeolite product. Studies conducted by Cao and Shah (2007) showed that if a higher Si concentration exists, more Si-O-Si linkages are formed instead of Si-O-Al linkages, which alters the crystallisation mechanism. Higher temperature and higher $\text{SiO}_2/\text{Al}_2\text{O}_3$ favour the formation of zeolite P, whereas low $\text{SiO}_2/\text{Al}_2\text{O}_3$ and low temperatures favour faujasite and zeolite A formation (Elliot and Zhang, 2005; Lin and Hsi, 1995).

As mentioned earlier, the main components of FA are amorphous aluminosilicate glass, quartz, mullite, iron oxides (magnetite and hematite) and unburned carbon. From these FA components, SiO_2 and Al_2O_3 come from the amorphous glass phase, quartz and mullite. Studies have shown that the aluminosilicate glass phase is the largest and most unstable FA phase in a hydrothermal environment (Elliot and Zhang, 2005; Murayama *et al.*, 2002; Querol *et al.*, 2001; Querol *et al.*, 1996). As a result, it has the highest dissolution rates and it is the largest contributor to the zeolites produced. Querol *et al.* (2001) reported that the Al and Si bearing phases of FA are dissolved during different stages of the zeolitisation process, with the glass phase being the most reactive phase followed by quartz and then mullite (Querol *et al.*, 2001). This makes the $\text{SiO}_2/\text{Al}_2\text{O}_3$ ratio of the glass very important during zeolite synthesis. Additionally, studies have shown that fly ashes with similar bulk $\text{SiO}_2/\text{Al}_2\text{O}_3$ produced different zeolites under the same synthesis conditions and this was attributed to the differences in the glass matrix (Querol *et al.*, 2001; Querol *et al.*, 1996). Therefore, the

$\text{SiO}_2/\text{Al}_2\text{O}_3$ ratios of the glass matrix and not that of the bulk fly ash, have a crucial influence on the type of zeolite produced.

The effects of changing $\text{SiO}_2/\text{Al}_2\text{O}_3$ ratio on the physical properties of a zeolite can be summarised as (Szostak, 1989):

- i. Increasing silica/alumina ratio
 - a. Increases acid resistance
 - b. Increases thermal stability
 - c. Increases hydrophobicity
 - d. Decreases affinity for polar adsorbates
 - e. Decreases cation content
- ii. Decreasing silica/alumina in a zeolite
 - a. Increases hydrophilicity
 - b. Increases cation exchange properties

2.2.9.2. Type of the charge balancing cations

The inorganic cations such as Na^+ , K^+ , Ca^{2+} and Li^+ are necessary as charge balancing cations in the zeolite synthesis process. These cations stabilise the zeolite framework structure during its formation by creating charge neutrality, since the substitution of the tetravalent silicon atoms by the trivalent aluminium atoms results in ionic sites in the vicinity of the aluminium atoms (Musyoka, 2009; Molina and Poole, 2004). The cations are situated in the pores and can be exchanged out of the crystalline solid upon completion of the synthesis, as they are not framework species. Many studies have shown that the use of NaOH in alkaline activation of the fly ash is far more effective than KOH (Querol *et al.*, 1996; Querol *et al.*, 1995). Murayama *et al.* (2002) reported that Na^+ ions favour crystallisation, resulting in shorter reaction times and a high crystallinity product, while K^+ ions and other cations depress crystallisation. The presence of excessive inorganic cations may disrupt the formation of the required phase. For example, if FA is being activated by NaOH solutions, Ca^{2+} and Mg^{2+} ions, if present, act as competing ions. This leads to interference in the crystallisation process.

2.2.9.3. NaOH concentration

Sodium hydroxide acts as a mineralising agent, which depolymerises the Si feedstock and forces the reactants into solution (Pfenninger, 1999). The concentration of NaOH has been

reported to have different effects on the zeolites synthesis, depending on the composition of the fly ash used in the synthesis (Querol *et al.*, 1996). Numerous studies conducted have reported that an increase in NaOH/FA ratio results in an increase in crystallinity and purity of the zeolite products formed (Musyoka, 2009; Molina and Poole, 2004; Querol *et al.*, 1996). Wang *et al.* (2008) investigated the effect of NaOH concentration on the synthesis of a pure phase of zeolite A. From their study, the authors reported that the NaOH concentration determines the molar ratio of the prepared initial gel. Moreover, the outcome of their study also showed that the concentration of the alkaline solution also affects the structural formation, morphology and particle size distribution of the zeolites. In addition, Wang *et al.* (2008) stated that crystal sizes and crystallisation time of zeolites A reduced with an increase in NaOH concentration.

2.2.9.4. Effect of synthesis time

Synthesis time is an important parameter during the synthesis of zeolites from FA, owing to the difficulties associated with the dissolution of quartz and mullite which always appear as secondary products even at longer crystallisation times (Molina and Poole, 2004). Time is a crucial parameter since it significantly affects the crystallisation of zeolites. For example, Nagy *et al.* (1998) stated that when preparing a pure phase zeolite, it is important to understand that a desired zeolite species can be a metastable product that can undergo further dissolution which can lead to more stable species. This was explained by the Ostwald rule of successive transformation which states that “the first phase to crystallise from a solution will be a hydrothermally least stable phase but with time, this phase is followed by more stable and denser phases” (Barrer, 2007). Molina and Poole (2004) reported that the amount of time the reacting species spend in the reactor determines the type of zeolite product formed. In addition, prolonged aging of the hydrogel at ambient temperatures prior to crystallisation may result in the formation of a product which contains a larger number of small crystals.

2.2.9.5. Effect of temperature

Temperature is also one of the imperative factors that influence zeolite synthesis. Temperature has been observed to influence crystallisation kinetics. According to Elliot and Zhang (2005) an increase in temperature results in an increase in the nucleation and the growth rate of the zeolite crystals. During zeolite synthesis from FA, an increase in temperature results in an increase in mullite dissolution (Elliot and Zhang, 2005; Querol *et al.*, 1996). Furthermore, this increase in temperature leads to an increased silicon (Si) dissolution compared to aluminium (Al) dissolution from FA (Elliot and Zhang, 2005; Catalfamo *et al.*, 1993). This result in an increase in the Si/Al ratio in solution, which influences the gel composition and subsequently the zeolite product produced. Temperature

also affects the nature of the zeolite phase formed. For example, higher temperatures favour the crystallisation of more dense phases. In addition, Elliot and Zhang (2005) stated that higher temperatures favour zeolite P formation, while lower temperatures favour faujasite and zeolite A formation.

2.2.9.6. Water concentration

Zeolite synthesis is a solution-mediated process. Thus, water is used as a solvent during the synthesis process. In addition to its solvating and hydrolysing ability, water acts as a template by interacting with the cations. According to Feijen *et al.* (1994), water molecules also enhance crystal growth by filling the void spaces, which stabilises the zeolite structure. Previous studies have shown that increasing the liquid to solid ratio during the hydrothermal synthesis of zeolites from FA increases the dissolution of mullite, quartz and the glass matrix (Querol *et al.*, 2001; Querol *et al.*, 1995). As a consequence, the yield of zeolites also increases. For most synthesis procedures, de-mineralised water is used to avoid the complicating effects of competing ions such as calcium (Casci, 2005), which are commonly present in tap waters.

However, in a study by Belviso *et al.* (2010), distilled water and seawater were used during the hydrothermal synthesis process in separate experiments. The findings of these studies indicated that zeolites can be synthesised from different kinds of coal FA under low crystallisation temperatures using both distilled water and seawater. In addition, the study showed that X-type zeolite, ZK-5-type zeolite and hydroxysodalite can be synthesised at lower temperatures when using seawater, whereas A-type zeolite could be synthesised only when using distilled water (Belviso *et al.*, 2010).

To quantify the amount of water in the synthesis, most researchers normally report it as a relative proportion to other reagents involved in the synthesis process. A good example is work by Elliot (2006) where he reported the ratio of water to aluminium (H_2O/Al) in the quantification of the water used during synthesis, although silicate to water (SiO_2/H_2O) or water to sodium hydroxide (H_2O/Na_2O) ratios can also be used.

2.2.9.7. Effect of agitation on zeolites synthesis

Zeolite synthesis studies have generally been carried out at laboratory scale under static conditions. Synthesis under static conditions is not always desirable since it can result in the uneven settling of the synthesis gel and cause the liquid phase to separate from the solid phase of the reaction mixture due to gravitational forces. For a large or industrial scale production of zeolites, the synthesis process must imperatively be conducted in an agitated reactor. This is because the reaction mixture produces a viscous gel and if mixing is inadequate or absent, an inhomogeneous reaction mixture may result, with pockets of gel

having different compositions and consistency. According to Casci (2005) each “pocket” behaves like a mini reactor and generates phases corresponding to the composition in that region. Moreover, Marrot *et al.* (2001) reported that the synthesis of zeolites in medium that is not agitated requires longer periods of time for growth of zeolites, and therefore is economically inappropriate. Casci (2005) reported that agitation assists in: the initial gel formation, reagent dissolution, maintaining a homogeneous gel, maintaining a uniform temperature across the reactor, assisting with gel structure break-up, transferring nutrients to growing crystals and keeping the zeolite crystals in suspension after the completion of the reaction.

Nonetheless, agitation introduces a significant parameter i.e. shearing, which must be taken into account during zeolite synthesis. Marrot *et al.* (2001) conducted a study on the influence of shearing during zeolite synthesis. In the study, it was observed that shearing seems to have a detrimental effect on the stability and purity of the zeolitic product being formed. This effect was observed during the crystallisation (hydrothermal treatment) step of the synthesis process. Weitkamp and Puppe (1999) reported that the effect of this physical parameter (agitation) can lead to a change in the attributes of the synthesis gel and also affect the outcome of the zeolite synthesis process.

2.2.10. Characterisation of zeolites

Characterisation techniques provide information about the structure and morphology of the zeolite, its chemical composition as well as its catalytic and adsorptive abilities. Several techniques are used to characterise the zeolite phases obtained. The most commonly used techniques are; X-ray powder diffraction, the Rietveld technique of structure refinement, Neutron scattering, nuclear magnetic resonance (NMR), Infra-red (IR), Thermal, Scanning electron microscopy (SEM), Laser Raman, measurement of sorptive capacity, particle size and pore size distribution, etc. This section gives a brief description of some of the methods that were applied in this study.

2.2.10.1. Mineralogy by X-Ray powder diffraction

X-ray powder diffraction (XRD) is the most widely used technique for determining the zeolite structure as well as its purity. This technique is used for phase identification of crystalline material and it is especially suitable for the characterisation of polycrystalline phases. X-ray diffraction produces the diffraction pattern by bombarding a single crystal with X-rays to determine the crystal structure. When x-rays interact with a crystalline phase, a diffraction pattern is recorded and then analysed to reveal the nature of the crystal. X-rays are diffracted by each mineral differently, depending on what atoms make-up the crystal lattice and how they are arranged. The spacing in the crystal lattice can be determined using Bragg's law;

Where;

- d = Distance between atomic layers in a crystal (interplanar spacing)
- λ = Wavelength of the incident x-ray beam
- θ = Diffraction angle
- n = An integer

This law relates the wavelength of electromagnetic radiation to the diffraction angle and the lattice spacing in a crystalline sample. The Bragg's formula provides a unique fingerprint identifying the mineral phase and giving lattice parameters of the structure. A typical diffraction spectrum consists of a plot of reflected intensities vs. the detector angle. The conversion of the diffraction peaks to d-spacing allows identification of the mineral phase because each mineral has a set of unique d-spacings. Thus, the X-ray diffraction method can be used for the identification of minerals and for the analysis of mixtures of minerals. The pattern is used for the identification of known structures by comparing with standard patterns listed by the Joint Committee on Powder Diffraction Standards (JCPDS). The JCPDS is the powder diffraction file database for inorganic compounds used for phase identification, which is done by searching and matching obtained spectra with the available standards.

2.2.10.2. Scanning electron microscopy

Scanning electron microscopy (SEM) is one of the best and most widely used techniques for the physical characterisation (i.e. the size and morphology of the crystal material) of fly ash and zeolites. This type of electron microscopy is capable of producing high-resolution images of a sample surface. SEM, using a highly energised focused electron beam to scan the surface of a sample, generates a variety of signals. These are collected, amplified, and displayed on a cathode ray tube. The electron beam and the cathode ray tube scan synchronously so that an image of the surface of the specimen is formed (Kutchko and Kim, 2006).

2.2.10.3. Chemical analysis by X-ray Fluorescence

X-ray fluorescence (XRF) is a method used for the qualitative and quantitative analysis of the chemical composition of a specimen. The analysis of major and trace elements in a material by XRF is made possible by the behaviour of atoms when they interact with radiation (Mantler and Schreiner, 2000). When a sample is illuminated by an intense X-Ray beam, known as the incident beam, some of the energy is scattered and some is absorbed in a characteristic manner within the sample. The sample becomes energised and in turn emits X-rays along a spectrum of wavelengths. Each atom has specific energy levels, so the

emitted radiation is characteristic of that atom. By measuring the energy of the radiation emitted, it is possible to identify which elements are present in the sample. In addition, by measuring the intensity of the emitted energy, it is possible to quantify how much of a particular element is present in a sample.

2.2.10.4. Structural configuration by infra-red spectroscopy

Vibrational spectroscopy obtainable by infrared spectroscopy (IR) provides information on a molecular level. This technique can be used to furnish direct information about the nature of surfaces and adsorbed surface species. The mid-infrared region of the spectrum is useful in the deduction of the structural information, since it contains fundamental vibrations of the framework TO_4 tetrahedra. Each zeolite exhibits typical characteristic infrared spectra and the spectra can be grouped into two classes, namely: (1) internal vibrations of the framework TO_4 , which are insensitive to structural variations; and (2) vibrations related to the external linkage of the TO_4 units in the structure (Breck, 1974). Some common features such as asymmetric and symmetric stretch, double ring vibrations, T–O bending modes and pore opening modes can be observed.

The stretching modes involving mainly tetrahedral atoms are assigned to the spectral lines in the region of $650 - 820 \text{ cm}^{-1}$. These stretching modes are sensitive to Si–Al composition in the framework and may shift to a lower frequency with increasing number of tetrahedral aluminium atoms (Fernandez-Jimenez and Palomo, 2005). The frequencies sensitive to the linkages between tetrahedral and the topology and the modes of arrangement of the secondary units of the structure in the zeolite occur in the region of $500 - 600$ and $3000 - 420 \text{ cm}^{-1}$.

A band in the $500 - 650 \text{ cm}^{-1}$ is assigned to the presence of double rings in the structural framework structure and is observed in all zeolites that contain the 4- and double 6-rings such as Zeolite X, Y, A and L. Frequencies between $300 - 420 \text{ cm}^{-1}$ are associated with external linkages and also related to pore opening or motion of the tetrahedral rings which form the pore openings in zeolites (Breck, 1974).

2.2.11. Gaps in the literature with respect to zeolites synthesis

An extensive literature review has revealed that FA is a suitable feedstock for zeolite synthesis. Although there are some reports on zeolite synthesis from FA in countries like Spain, Japan, Korea, UK and China (Querol *et al.*, 2007; Inada *et al.*, 2005; Querol *et al.*, 2002; Querol *et al.*, 2001; Rayalu *et al.*, 2000; Kim *et al.*, 1997; Querol *et al.*, 1996; Querol *et al.*, 1995), there is limited research on the use of different South African fly ash as a feedstock for zeolite synthesis. The class of FA differs from country to country and most of the previous studies were conducted using class C type of FA. Given that South African FA

belongs to class F and its composition varies from source to source within the country, zeolite synthesis conditions from previous studies may not apply to South African fly ashes.

Recent studies in South Africa have shown that a pure phase of zeolite Na-P1 and zeolite A can be produced from South African FA. However, these studies were conducted at laboratory scale. As aforementioned, the production of zeolites from FA on an industrial/pilot scale would contribute to the mitigation of the environmental problems caused by the disposal of FA. However, there has never been a pilot or industrial study on the synthesis of zeolites from FA using South African fly ashes as a feedstock. There are also very limited studies on the synthesis of zeolites from FA on a pilot or industrial scale worldwide. Therefore, a detailed investigation on the use of South African fly ashes is required, especially with respect to operating parameters for large scale operations as well as FA compositional variability. These factors would affect zeolite synthesis significantly. It is also clear that the optimum conditions obtained from laboratory scale synthesis cannot be applied for a large scale production. Therefore, it is important to attempt to develop synthesis conditions that can be applied (for a specific zeolite) for a large scale production of zeolites from South African coal FA.

2.3. Chapter summary

Knowledge of the physical characteristics, chemical composition and properties of fly ash is essential to understanding any possible environmental impacts. The properties and morphological features of the fly ash formed during the combustion of coal is influence by the chemical and morphological characteristics of the minerals in coal, coal source, type of coal burned, the boiler and its operating conditions and the process undergone by coal before combustion. Due to some compositional similarity of fly ash to some volcanic material, fly ash has been used as a feedstock for zeolite synthesis.

The most relevant information concerning fly ash and zeolite synthesis from fly ash has been presented in this chapter. The analytical techniques used to identify and quantify the minerals in fly ash and zeolites and their morphological features are also highlighted in this chapter. X-ray powder diffraction is probably the most widely used technique for determining the zeolite structure as well as its purity.

The next chapter describes the experimental materials, setup, sample preparation and synthesis procedures, together with a description of the characterisation techniques used in this study.

3. EXPERIMENTAL AND ANALYTICAL TECHNIQUES

This chapter describes the chemicals, experimental and analytical methods used in this study. It is divided into three sections. Section A focuses on the methods used to investigate and assess the scale-up conditions for the synthesis of zeolite Na-P1 and Section B is concerned with the methods used for the synthesis of zeolite A and Section C describes the analytical techniques used in this study.

3.1. SECTION A: Synthesis of Zeolite Na-P1

This investigation began by synthesising a pure phase of zeolite Na-P1. The effects of impeller design, agitation and reaction time were investigated, together with the use of different water sources as a substitute for ultrapure water. The main focus of this investigation was to optimise the aging step with the view of synthesising a pure zeolite Na-P1 phase and establishing base conditions for the scale-up process.

3.1.1. Materials

Pulverised fly ash used in this study was collected from the Arnot Eskom power station situated in Mpumalanga in South Africa. Two batches were collected from this power station and are indicated as batch 1 and batch 2. This fly ash was chosen because it was shown to produce a pure phase of zeolite Na-P1 under the conditions reported by Musyoka (2009). The chemical and mineralogical compositions of the two samples of fly ash were analysed using XRF and XRD analytical techniques respectively and are given in the next chapter. A list of chemical reagents used in the current study is given in Table 3.1.

Table 3-1: List of chemicals used in this study

Chemicals	Supplier	Purity
Sodium Hydroxide pellets	Merck Chemicals	Min 98.00 %
Hydrofluoric acid	B & M Scientific cc.	40.00 %
Nitric acid	B & M Scientific cc.	55.00 %
Hydrochloric acid	Kimix	32.00 %
Boric acid	Merck Chemicals	99.00 %
Acetic acid	Kimix	99.80 %
Perchloric acid	Merck Chemicals	60.00 %
Sodium Aluminate Powder	Sigma-Aldrich	-

3.1.2. Sample storage

The fly ash samples were stored in tightly sealed plastic containers to exclude air. These containers were then kept in a dark cool room away from direct sunlight to avoid temperature fluctuations. This was because upon exposure to the atmosphere many of the metastable assemblies of minerals phases in fly ash which are initially formed at high temperatures during coal combustion will alter to form thermodynamically stable minerals which might alter the overall initial composition of the fly ash (Musyoka, 2009; Sonqishe *et al.*, 2009; Catalfamo *et al.*, 1993). The acid mine drainage used in this study was stored in tightly sealed 5 L plastic containers under refrigeration at 4 °C. This was done in order to preserve the cation and anion species in the water.

3.1.3. Synthesis equipment

The experimental setup for the aging step is shown in Figure 3.1. It consisted of a 150 ml (working volume) jacketed stirred glass reactor. The reactor was connected to a SMC water bath (Model: TTM-J4) which maintained the temperature of the reactor contents. The reactor was equipped with an IKA mechanical overhead stirrer (Model: RW20 DZM.N). Three types of impellers were used in this investigation i.e. the 4 flat-blade, anchor and screw impellers as shown in Figure 3.2. The blade thickness of all three impellers were 0.5 mm. 23 ml Parr bombs with Teflon lining (Figure 3.3) were used for the hydrothermal treatment stage. The hydrothermal treatment process was conducted by placing the Parr bombs in a Term-O-Mat hot air oven where the temperature was controlled.

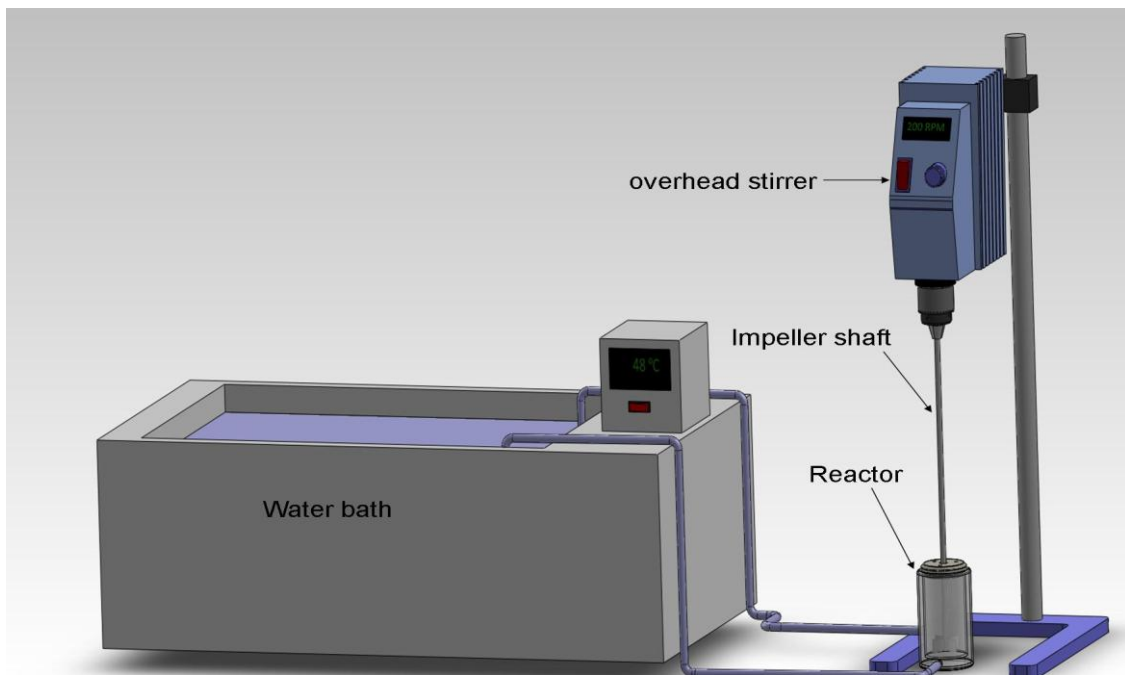


Figure 3-1: Experimental set-up of the aging process

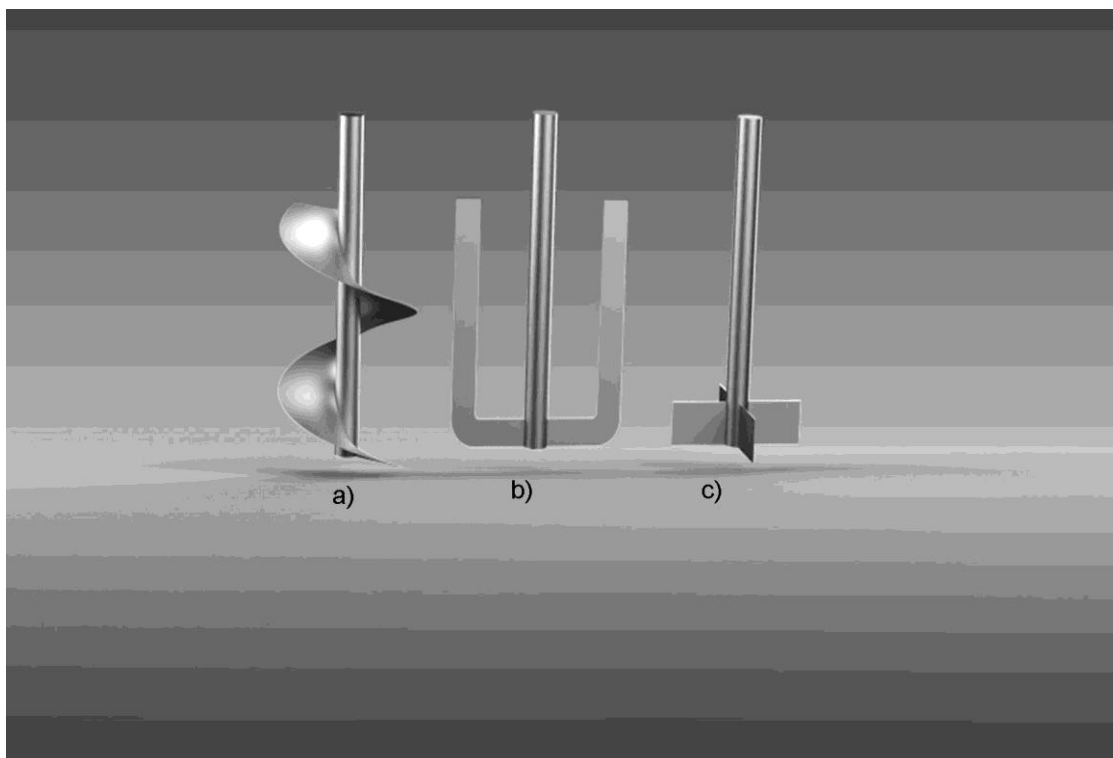


Figure 3-2: Three types of impellers used in this study i.e. A). Archimedes Screw B). Anchor C). 4 flat-blade impeller

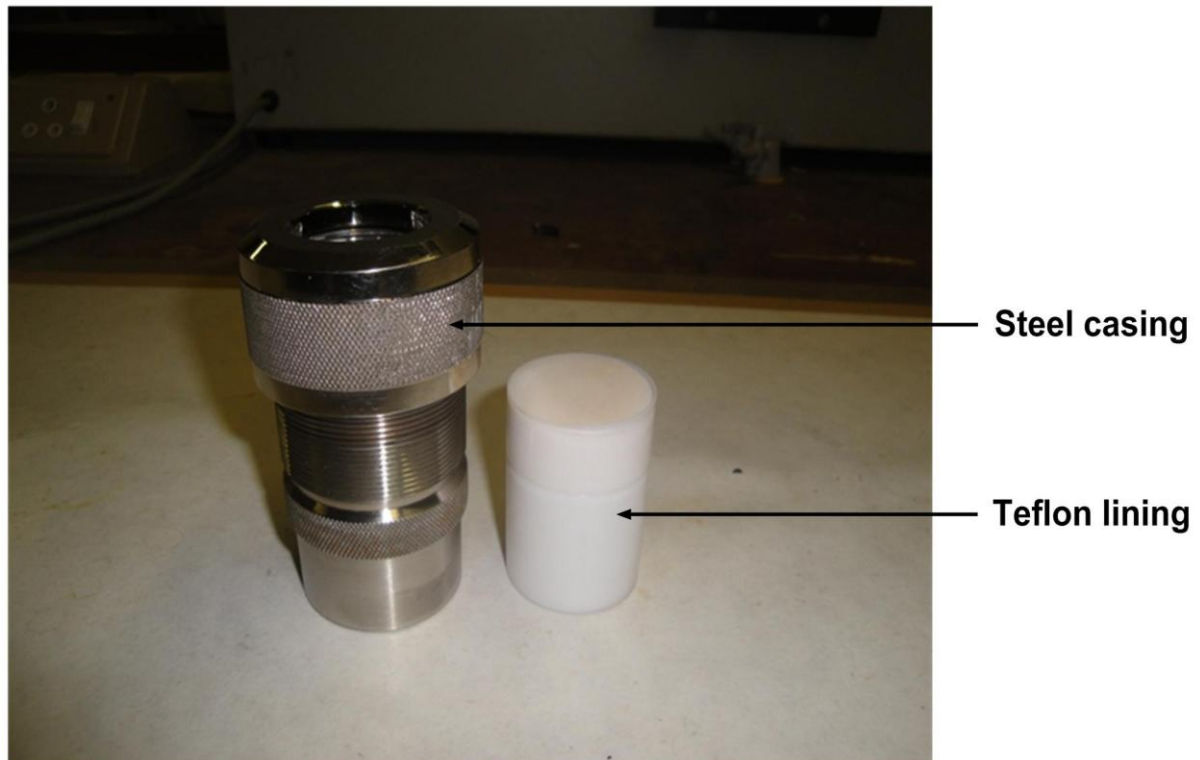


Figure 3-3: Parr bomb and Teflon lining used as small scale reactors in the hydrothermal treatment process

3.1.4. Synthesis procedure

The synthesis procedure involved a two-step process which was adopted from Hollman *et al.* (1999). This two-step process consisted of (1) the aging step where the fly ash was mixed with the alkaline solution for dissolution of the fly ash feedstock and the (2) hydrothermal treatment step where the synthesis gel from the aging step was subjected to high temperatures for the crystallisation of zeolites to occur.

3.1.4.1. Aging step

The experimental setup for this step has been illustrated in Figure 3.1. This step was conducted by mixing 20 g fly ash with 100 ml of a 5 M sodium hydroxide (NaOH) solution on a 1:1 mass ratio (fly ash to sodium hydroxide (NaOH) pellets). The 5 M NaOH solution was prepared by dissolving 20 g of Sodium hydroxide pellets in 100 ml of ultrapure water in a beaker. The resulting NaOH solution was then mixed with fly ash in a 150 ml glass reactor. Agitation was induced by using either a magnetic stirrer, Archimedes screw, 4 flat-blade or an anchor impeller at various stirring speeds. The aging temperature was kept at 47 °C for various periods of time (12 to 48 hours) depending on the parameter that was being investigated. Previous studies have shown that these conditions were optimum for dissolution of silicon and aluminium from fly ash into the liquid phase (Musyoka, 2009; Ríos *et al.*, 2009).

3.1.4.2. Hydrothermal treatment

After the aging period, the pre-synthesis gel obtained was transferred into a 250 ml plastic bottle and 150 ml ultrapure water was added while stirring as recommended by Musyoka (2009). The resulting homogeneous mixture was then transferred in aliquots of 10 ml into 23 ml Parr bombs. Crystallisation of the feedstock was achieved by placing the mixture in sealed Parr bombs in a hot air oven for different periods of time ranging from 12 to 48 hours at a temperature of 140 °C.

3.1.4.3. Recovery of zeolites

After the hydrothermal treatment stage, the Parr bombs were removed from the oven and allowed to cool down to room temperature. The zeolitic products were recovered by filtration followed by thorough washing with de-ionised water until the pH of 9-10 of the filtrate was achieved. The zeolites products were then dried in an oven overnight at 90 °C and ground into a powder for further analysis.

3.1.5. Experiments

All the experiments reported below were conducted following the procedure outlined above; however slight changes were made, depending on the investigated parameter or the experiment. However, the concentration (5 M) and the volume (100 ml) of the NaOH solution, mass of fly ash (20 g) and the 1:1 mass ratio (FA to NaOH pellets) stated in section 3.1.4.1 above were used for all the experiments reported below. The hydrothermal treatment step was kept static, meaning there was no agitation in this step, but only during the aging step.

3.1.5.1. Synthesis of a pure phase of zeolite Na-P1

This set of experiments was carried out based on the optimum synthesis conditions reported by Musyoka (2009). According to the author, the optimum conditions to obtain a pure phase of zeolite Na-P1 from South African fly ash were: aging step at 47 °C for 48 hours (stirred at 800 rpm using a magnetic stirrer) followed by the hydrothermal treatment step at 140 °C, maintained for 48 hours. In these experiments, batch 1 of Arnot coal fly ash was used as a source of silica and alumina. The main aim of these experiments was to demonstrate the reproducibility of the data that was reported by Musyoka (2009) with the view of creating base conditions for the current study. Raw materials and synthesis products were characterised using XRD and FTIR techniques described below.

3.1.5.2. Effects of impeller design and agitation during the aging step

These experiments were also conducted based on the conditions recommended by Musyoka (2009). Batch 1 of Arnot coal fly ash was used in these experiments. However, in these

experiments three types of impellers (i.e. 4-flat blade, Anchor and Archimedes Screw impellers (Figure 3.2) were used to induce agitation during the aging step at three agitation speeds i.e. 150, 200 and 300 rpm (see experimental conditions in Table 3.2). The choice of the impellers and the agitation speeds was based on previous studies reported in literature (Casci, 2005; Bebon *et al.*, 2002; Marrot *et al.*, 2001). The zeolitic products obtained from these experiments were characterised using XRD, FTIR and SEM analytical techniques. These experiments were conducted in duplicate in order to minimise the error in the results.

Table 3-2: Experimental conditions for the investigation of effect of the impeller design and agitation during the aging step

Impeller Type	Agitation speed (rpm)	Aging Temperature (°C)	Aging time (hours)	HT* Time (hours)	HT* Temperature (°C)
4-Blade	150	47	48	48	140
	200	47	48	48	140
	300	47	48	48	140
Screw	150	47	48	48	140
	200	47	48	48	140
	300	47	48	48	140
Anchor	150	47	48	48	140
	200	47	48	48	140
	300	47	48	48	140

*HT-Hydrothermal Treatment

3.1.5.3. Effect of fly ash composition as a feedstock

In these experiments, batch 1 and batch 2 of Arnot coal fly ash were used as the starting material in order to determine the effect of variation in FA feedstock. The experimental conditions for these experiments were as follows; aging was conducted at 47 °C for 48 hours (stirred at 200 rpm using a 4 flat-blade impeller) followed by the hydrothermal treatment step at 140 °C maintained for 48 hours. The zeolitic products obtained from these experiments were characterised using XRD, FTIR and SEM analytical techniques. These experiments were conducted in duplicate in order to minimise the error in the results.

3.1.5.4. Effects of water chemistry on the quality of zeolite Na-P1

Batch 2 of the Arnot coal fly ash with various solvents, namely distilled water, municipality tap water and Acid Mine Drainage (AMD) collected from a uranium mine located in Gauteng, South Africa were used as the starting materials for the zeolite synthesis in this set of

experiments in order to determine the effect of impurities in the solvents. The elemental composition of the various solvents was determined using the ICP-AES/MS technique and the results are given in Table 5.3.

In this set of experiments, the aging step conditions were kept at 47 °C for 48 hours. However, the alkaline solution (NaOH) used in this investigations was prepared by dissolving 20 g of NaOH pellets in 100 ml of either ultrapure water, distilled water, tap water or AMD. The hydrothermal treatment step was performed at 140 °C for 48 hours. Zeolitic products were characterised using XRD and SEM techniques. FTIR was not used for this set of experiments due to experimental constraints.

3.1.5.5. Effects of hydrothermal reaction time

In these experiments, batch 2 of Arnot coal fly ash was used as the starting material. These experiments were carried out by keeping the aging temperature constant at 47 °C and varying the aging time i.e. 12, 24, 36 and 48 hours. A 4-flat blade impeller was used to induce agitation at 200 rpm. After each aging period, samples were taken, filtered and analysed for major cations in the synthesis solution using ICP-AES/MS. During the hydrothermal treatment step, 12 hourly samples were taken for each aging time in order to monitor the evolution of the zeolite crystals. This means that samples were taken after 12, 24, 36 and 48 hours of the hydrothermal treatment. The hydrothermal treatment temperature was kept constant at 140 °C. The experimental conditions for this set of experiments are depicted in Table 3.3. These experiments were carried out in order to establish optimum conditions for the synthesis of a pure phase of zeolite Na-P1 from low amorphous phase fly ash and to optimise the zeolite synthesis period, i.e. to get as much zeolites (zeolite Na-P1) as possible in the shortest reaction time. Zeolitic products were characterised using XRD and SEM techniques.

Table 3-3: Experimental conditions for the investigation of effect of aging time using a 4 flat-blade impeller at 200 rpm.

Impeller Type	Agitation speed (rpm)	Aging Temperature (°C)	Aging time (hours)	HT* Time (hours)	HT* Temperature (°C)
4-Blade	200	47	12	12	140
	200	47	12	24	140
	200	47	12	36	140
	200	47	12	48	140
	200	47	24	12	140
	200	47	24	24	140
	200	47	24	36	140
	200	47	24	48	140
	200	47	36	12	140
	200	47	36	24	140
	200	47	36	36	140
	200	47	36	48	140
	200	47	48	12	140
	200	47	48	24	140
	200	47	48	36	140
	200	47	48	48	140

*HT-Hydrothermal Treatment

3.2. SECTION B: Synthesis of zeolite A

This section investigates the synthesis of zeolite A from South African coal fly ashes with the view of establishing suitable scale-up conditions. This investigation began by synthesising a pure phase of zeolite A and then investigating the use of mine water as a replacement for ultrapure water together with the use of five different sources of South African coal fly ash to synthesise zeolite A.

3.2.1. Materials

South African coal fly ash samples collected from five different ESKOM power stations in Mpumalanga were used in this investigation, i.e. Arnot, Matla, Hendrina, Lethabo and Tutuka power stations. The chemical and mineralogical compositions of the various fly ashes were analysed using XRF and XRD analytical techniques respectively and are given in the next

chapter. The chemical reagents used in this investigation are listed in Table 3.1 in section 3.1.1. These fly ashes were stored following the procedure outlined in section 3.1.2 of this chapter.

3.2.2. Synthesis Procedure and conditions

The procedure used for the synthesis of zeolite A in this study involved the introduction of an alkali fusion step prior to the hydrothermal treatment. This method was adopted because it plays an important role in enhancing the dissolution of the FA precursor and impacts upon the hydrothermal conditions for the synthesis of zeolites. This synthesis process consisted of three steps; fusion, dissolution of the fused product in water followed by the hydrothermal crystallisation. The synthesis conditions for zeolite A used in the investigation using different feedstock FA and solvents were optimum conditions reported by Musyoka *et al.* (2011) for Arnot FA using ultrapure water.

3.2.2.1. Fusion

A homogenous mixture of fly ash and sodium hydroxide was prepared by grinding and mixing the fly ash and sodium hydroxide powder in a ratio of 1: 1.2 (fly ash:NaOH powder). This ratio was reported to be optimum for the synthesis of zeolites with a maximum value of cation exchange capacity (Musyoka *et al.*, 2011; Ríos *et al.*, 2009; Rayalu *et al.*, 2000). The resultant mixture was fused at 550 °C for 1.5 hours in an electric furnace. Thereafter, the alkali fused fly ash was allowed cool down, ground and thoroughly mixed.

3.2.2.2. Extraction step

In this step, the water soluble phases in the fused fly ash were dissolved in water in order to prepare a homogeneous gel. The alkali fused FA was thus dissolved in ultrapure water in a H₂O to fused fly ash ratio of 5 ml/g and this mixture was stirred at 1400 rpm for two hours at ambient temperature and atmospheric pressure. The FA slurry was thereafter filtered to remove the remaining solids. The volume of the clear solution obtained after filtration varied (between 700 ml and 800 ml) depending of the effectiveness of the filtration process. The resulting clear solution was mixed with the aluminate solution in a 2.5:1 volume ratio (clear solution:sodium aluminate) and was stirred for ten minutes. This means that for every 50 ml of the clear solution, 20 ml of the aluminate solution was added. The purpose of the addition of the aluminate solution was to control the molar ratio of the clear solution for the subsequent synthesis of a single phase zeolite A product.

3.2.2.3. Preparation and addition of the aluminate solution

The aluminate solution was prepared by mixing sodium aluminate solution with sodium hydroxide solution and stirred using a magnetic stirrer for 30 minutes. Sodium aluminate

solution was prepared by mixing sodium aluminate powder with ultrapure water such that for every 2.4 g of NaAlO_2 , 25 ml of water was added, resulting in a 1.2 M solution. Sodium hydroxide solution was prepared by mixing sodium hydroxide pellets with water such that for every 4.8 g of NaOH pellets, 25 ml of water was added resulting in a 4.8 M solution.

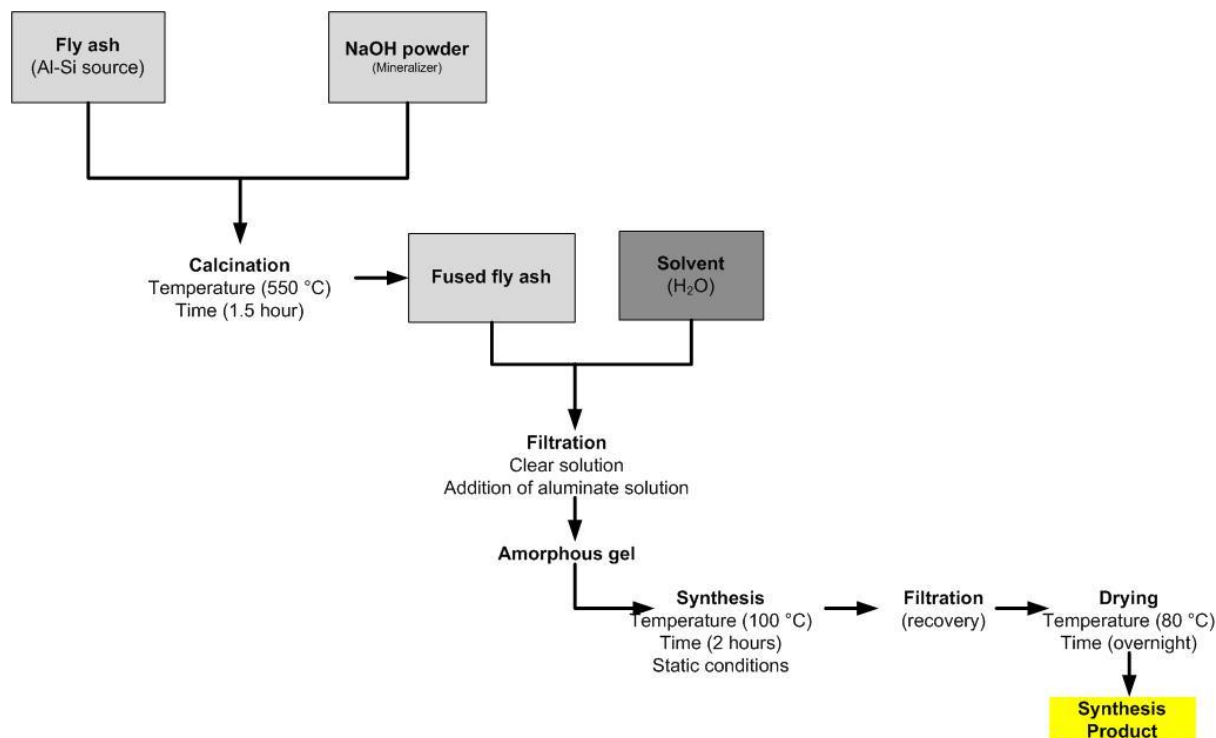


Figure 3-4: Flowchart illustrating the synthesis process of zeolite A from fly ash

3.2.2.4. Crystallization step

After the addition of the aluminate solution, the resulting milky solution was then transferred into 250 ml glass bottles with air tight seals. The crystallisation of zeolites was achieved by placing the bottles with the mixture in an air heated oven kept at 100°C for two hours under static conditions (no stirring).

3.2.2.5. Recovery of zeolites

The zeolite products were separated from the solution and recovered by filtration followed by washing the zeolite crystals with de-ionised water several times until the pH of 9-10 of the filtrate was achieved. The zeolitic products were then dried in an oven overnight at 80°C and ground into powder for further analysis.

3.2.3. Experiments

All the experiments reported below were conducted following the procedure outlined above; however slight changes were made depending on the investigated parameter in the experiment.

3.2.3.1. Synthesis of a pure phase zeolite A

This set of experiments was conducted using Arnot fly ash as the starting material. In this case, 120 g of NaOH powder was mixed with 100 g of fly ash and fused for 1.5 hours at 550 °C. After the fusion step, about 195 g of fused fly ash was obtained and was dissolved in about 980 ml of ultrapure water for 2 hours under stirring (1400 rpm using 4-flat-blade impeller) in a 1.8 L stainless reactor with Teflon lining. The resulting slurry was then filtered and about 720 ml of the clear solution was obtained. 288 ml of the aluminate solution was prepared and added to the clear solution under stirring for 10 minutes. The mixture was then subjected to crystallisation at 100 °C for two hours.

In another set of experiments, ultrapure water was substituted with raw untreated circumneutral mine water (CMW) collected from Middleburg coal mine in Mpumalanga, South Africa. This was done in order to test the robustness of the synthesis conditions when impurities were introduced from the solvent. The zeolitic products obtained were characterised using XRD, SEM and XRF analytical techniques. The chemical composition of the CMW solvent was determined using the ICP technique and the results are given in Table 6.1.

3.2.3.2. Synthesis of zeolite A using South African fly ash from different sources

In this case, the same procedure as that given in section 3.2.4.1 above was followed. However, Arnot fly ash was replaced by four other fly ash samples sourced from other power stations, namely: Matla, Lethabo, Hendrina and Tutuka fly ash. The main aim of these experiments was to demonstrate the possibility of synthesising zeolite A from fly ashes with varying chemical and mineralogical compositions. XRD, SEM and XRF analytical techniques were used to characterise the ash and the zeolitic products obtained.

3.3. SECTION C: Techniques of characterisation

This section describes the analytical techniques used in this study to carry out the characterisation of raw materials and synthesis products. Each technique typically probes only a particular aspect of the material and, therefore, the use of a combination of methods was necessary to obtain a complete description of the starting materials as well as the zeolitic products. Several techniques were used for the characterisation of zeolites to provide information on: (1) its structure and morphology; (2) its chemical and mineralogical composition.

3.3.1. X-ray Fluorescence spectrometry

X-ray fluorescence (XRF) analysis was carried out to quantify the chemical/elemental composition of the fresh ash. XRF analyses were however not performed on the zeolite Na-P1 products due to the small quantity of the zeolite produced.

3.3.1.1. Sample preparation and procedure

The samples were prepared by mixing 9 g of fly ash with 2 g of a binder which was made up of 10 % C-wax binder and 90 % EMU powder. The mixture was thoroughly shaken, poured into the mould and pelletized at a pressure of 15 tonnes for about one minute using a Dickie and Stockler manual pelletiser. Loss on ignition (LOI) was measured by placing the samples in a furnace at 1000 °C for at least 45 minutes.

Analyses were done on a Philips PW 1480 X-ray spectrometer. The spectrometer was fitted with a chromium tube and five analysing crystals (LIF 200, LIF 220, GE, PE and PX). The detectors were a combination of gas-flow proportional counter and a scintillation detector. The gas-flow proportional counter used a P10 gas (which is a mixture of 90 % argon and 10 % methane). Major elements were analysed on a fused glass bead at 40 kV and 50 mA tube operating conditions and trace elements were analysed on a powder briquette at 50kV and 40 mA tube operating conditions. Matrix effects in the samples were corrected for by applying theoretical alpha factors and measured line overlap factors to the raw intensities measured with the SuperQ Philips software.

3.3.2. Inductively Coupled Plasma (Atomic Emission and Mass) Spectroscopy

Elemental analysis of the pre-synthesis solution collected after the aging step was carried out to gain a better understanding of the trace and major heavy metal species released from the fly ash into the solution, and also to determine the Si/Al ratio in the solution. This was achieved with the use of an inductively coupled plasma atomic emission spectrometry (ICP-AES) and a mass spectrometry technique (ICP-MS). This technique was also used to determine the elemental composition of the solvents (water sources) used during zeolite synthesis. All the samples were filtered to remove suspended solids and then diluted with a 2 % (v/v) solution of nitric acid. The instrument used for determining the major elements was a Varian Radial ICP-AES, while trace elements were determined using an Agilent 7500ce ICP-MS, using a High Matrix Introduction (HMI) accessory and Helium (He) as a collision gas. For both instruments, external calibration was performed daily, and results of a quality control standard verifying accuracy was included with every batch of samples analysed. For ICP-MS analysis, internal standards were used to correct for matrix effects and instrument drift.

3.3.3. Ion chromatography

Ion chromatography (IC) was used to analyse the anion concentration in the mine water. The samples were filtered through 0.45 μm nucleopore membrane filter paper and preserved at 4 °C until the analysis was conducted. The samples were diluted as required. A Dionex DX-120 Ion Chromatograph with a AS40 automated sampler, ASRS-300 suppresser, AS14 analytical column, AG14 guard column and a conductivity detector was used for the analysis. The eluant used was a mixture of 3.5 mM NaHCO_3 and 1.0 mM Na_2CO_3 .

3.3.4. X-ray Diffraction Spectroscopy

X-ray diffraction (XRD) analyses were carried out to identify and also quantify the different phases in the fresh ash as well as in the zeolite materials. For the identification and quantification of mineral phases, qualitative and quantitative XRD analyses were done respectively.

3.3.4.1. Qualitative XRD analysis

3.3.4.1.1. Sample preparation and procedure

For these analyses, samples were analysed without any additional sample preparation. The fly ash and synthesised zeolite samples (after being ground to a fine powder) were placed in a sample holder and the crystalline phases were characterised using a Philips X-ray diffractometer with Cu-K α radiation. The XRD instrument operating conditions are shown in Table 3.4. The phase identification was performed by searching and matching obtained spectra with the powder diffraction file data base of JCPDS (Joint Committee of Powder Diffraction Standards) files for inorganic compounds.

Table 3-4: XRD operating parameters

Radiation source	Cu-K α
Radiation wavelength (λ)	1.542 Å
Range	104
Time constant	1 s
Preset	1000 counts/s
Voltage	40 kV
Current	25 mA
2θ range	$4^\circ < 2\theta < 60^\circ$
2θ /step	0.1°
Anti-scatter slit	1°

3.3.4.1.2. Determination of percentage crystallinity

Percentage crystallinity of the samples was defined on the basis of the major (most intense) characteristic peaks of Zeolite Na-P1. The major peaks were selected specifically because they are least affected by factors such as the degree of hydration of the samples and the type of cation compensation (Ojha *et al.*, 2004; Marrot *et al.*, 2001). Percentage crystallinity was calculated by using Equation 3.1. (Gosh *et al.*, 1994).

$$\% \text{ crystallinity} = \frac{\text{sum of the area under the XRD peaks of the product}}{\text{sum of the area under the XRD peaks of the std sample}} \times 100 \quad (3.1)$$

Among all the synthesised zeolite Na-P1 samples, the one in which the sum of the diffraction intensities of these major peaks was highest was selected as the standard with 100 % crystallinity and the relative crystallinity of the other samples was calculated according to that standard.

3.3.4.1.3. Quantification of the zeolite phase

The area under each XRD peak was measured. The sum of the areas under the diffraction peaks corresponding to each of the phases was calculated. The total area was assumed to be 100 %. Thus, the percentage of each phase detected was calculated according to the following equation 3.2 (Dyer, 1988):

$$\text{Percentage of crystalline phase(A)} = \frac{\text{sum of area under peaks of phase(A)}}{\text{Total area}} \times 100 \quad (3.2)$$

3.3.4.2. Quantitative XRD analysis

This technique was only used to quantify the mineral and amorphous phases in the Arnot fly ash samples.

3.3.4.2.1. Sample preparation and procedure

After the addition of a 20 % Si (Aldrich 99 % pure) for the determination of the amorphous content and milling in a McCrone micronizing mill, the samples were prepared for XRD analysis using a back loading preparation method. Samples were analysed with a PANalytical X'Pert Pro powder diffractometer with X'Celerator detector and variable divergence and receiving slits with Fe filtered Co-K α radiation. The phases were identified using X'Pert Highscore plus software. The relative phase amounts (weight %) were estimated using the Rietveld method (Autoquan Program).

3.3.5. Fourier Transform Infrared Spectroscopy

Attenuated total reflectance (ATR) FTIR analysis was carried out in order to monitor the evolution of crystallinity during the synthesis and also to gain an insight about the molecular structure of the product. ATR-FTIR analysis is fast; a very small amount of sample is needed and requires virtually no sample preparation. A mass of 15 mg of the zeolite sample was placed on the Attenuated Total Reflectance (ATR) sample holder of a Perkin Elmer spectrum 100 FT-IR spectrometer. The FT-IR spectra of the fly ash and zeolitic materials were recorded in the range of 1800 to 250 cm^{-1} . The baseline was corrected and the spectra smoothed. Vibrations common to zeolites were identified. The use of diamond cells with a beam condenser or microscope allowed adjustment of the thickness of a sample by squeezing, which enables analysis of microgram samples to be performed.

3.3.6. Scanning Electron Microscopy

The morphology of the fly ash and zeolites prepared in this investigation was examined using the Cambridge S200 SEM, which is equipped with an energy dispersive X-ray analyser. The samples were sprinkled on special glue mixed with carbon graphite and mounted onto aluminium stubs. Samples were then coated with a thin film of copper to make them conductive. The “photo” imaging was used to identify regions of relative homogeneity.

3.4. Summary

In this chapter, the experimental set-up together with the synthesis procedure for both the synthesis of zeolite Na-P1 and zeolite A were described. The characterisation techniques used in this study and sample preparation were also outlined in this chapter. The next chapter (Chapter 4) focuses on the characterisation of the raw materials used in this study.

CHAPTER 4

4. CHARACTERISATION OF RAW MATERIALS

4.1. Introduction

Since fly ash was the main raw material used in this study, the main aim of this section was to describe the characterisation of fly ash from the various sources used. The knowledge of the characteristics of the fly ash is very important for zeolite synthesis since the properties of the zeolitic products are dependent on these characteristics (i.e. physical, chemical and mineralogical). As aforementioned, the fly ash samples used in this study were collected from five ESKOM power stations situated in Mpumalanga, South Africa (i.e. Arnot, Hendrina, Tutuka, Lethabo and Matla power stations). These fly ashes were characterised chemically, mineralogically and structurally using XRF and XRD techniques. The SEM technique was also used in order to get a clear understanding of the morphology of the fly ash.

4.2. Chemical composition of the fly ashes

Chemical composition of fly ash has a significant influence on both its potential applications and on the environmental impact of its subsequent use. The XRF results of the chemical/elemental composition of the fly ashes used in this study are depicted in Table 4.1. The results obtained give fundamental information on the major and trace elemental composition of the fly ash matrix. The analysis was done in duplicate in order to minimise the error in the results obtained.

Table 4-1: Major elemental composition of coal fly ashes used in this study

Major Oxides (Mean Mass %)	Arnot		Tutuka	Hendrina	Lethabo	Matla
	Batch 1	Batch 2				
SiO ₂	55.66	55.44	52.63	49.79	58.32	58.44
Al ₂ O ₃	27.95	31.51	26.49	31.75	31.36	31.25
Fe ₂ O ₃	3.22	4.94	4.87	3.17	3.04	3.09
MnO	0.04	0.03	0.05	0.00	0.02	0.02
MgO	1.91	1.18	1.31	0.98	1.13	1.14
CaO	4.38	3.76	5.33	4.62	3.16	3.21
Na ₂ O	0.31	0.04	0.55	0.09	0.46	0.46
K ₂ O	0.45	0.47	0.82	0.63	0.54	0.54
TiO ₂	1.13	1.11	1.46	0.67	1.16	1.17
P ₂ O ₅	0.26	0.30	0.38	1.46	0.39	0.40
SO ₃	0.03	0.06	0.06	0.23	0.02	0.02
Loss On Ignition	4.74	1.22	6.09	6.59	0.40	0.28
Sum (%)	100.07	100.07	100.04	99.98	100.00	100.00
SiO ₂ /Al ₂ O ₃	1.99	1.76	1.99	1.57	1.86	1.87

Table 4-2: Trace elements in the coal fly ashes used in this study

Trace elements (ppm)	Arnot		Tutuka	Hendrina	Lethabo	Matla
	Batch 1	Batch 2				
As	49.10	-	85.70	-	41.09	41.09
Ba	708.93	485.7	913.11	-	918.23	917.53
Ce	128.45	254.0	155.80	-	112.73	107.75
Co	43.87	30	39.52	12.55	14.84	17.97
Cu	46.88	109.9	51.43	51.03	53.85	55.71
Nb	58.10	37.2	65.92	39.67	53.05	57.66
Ni	24.40	124.9	22.04	58.12	21.95	20.45
Pb	56.56	90.3	48.83	65.37	51.71	51.81
Rb	29.29	56.2	41.01	31.18	27.57	35.77
Sr	1011.45	988.9	1384.72	1194.85	970.66	976.19
V	113.49	78.6	122.29	85.12	123.49	110.70
Y	84.78	93.8	98.29	15.31	73.72	71.71
Zn	42.09	135.3	38.03	93.69	39.54	39.48
Zr	442.60	-	492.99	424.09	385.24	384.58
Mo	11.28	-	7.48	-	7.86	10.58
Th	384.21	-	558.96	-	372.75	373.09

The XRF results in Table 4.1 revealed that the glass phase in all the fly ashes used in this study accounts for more than 60 to 80 % of the fly ash and this indicated that South African FA would supply a readily available source of Si and Al for zeolite synthesis. The average $\text{SiO}_2/\text{Al}_2\text{O}_3$ ratio of the fly ashes in this study was found to be 1.99, 1.76, 1.99, 1.57, 1.86 and 1.87 for Arnot batch 1, Arnot batch 2, Tutuka, Hendrina, Lethabo and Matla fly ashes, respectively. This ratio is appropriate for the synthesis of low Si-zeolites with high cation exchange capacity (Querol *et al.*, 1996). This ratio plays an important role during zeolite synthesis since it places constraints on the framework composition of the zeolite produced (Szostak, 1989). Changing this ratio may result in a change in the final structure obtained and may also lead to the crystallisation of unwanted phases (Szostak, 1989). Although the chemical compositions of the two batches of Arnot fly ash were similar, these samples exhibited a different $\text{SiO}_2/\text{Al}_2\text{O}_3$ ratio i.e. 1.99 and 1.76 for batch 1 and batch 2 respectively. This is due to increased alumina content in batch 2.

These South African fly ashes are classified as class F type (according to the ASTM standard C618) because their $\text{SiO}_2 + \text{Al}_2\text{O}_3 + \text{Fe}_2\text{O}_3$ content was assessed to be greater than 70 %. This type of fly ash results from the burning of the harder, older anthracite and bituminous coal (Vassilev and Vassileva, 2007). These fly ashes were also found to contain low content of CaO and MgO. These oxides play a significant role during zeolite synthesis. Ca^{2+} and Mg^{2+} were reported to act as competing ions during zeolite synthesis. Ca^{2+} was also reported to have structure breaking properties which lead to the interference with the zeolite crystallisation process (Catalfamo *et al.*, 1993). It was also reported that Ca-bearing phases can act as an inhibitor for the synthesis of zeolites through the formation of Calcium Silicates (Ríos *et al.*, 2009; Juan *et al.*, 2007). Fe-bearing minerals, such as magnetite, were also found to show an inert behaviour during zeolite synthesis (Juan *et al.*, 2007). Thus the lower the content of Ca and Fe bearing minerals, the less the interference during the crystallisation of zeolites. Nonetheless, all the fly ashes used in this study contained low content of Fe-bearing minerals ranging between 3 to 5 %.

The fly ashes used in this study contained low contents of sodium (Na), as can be seen in Table 4.1. Sodium plays a crucial role during zeolite synthesis as a charge-balancing cation. Therefore, most of the sodium available during the synthesis of zeolites in this study came from the NaOH solution and the sodium aluminate source used, since the fly ash contained low concentration of this element. The sulphur trioxide (SO_3) content in the fly ashes used in this study was low (ranging between 0.02 to 0.06 %). This may be due to the fact that these fly ashes were produced from low sulphur containing coals. However, the Hendrina FA showed a high SO_3 content. Although low sulphur coals may have been used, the content of SO_3 in the FA may increase due to the injection of SO_3 in the electrostatic precipitator. Therefore, FA collected from electrostatic precipitators may contain high amounts of SO_3 . Hendrina FA might have been collected from the electrostatic precipitators, resulting in a high SO_3 content.

The Loss-On-Ignition (LOI) measures the amount of unburned carbon remaining in the fly ash and it is an important chemical parameter, since it can be used as a screening tool for fly ash for use in concrete and cement manufacturing and also assists in the prediction of the quality of zeolites synthesised from fly ash. Rayalu *et al.* (2001) pointed out that large amounts of unburned carbon (high values of LOI) interferes with the fusion step, thereby affecting the quality of the fused product. Compared to the other fly ashes, Hendrina fly ash had the largest amount of unburned carbon (6.59 %) followed by Tutuka fly ash (6.09 %) then batch 1 of Arnot fly ash (4.74 %). It was noticeable that Arnot batch 1 and 2 fly ashes differed considerably in terms of the LOI (i.e. 4.74 % for batch 1 and 1.22 % for batch 2). This indicated that the power station burner conditions were altered during the time the samples were taken.

These fly ashes were also found to contain some potentially toxic trace elements such as As, Pb and Ba (Table 4.2). Amongst the dominant trace elements present in the fly ash, Sr, Ba, Ce, Zr and Th were found to be in significantly higher concentration relative to the other trace elements in all the fly ashes. It is important to highlight that although other trace elements such as As, Ba and Ce in Hendrina fly ash were not indicated in the table, it does not mean that this fly ash did not contain these elements. These elements were not analysed due to experimental constraints. Strontium (Sr) was found to be the highest trace element in all the fly ashes with concentrations between 970 to 1384 ppm (Table 4.2) being observed. Similarly, Barium (Ba) also existed in high concentrations, especially in Tutuka (913.11 ppm), Lethabo (918.23 ppm) and Matla (917.53 ppm) fly ashes. Ba concentrations ranged between 485 and 919 ppm. Fly ashes used in this study were also found to contain large amounts of zirconium (Zr) and thorium (Th) with concentrations ranging between 384 to 493 ppm and 372 to 559 ppm respectively. Nevertheless, none of the abovementioned trace elements were ever reported to affected zeolite synthesis. However, they may be detrimental to the environment.

4.3. Mineralogical composition of the fly ashes

4.3.1. Qualitative X-ray diffraction analysis

Figure 4.1 and 4.2 illustrate the qualitative XRD analysis of all the fly ash samples used in this study.

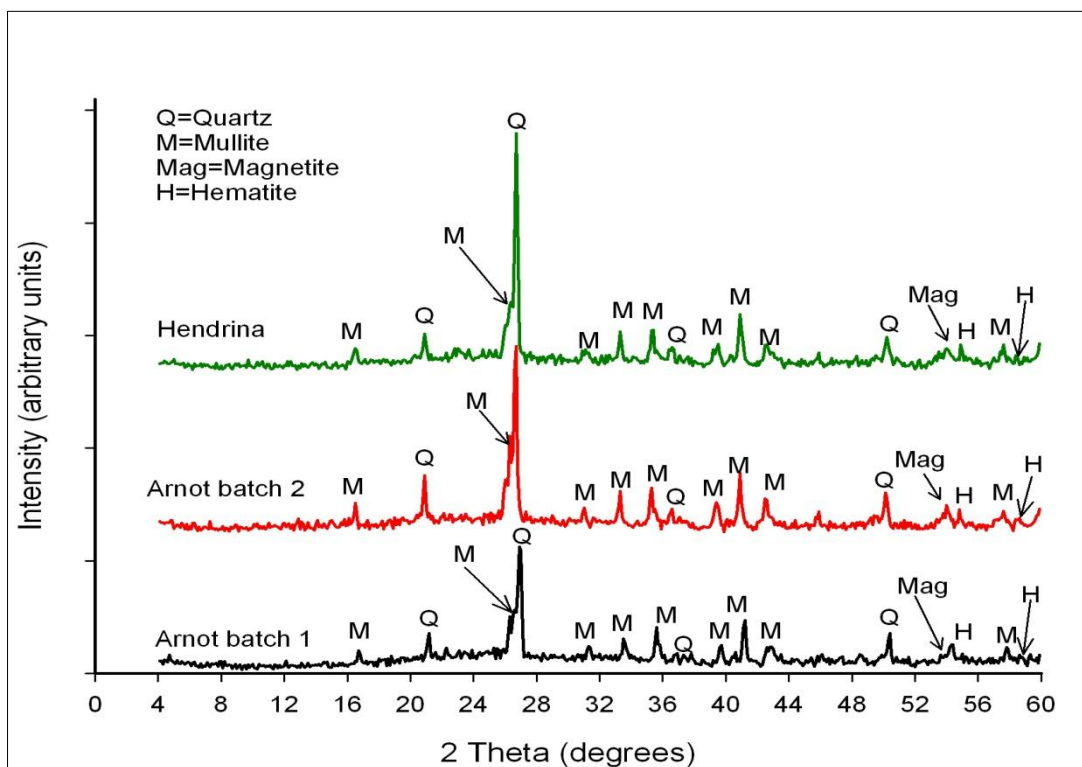


Figure 4-1: XRD spectra of Arnot (Batch 1 and 2) and Hendrina fly ash

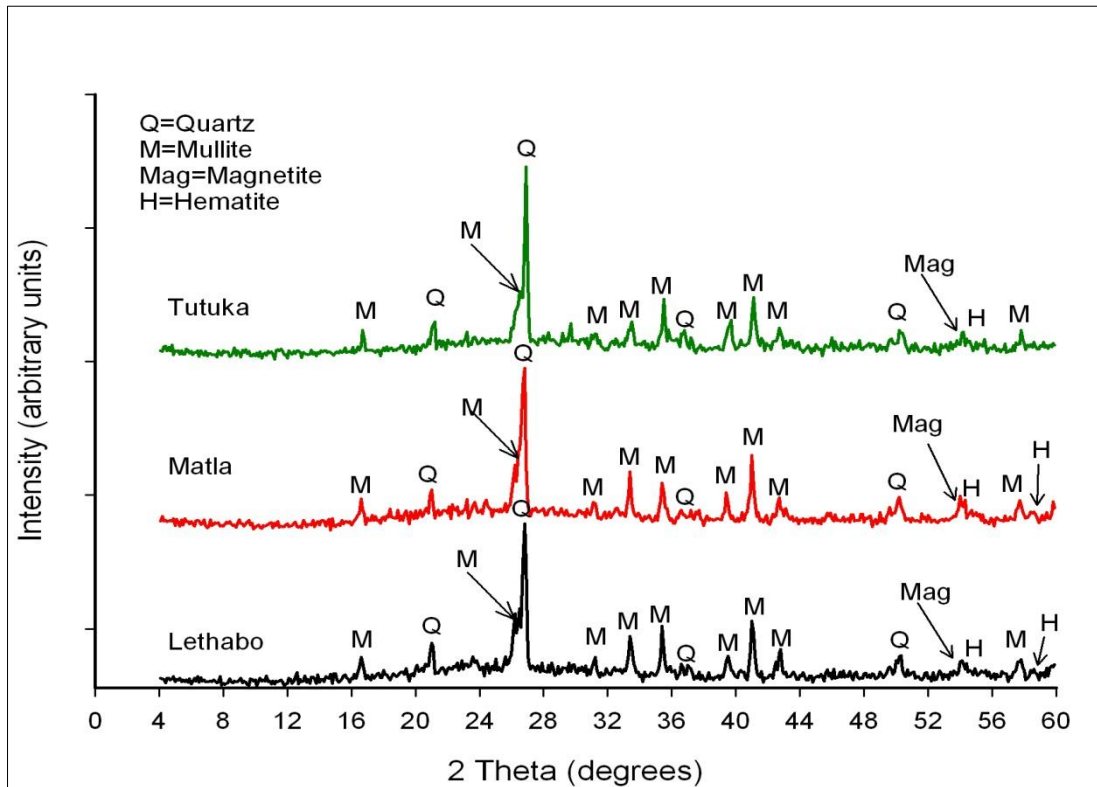


Figure 4-2: XRD spectra of Lethabo, Matla and Tutuka fly ash

Qualitative XRD analysis of all the South African fly ashes (Arnot, Hendrina, Tutuka, Matla and Lethabo) used in this study showed a direct parallelism in terms of characteristic peaks observed (Figure 4.1 and 4.2). As such, all these South African fly ashes showed a similar mineralogical composition. The major crystalline phases in the fly ashes used in this study were found to be quartz (SiO_2), mullite ($3\text{Al}_2\text{O}_3 \cdot \text{SiO}_2$) with small quantities of magnetite and hematite as indicated in the X-ray diffraction pattern in Figure 4.1 and 4.2. Quartz had the most intense peak at 26.85 degrees 2θ while the less intense peaks on the XRD patterns were identified as mullite, hematite and magnetite. The fly ashes contained an amorphous glassy phase, giving rise to a broad hump in the region between 18 to 32 degrees 2θ , as indicated in the XRD spectra above. This hump was also identified by several authors in their studies (Musyoka, 2009; Ríos *et al.*, 2009; Criado *et al.*, 2007; Inada *et al.*, 2005).

4.3.2. Quantitative X-ray diffraction analysis

The overall quantitative XRD analysis confirmed that all the fly ashes used in this study were composed of phases that had been observed through qualitative XRD analysis (i.e. quartz, mullite, amorphous phase, magnetite and hematite). However, another minor phase (calcite), occurring in small quantities that was not detected through the qualitative XRD analysis, was

also observed in all fly ashes except for Arnot fly ash. The results of the quantitative XRD analysis are depicted in Figure 4.3 and Table 4.3.

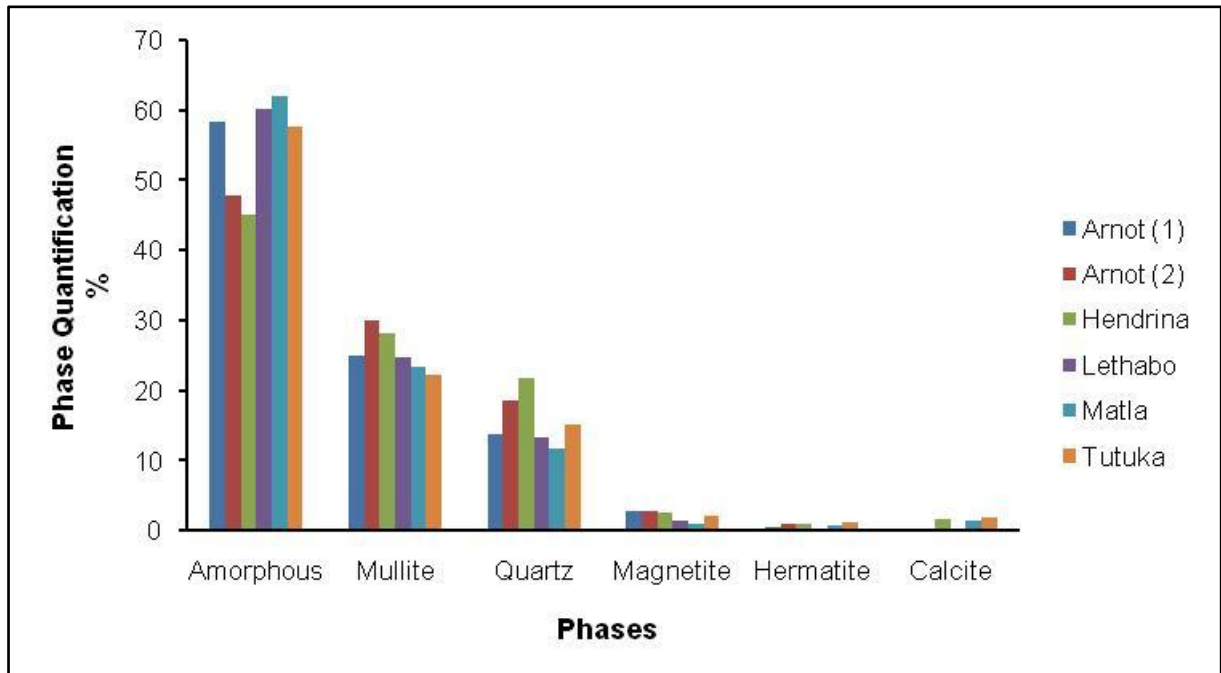


Figure 4-3: Quantification of the fly ash phases

Matla fly ash was found to contain the highest content of the amorphous glassy phase (61.96 %) and very low contents of mullite (23.4 %) and quartz phases (11.6 %). Hendrina fly ash contained the lowest amorphous glassy phase content (44.99 %) and highest content of quartz (21.8 %) compared to the other fly ashes used in this study (Table 4.3). The mullite content in this FA (Hendrina) was also found to be high, i.e. 28.2 %. However, batch 2 of Arnot FA was found to contain the highest amount of mullite (29.93 %) and high quartz content (18.6 %). Similar to Hendrina FA, batch 2 of Arnot FA had a low content of the amorphous glassy phase (47.85 %). The two batches of Arnot FA had similar chemical composition (Table 4.1). However, the mineralogical composition of the two batches was found to vary considerably-see Table 4.3. Batch 1 of Arnot FA was found to contain a larger amount of the amorphous glassy phase with a lower content of mullite and quartz when compared to batch 2. The difference between the contents of the mineral phases in these batches was found to be; ± 10 % for the amorphous glassy phase, ± 5 % for mullite and ± 5 % for quartz. However, the magnetite content in batch 1 was slightly higher than that of batch 2 of Arnot FA (i.e. 2.75 % for batch 1 and 2.7 % for batch 2). Calcite was not detected in the two batches of Arnot FA.

Table 4-3: Quantification of the fly ash phases

Source (mass %)	Amorphous	Mullite	Quartz	Magnetite	Hematite	Calcite
Arnot (batch 1)	58.22	24.84	13.66	2.75	0.53	ND
Arnot (batch 2)	47.85	29.93	18.6	2.7	0.92	ND
Hendrina	44.99	28.2	21.8	2.5	0.97	1.55
Lethabo	60.13	24.76	13.21	1.31	0.3	0.29
Matla	61.96	23.4	11.6	1.02	0.63	1.4
Tutuka	57.74	22.1	15.09	2.08	1.12	1.87

*ND-not detected

The amorphous glassy phase has been reported to be the most unstable phase compared to quartz and mullite. According to Querol *et al.* (2001), quartz is less stable than mullite. This means that the amorphous phase will be the first to dissolve, followed by quartz, then mullite. Although quartz is less stable than mullite, these crystalline phases are significantly stable, to an extent that some authors reported little to no reactivity during zeolite synthesis (Berkhaut and Singer, 1996; Catalfamo *et al.*, 1993; Mondragon *et al.*, 1990). Mullite has also been found to be resistant to direct caustic treatment; therefore higher levels of mullite in the fly ash would inhibit zeolite formation (Moreno *et al.*, 2002; Rayalu *et al.*, 2001). A previous study has reported that the Si/Al ratio in the synthesis solution at an early stage is important for deciding the type of zeolite to be synthesised (Inada *et al.*, 2005). This makes the amorphous glassy phase very important since it easily dissolves into the alkaline solution.

Based on this information it can be said that Matla FA was the most reactive fly ash, since it contained a high quantity of the amorphous glass phase and low contents of mullite and quartz. Lethabo FA was found to be the second most reactive FA followed by Tutuka and batch 1 of Arnot FA, with Hendrina and batch 2 of Arnot FA being the least reactive fly ashes. Batch 1 of Arnot FA was found to be more reactive than batch 2. This is because batch 1 contained a large amount of the reactive amorphous glassy phase and a low content of the less reactive mullite and quartz phases compared to batch 2.

Fe-bearing minerals in these fly ashes were found to exist as magnetite and hematite. As aforementioned, these Fe-bearing ashes were reported to show an inert behaviour during zeolite synthesis. Querol *et al.* (1996) reported that magnetite was not affected by the activation of fly ash with NaOH solution. Furthermore, the study reported that magnetic separation of iron oxides (magnetite and hematite) during prior zeolite synthesis resulted in an increase in fly ash conversion efficiency. Advantageously, the fly ashes used in this study consisted of low contents of both magnetite and hematite (ranging between 1 to 2.8 % for magnetite and 0 to 1.2 % for hematite).

4.4. Morphology of fly ash particles

In addition to chemical and mineralogical composition, fly ash can also be characterised morphologically using SEM analytical technique. Kutchko and Kim (2006) stated that the morphology of fly ash depends on the combustion temperature and cooling rate. Figure 4.4 illustrates several aspects about the morphology of fly ash.

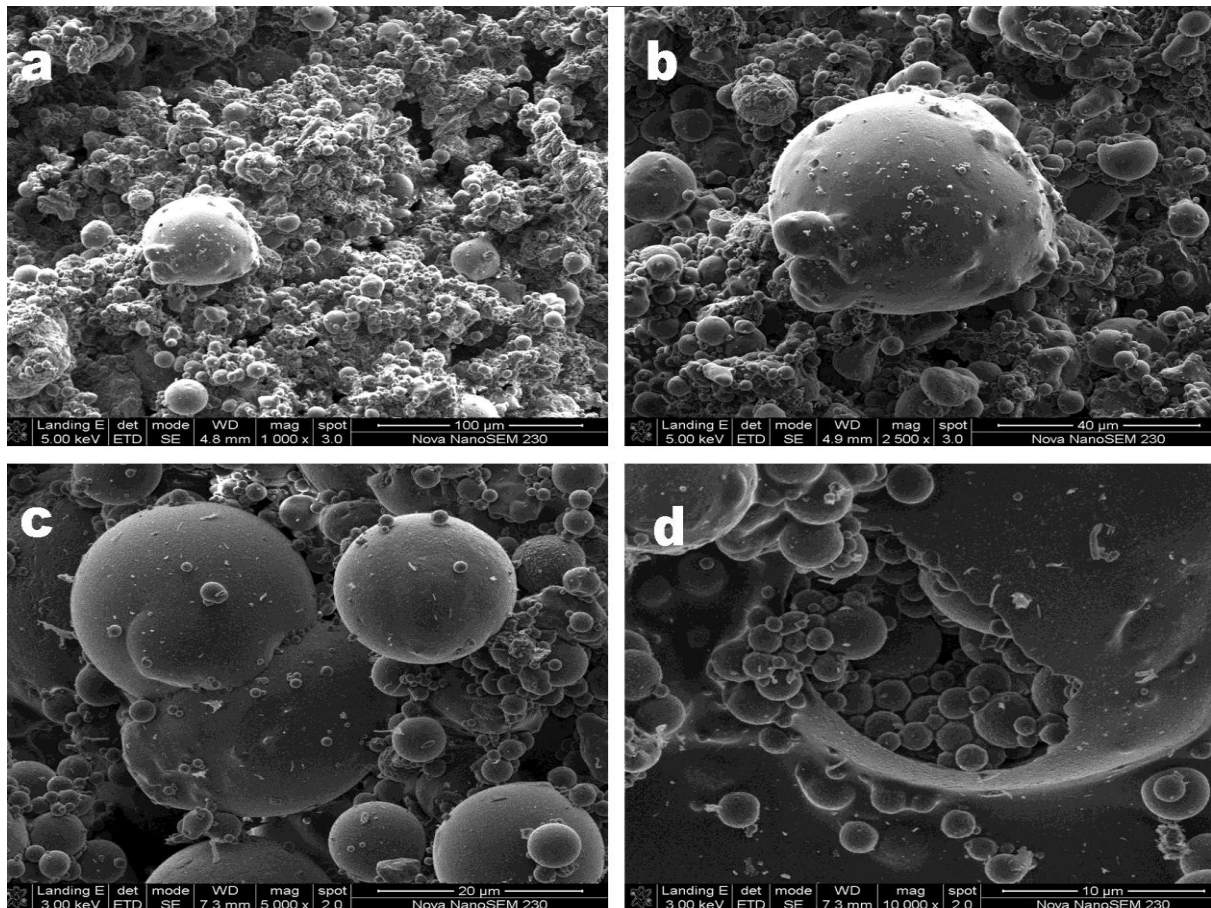


Figure 4-4: SEM images of fly ash morphology. (a) Typical view of the FA particles with a predominantly spherical morphology. (b) Smaller particles attached to the surface of a larger particle. (c) Hollow spheres (cenospheres). (d) Hollow sphere containing smaller spheres (plerospheres).

The SEM images above revealed that fly ash particles are predominantly spherical in shape with a relatively smooth surface texture and a wide particle size range (Figure 4.4b). The smoothness of the surface of the fly ash particles can be attributed to the fact that these particles are covered with the amorphous glass phase (Inada *et al.*, 2005). In some cases, smaller particles are attached to the surface of larger particles, serving as substrates (Figure 4.4). The spherical shape of fly ash particles is formed as a result of the relatively sudden cooling during combustion (Kutchko and Kim, 2006). The spherical particles are either solid or hollow (Figure 4.4c). The hollow spherical particles are known as cenospheres and are believed to be formed by the expansion of CO₂ and H₂O gas, evolved from minerals within

the burning coal (Reyes, 2008; Landman, 2003; Fisher *et al.*, 1976). Cenospheres may contain some smaller particles in their interiors (plerospheres, Figure 4.4d).

4.5. Particle size distribution

Particle size distribution (PSD) is a physical characteristic of fly ashes that strongly affects their reactivity (Fernandez-Jimenez and Palomo, 2003). PSD is an important criterion in ascertaining the utilisation potential of fly ash. In addition, particle characterisation of fly ash is also important in understanding the enrichment of trace elements, which might affect the quality of the synthesised zeolite product (Liu *et al.*, 2004). PSD of fly ash can vary from time to time depending on the coal combustion conditions in the power station (Vadapalli *et al.*, 2007; Vassilev and Vassileva, 2007; Iyer and Scott, 2001). Such variability in PSD of fly ash could influence the conversion of fly ash into zeolites. PSD of the different fly ashes used in this study is illustrated in Figure 4.5.

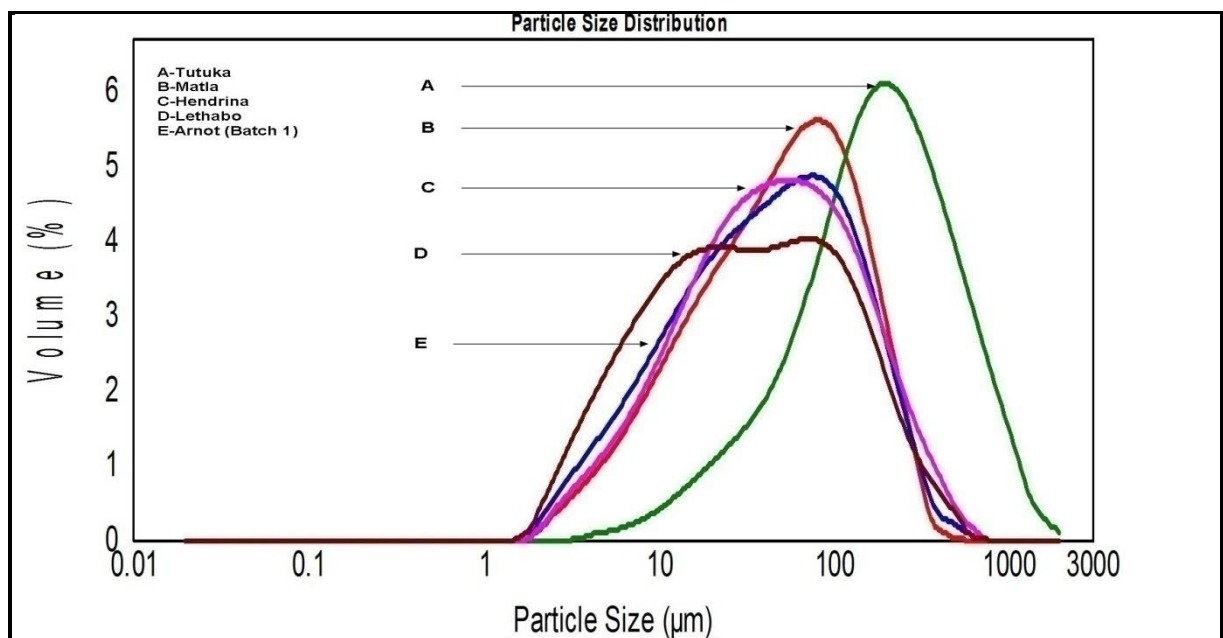


Figure 4-5: Particle size distribution of coal fly ashes. A) Tutuka, B) Matla, C) Hendrina, D) Lethabo and E) Arnot (batch 1) fly ash

Figure 4.5 reveals that the PSD of the fly ashes used in this study had the expected normal bell-shaped distribution curve. It is well documented that particle size distribution of fly ashes ranges between 0.5 and 200 μm although coarser particles ($>200 \mu\text{m}$) may exist (Goodarzi, 2006; Scheetz and Earle, 1998). However, the particle sizes of the fly ashes in this study generally ranged between 1 to 3000 μm . Among all these fly ashes, Tutuka fly ash was observed to have large particle sizes, ranging between 3 to 3000 μm . The particle diameter of Tutuka fly ash was found to be mainly between 180 to 247 μm .

Matla, Hendrina, Lethabo and Arnot fly ashes were observed to have similar particle sizes ranging between 1 to 1000 μm . However, Matla fly ash exhibited the largest particle diameter lying between 77 to 104 μm when compared to the other three fly ashes (i.e. Hendrina, Lethabo and Arnot fly ash). Interestingly, the distribution pattern of Lethabo fly ash was observed to have an additional shoulder between 17-23 μm particle diameters. Nonetheless, this ash (Lethabo) was found to have the lowest maximum volume percentage (4 %). Although Arnot fly ash (4.9 %) had a maximum particle diameter slightly higher than that of Hendrina fly ash (4.8 %), these fly ashes exhibited similar PSD patterns, ranging between 1 to 1000 μm .

4.6. Conclusions

From the physio-chemical characterisation results, it can generally be concluded that the raw materials (South African fly ashes) used in this study have properties suitable for zeolite synthesis and can be, in principle, useful sources of silica and alumina. The $\text{SiO}_2/\text{Al}_2\text{O}_3$ ratio of the fly ashes was deemed to be appropriate for the synthesis of low-Si zeolitic materials with high cation exchange capacity (CEC). In addition, the very low contents of impurities, such as Fe and Ca, is also important, taking into account that Fe-bearing and Ca-bearing phases can show an inert behaviour and promote the formation of C-S-H phases, respectively. Considering new applications for these raw materials, their thorough characterisation provided very important data useful in predicting their behaviour in zeolite synthesis. Finally, this study also showed that the mineralogical and chemical composition of the FA sourced from different South African power stations or sampled from the same power station at different times varied considerably.

5. SYNTHESIS OF ZEOLITE NA-P1 FROM SOUTH AFRICAN COAL FLY ASH: investigation of scale-up conditions

5.1. Introduction

A recent study has shown that zeolite Na-P1 can be synthesised from South African fly ash. In that study, a pure phase of zeolite Na-P1 was obtained in a small scale laboratory experiment with a 23 ml working volume (Musyoka, 2009). Although the study reported optimum conditions for the synthesis, it is clear that these conditions may not be valid in a scale-up operation. Most studies in the literature that were conducted on the synthesis of zeolites from fly ash were performed at a small laboratory scale. Determination of the scale-up parameters on the synthesis of the fly ash zeolites from a lab-scale to a pilot scale is problematic. It is important that before scale-up commences, its implications on the zeolite product quality be examined. Therefore, it is necessary to investigate the effects of some fundamental parameters that may influence the zeolitisation process on a large scale (for example; synthesis temperature, time, agitation as well as starting materials).

However, for a large or industrial scale production of zeolites, the synthesis process must imperatively be conducted in an agitated reactor. This is because the reaction mixture produces a viscous gel and if mixing is inadequate or absent, an inhomogeneous reaction mixture may result, with pockets of gel having different compositions and consistency. According to Casci (2005) each “pocket” behaves like a mini reactor and generates phases corresponding to the composition in that region. Moreover, Marrot *et al.* (2001) reported that the synthesis of zeolites in a non-agitated medium requires longer periods of time for growth of zeolites, and is therefore economically inappropriate.

Generally, the type and chemical composition of the synthesised zeolites is strongly dependent on the chemical composition of the feedstock. However, other physio-chemical factors may play an important role in the thermodynamics and kinetics of zeolite formation. Thus, the mineral and chemical composition of fly ash and the chemistry of water are very important, since FA and water are the main starting materials during the zeolite synthesis from fly ash. Fly ash acts as the main source of $\text{SiO}_2/\text{Al}_2\text{O}_3$. Water is used as a solvent to facilitate the dissolution of the feedstock. In addition to its solvating ability, water acts as a hydrolysing agent and as a template by its interaction with cations (Elliot and Zhang, 2005). Water molecules have been found to enhance the formation of zeolite structure during crystal growth by filling the void space, which stabilises the structure (Musyoka, 2009; Elliot and

Zhang, 2005). Most of the studies on zeolite synthesis have been performed with the use of ultrapure water to avoid the complicating effect of ions such as calcium (Casci, 2005). However, the use of ultrapure water on an industrial scale would have serious implications on the operation costs.

Synthesis time is also an imperative factor in zeolite synthesis. The amount of time the reacting species spend in the reactor determines the type of zeolite product formed. Prolonged aging of the hydrogel at ambient temperatures prior to crystallisation may cause the formation of a product which contains a larger number of small crystals. In addition, it was reported in a study by Molina & Poole (2004) that crystallisation for a short period showed no peaks, which normally represents the absence of a crystalline material.(Molina and Poole, 2004). It is very important that the synthesis period be optimised before scale-up commences.

Therefore, this section of the current study investigated the effects of impeller design and agitation during the aging step, as well as fly ash composition together with the use of different water sources as a substitute for ultrapure water on the synthesis of zeolite Na-P1. As aforementioned, the main aim of this investigation was to optimise the aging step with a view to synthesising a pure zeolite Na-P1 phase and establishing base conditions for the scale-up process.

5.2. Materials and Method

5.2.1. Experimental procedure

Experimental procedure and conditions together with the experiments conducted for this part of the study were previously explained in section A of Chapter 3.

5.2.2. Analytical Techniques

The analytical techniques used for this part of the study were previously explained in section C of Chapter 3.

5.3. Results and discussion

This section is divided into four parts. The first part was aimed at investigating the effect of impeller design and agitation during the aging step in order to obtain the best impeller and agitation rate suitable for the scale-up synthesis process. The second part was aimed at synthesising zeolite Na-P1 from two different fly ash samples from the same power station. The third part studied the use of other sources of water as a substitute for ultrapure water in order to reduce the cost associated with the use of this water on an industrial scale. Lastly,

the effect of the reaction time on the phase purity and crystallinity of zeolites was investigated with a view to optimise the synthesis time.

5.3.1. Effect of impeller design and agitation during the aging step

Although Musyoka (2009) reported the use of magnetic stirring at 800 rpm during the aging step of the zeolite synthesis as part of his optimum conditions for the synthesis of a pure phase of zeolite Na-P1, it is clear that the use of a magnetic stirrer at 800 rpm may not be suitable for a scale-up operation. However, it is believed that agitation during aging using different impellers at lower speeds would increase the dissolution rate of SiO_2 and Al_2O_3 from the fly ash into the solution as compared to a magnetic stirrer at a higher speed. There is limited to no information about the effect of impeller design and agitation rate and/or period on the dissolution of fly ash during the aging step of the zeolite synthesis process. These experiments were conducted in order to determine the best impeller design and its optimum speed that can be used for agitation during aging in a scaled-up process. This was achieved by determining the impact of the impeller design on the purity and the quality of zeolite Na-P1, since it was the desired product. This section discussed the results obtained for the synthesis of a pure phase of zeolite Na-P1 together with the effect of impeller design and agitation during the aging step. As aforementioned in Chapter 3-section A, the zeolitic products obtained after aging under stirred conditions, followed by hydrothermal synthesis under static conditions, were characterised with XRD, FTIR and SEM analytical techniques and the results are illustrated below.

5.3.1.1. Mineralogical analysis of the synthesised zeolites

Musyoka (2009) indicated that a pure phase of zeolite Na-P1 ($\text{Na}_6\text{Al}_6\text{Si}_{10}\text{O}_{32}\cdot 12\text{H}_2\text{O}$) can be synthesised from coal fly ash using a magnetic stirrer during aging to facilitate the dissolution of fly ash in to the alkaline solution at 800 rpm. The conditions from that study (Musyoka, 2009) were adopted in this study in order to demonstrate the reproducibility of the data as well as creating a reference point for the current study. The results obtained from this experiment provided a confirmation of Musyoka's findings. A pure phase of zeolite Na-P1 with a crystallinity of 93.0 % was obtained as indicated in Figure 5.1a and Table 5.1.

In another set of experiments, various designs of impellers were used during the aging step prior to the static hydrothermal synthesis step in order to facilitate the dissolution of fly ash into the alkaline solution during aging instead of a magnetic stirrer. The results obtained with the use of impellers during the aging step were compared to those obtained with the use of a magnetic stirrer during aging (see Figure 5.1). It was observed that all the three impellers investigated in this study could produce a pure phase of zeolite Na-P1 at lower agitation speeds. The percentage crystallinity of zeolite Na-P1 was determined using equation 3.1 and

using the zeolitic product obtained at 200 rpm with a 4 flat-blade impeller as a standard. This product was selected to be the standard because its XRD spectra showed the highest intensity for the major peaks. The sum of the area under five major peaks of zeolite Na-P1 (around $2\theta = 12, 18, 22, 28$ and 33 degrees) was used for the crystallinity calculation. The results for the percentage crystallinity are given in Table 5.1.

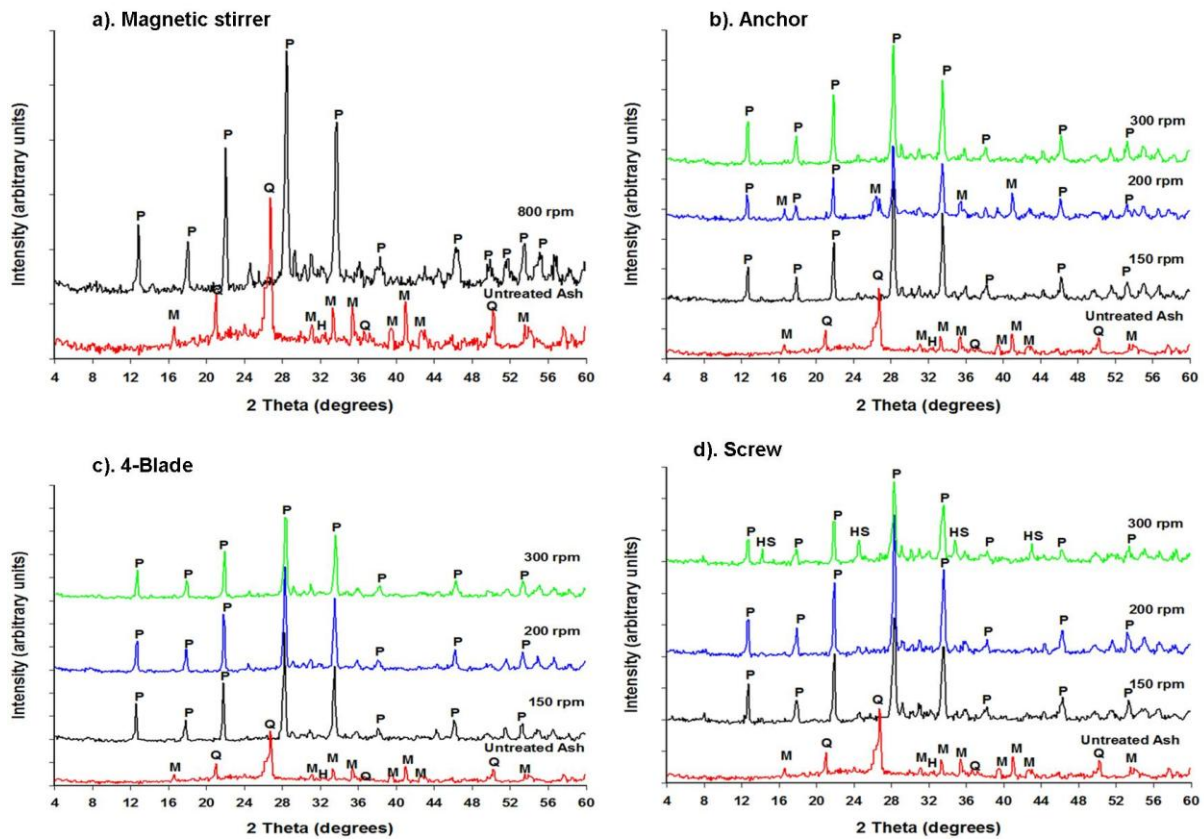


Figure 5-1: XRD spectra of the products synthesised using Magnetic stirrer, 4 flat-blade, Anchor and Archimedes screw impeller at different stirring speeds. (P=Zeolite Na-P1, Q=Quartz, M=Mullite, HS=Hydroxysodalite)

The most distinct changes in the XRD patterns of the fly ash when compared to those of the zeolitic products are the disappearance of the quartz and mullite peaks (showing complete conversion of the FA mineral phase) and the appearance of new crystalline phases. Another significant change observed in the XRD patterns of the zeolitic products was the disappearance of the broad hump (between 18 to 32 degrees 2θ) signifying the presence of the amorphous phase that was observed in the patterns of the raw fly ash. The disappearance of this hump signifies that the amorphous glassy phase was used up during the zeolite formation process. The major crystalline phase obtained after the activation of FA with NaOH solution and hydrothermal synthesis was zeolite Na-P1 ($\text{Na}_6\text{Al}_6\text{Si}_{10}\text{O}_{32}\cdot 12\text{H}_2\text{O}$) (with the strongest peak at $28^\circ = 2\theta$), with different yields, depending on the experimental

conditions. Along with this zeolitic product, hydroxysodalite crystallised as a trace phase in some cases.

The XRD spectra of the products obtained with an anchor impeller (Table 3.2, Figure 5.1b) showed that zeolite Na-P1 ($\text{Na}_6\text{Al}_6\text{Si}_{10}\text{O}_{32}\cdot 12\text{H}_2\text{O}$) was the only zeolite phase synthesised. The XRD spectra of the products obtained with the abovementioned impeller at 150 and 300 rpm demonstrated a pure phase of zeolite Na-P1 with percentage crystallinity of 91 % and 96.1 % respectively. Unexpectedly, the characteristic XRD peaks of mullite and quartz still remained after 48 hours of hydrothermal reaction at a stirring rate of 200 rpm. This meant that the product obtained under these conditions was a mixture of zeolite Na-P1 and fly ash, since quartz and mullite remained undissolved. As aforementioned in Chapter 4, these phases have been observed by several authors to show low or no reactivity in alkaline solutions. Under these conditions (anchor impeller, 200 rpm), the crystallinity of zeolite Na-P1 was found to be 56.0 %. In this case, it was concluded that the only source of Si and Al for zeolite crystallisation was the amorphous glass phase. These experiments were repeated in order to show the reproducibility of the results, and similar results were obtained. The reason for the results obtained with the anchor blade at 200 rpm was unknown. However, it can be said that in order to obtain a pure high crystalline zeolite Na-P1 product with the anchor impeller, agitation must be performed at high speeds (>300 rpm). A 4 flat-blade impeller was also investigated for the same activation conditions and agitation speeds.

In the set of experiments conducted with the use of a 4 flat-blade impeller (Table 3.2, Figure 5.1c), XRD showed that Na-P1 ($\text{Na}_6\text{Al}_6\text{Si}_{10}\text{O}_{32}\cdot 12\text{H}_2\text{O}$) was the only phase that crystallised after the activation of fly ash with NaOH at all agitation speeds investigated (150, 200 and 300 rpm). The results obtained with the use of this impeller showed complete dissolution of fly ash resulting in the crystallisation of a pure phase of zeolite Na-P1. The crystallinity of the products obtained under these conditions (Table 3.2.) is shown in Table 5.1. It was observed that highly crystalline products with a 100 % crystallinity were obtained at lower speeds i.e. 150 and 200 rpm. The crystallinity of zeolite Na-P1 decreased with an increase in agitation speed during aging i.e. from 100 % at 200 rpm to 94.9 % at 300 rpm. Based on these results, it can therefore be said that the use of a 4 flat-blade impeller for agitation during the aging step leads to the crystallisation of a pure phase zeolite Na-P1 at lower agitation speeds. This can be attributed to high shearing that is produced by this type of impeller. 4 flat-blade impellers are known to produce regions of high shearing around their blades (localised shearing) (Hemrajani and Tatterson, 2004). This facilitates the breaking of the Al-O and Si-O bonds in the fly ash and therefore a faster rate of dissolution of Al_2O_3 and SiO_2 from the fly ash into the alkaline solution. Therefore, shearing is required during the aging step of the zeolite synthesis process in order to increase the amounts of Si^{4+} and Al^{3+} extracted from fly ash into the alkaline solution. Consequently, the use of a 4-blade impeller leads to complete

dissolution of fly ash into the alkaline solution. Complete dissolution of fly ash is necessary in order to make available the nutrients required for the growth of zeolite crystals and this may lead to an increase in the yield of zeolites.

When comparing the results obtained with a 4 flat-blade to those obtained with an anchor impeller (Figure 5.1b and c), it can be noticed that at low agitation speeds i.e. 150 and 200 rpm, a 4-blade impeller produced high crystalline products with 100 % crystallinity for both speeds compared to 91.0 % at 150 rpm and 56.0 % at 200 rpm with an anchor impeller. When comparing the 4-blade impeller to the other two impellers (Anchor and Archimedes screw) at all the speeds (150, 200 and 300 rpm), the 4-blade impeller appears to be the best impeller for agitation in the aging step (Table 5.1).

Table 5-1: Percentage crystallinity of zeolite Na-P1

Impeller	Speed (rpm)	% Crystallinity	Impurities
4 flat-blade	150	100	-
	200	100	-
	300	94.9	-
Screw	150	92.1	-
	200	94.7	-
	300	69.4	±30 % hydroxysodalite
Anchor	150	91.0	-
	200	56.6	±40 % mullite
	300	96.1	-
Magnetic Stirrer	800	93.0	-

In the set of experiments conducted with the use of an Archimedes screw impeller (Table 3.2, Figure 5.1d), XRD showed that Na-P1 was still the dominant phase, accompanied by traces of hydroxysodalite at 300 rpm and a pure phase of Na-P1 was obtained at 150 and 200 rpm. Since the product obtained at 300 rpm was a mixture of Na-P1 and hydroxysodalite, this was therefore regarded as an impurity. The formation of the hydroxysodalite phase may be due to several reasons. The successive transformation of zeolite Na-P1 into hydroxysodalite based on Ostwald's rule of successive phase transformation may be one reason. This rule states that "the first phase to crystallise from a solution will be a hydrothermally least stable phase but with time, this phase will transform to more stable and denser phases" (Barrer, 2007). In addition, studies by Singer and Berggaut (1995) also pointed out that zeolite Na-P1 would be the first zeolite to form but found that it

can be gradually replaced by hydroxysodalite with increasing reaction time and temperature. Since the hydrothermal temperature and time were kept constant (i.e. 140 °C and 48 hours respectively), the extended synthesis time might not be the reason for the formation of hydroxysodalite. Another reason may be that since the reaction mixture produces a viscous gel if agitation is inadequate, an inhomogeneous reaction mixture may result with pockets of gel having different compositions and consistency. This leads to the crystallisation of unwanted or different zeolitic materials (Caschi, 2005). The only difference noticed between the products obtained at 150 and 200 rpm with the screw impeller was the increase in the crystallinity of zeolite Na-P1 from 92.1 % at 150 to 94.7 % at 200 rpm. It can therefore be said that with a screw impeller, it is not necessary to stir at higher stirring speeds (>300 rpm) during aging since a pure phase of zeolite Na-P1 with high crystallinity can be obtained at lower impeller speeds.

These investigations proved for the first time that different impeller designs and agitation during the aging step can have a profound impact on the zeolitic product quality. Therefore, it is not only the hydrothermal synthesis conditions and the molar regime, but also the dissolution kinetics of the feedstock, which influence the outcome of the zeolite synthesis process.

5.3.1.2. Structural analysis of the synthesised zeolites

The infrared spectrum allows the differentiation of various types of bonding modes in a material on a molecular level and also provides information with regard to the ordering and arrangement of the three-dimensional network structures. The FTIR spectra bands were assigned in accordance with the generally accepted practice for the silicate and zeolite families of compounds, as shown in Table 5.2.

Table 5-2: Overview of mid-infrared vibrations of zeolites (cm^{-1}) (Breck, 1974)

Internal tetrahedra	Asym. stretch	1250-950
	Sym. stretch	720-650
	T-O bend	500-420
External tetrahedra	Double rings	650-500
	Pore opening	420-300
	Sym. stretch	750-820
	Asym. stretch	1150-1050

The FT-IR spectrum for FA (Figure 5.2, green) shows the three wide bands characteristic of aluminosilicates. The peak observed at 1053 cm^{-1} is associated with T-O (T=Si, Al)

asymmetric stretching vibrations and may be attributed to the presence of quartz. The broadening of this peak may be due to the merging of FT-IR peaks corresponding to the other metal oxides present in the FA. The broad bands appearing at 800 and 550 cm^{-1} correspond to quartz and mullite, respectively, present in the FA. The band at 420 cm^{-1} is associated with T-O bending vibrations. (Reyes, 2008).

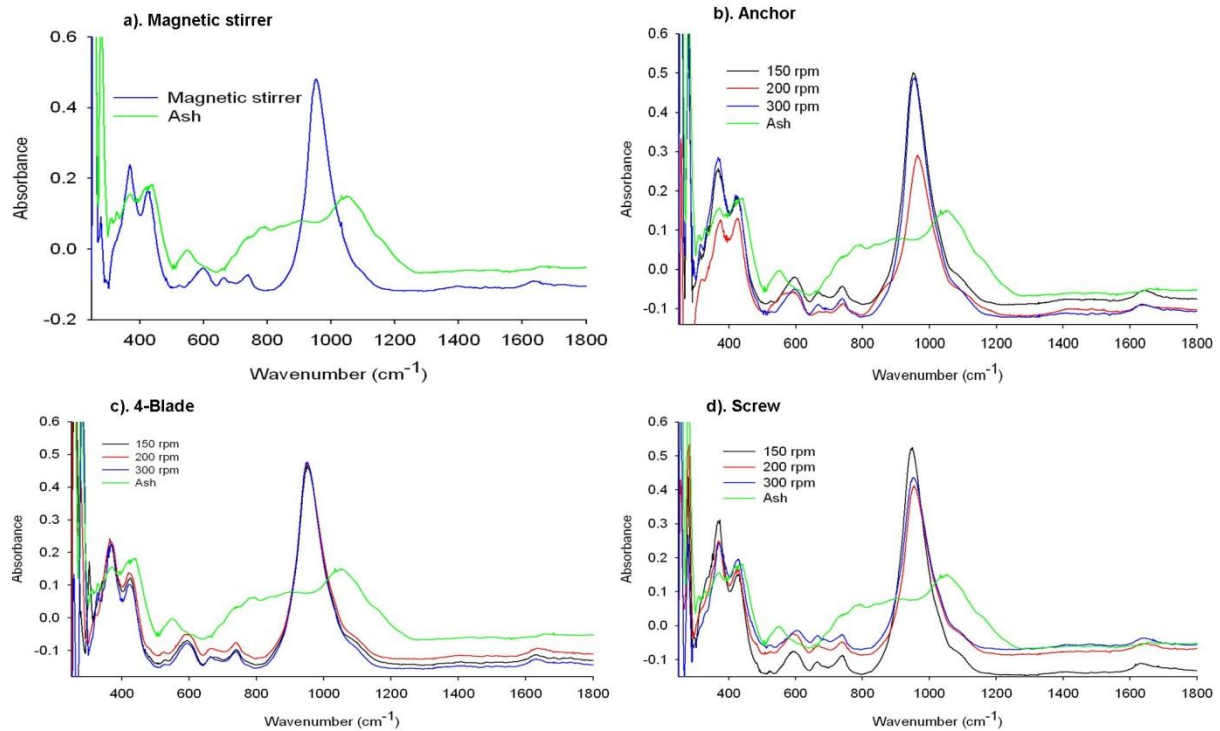


Figure 5-2: FTIR spectra of the zeolitic products synthesised using different impellers with variation of stirring speed.

In the FTIR spectra of the synthesised zeolites, the characteristic vibration bands of fly ash disappeared, accompanied by the appearance of new peaks that reveal the typical vibrations of zeolites. The IR vibrations common to all zeolites are the asymmetric stretching modes, which appear in the region 950 to 1250 cm^{-1} (Musyoka, 2009; Breck, 1974). These bands have been reported to be sensitive to the Si/Al ratio of the product analysed (Fernandez-Jimenez and Palomo, 2005; Breck, 1974). It can be seen that in all the IR spectrum of the synthesised zeolites (Figure 5.2a, b, c and d), the T-O band at 1053 cm^{-1} of the original fly ash (Figure 5.2c, green) became sharper and shifted perceptibly to lower frequencies. All these displacements denote that the vitreous component of the fly ash reacted with NaOH to form the zeolite structure. Since this section focuses on the effect of impeller design and agitation on the phase and purity of the zeolites synthesised, discussion on the effects of these parameters will be based on the changes that this band (T-O asymmetric stretching) undergoes, depending on the experimental conditions. However, other bands common to all zeolites are discussed below. The next strongest bands are found in the 420 to 500 cm^{-1} region and are attributed to the internal tetrahedron vibrations of the T-O bending mode

(Breck, 1974). These bands are also found in all zeolites. Bands in the region 300 to 400 cm^{-1} are assigned to the external linkages and are related to pore opening or the motion of the tetrahedral rings which form the pore opening of zeolites.

In the spectra shown in Figure 5.2a, b, c and d, it can be seen that the main zeolite band associated with the T-O asymmetric stretching vibrations (950 to 1250 cm^{-1}) shifts perceptibly when compared to that in the original fly ash. This band shifted to the lower frequencies (around 850 to 1160 cm^{-1}) with its centre at approximately 950 cm^{-1} . This can be attributed to the increase in the number of tetrahedrally positioned Al atoms in the zeolite product as compared to those in the fly ash (Rees *et al.*, 2007; Fernandez-Jimenez and Palomo, 2005; Breck, 1974).

According to Criado *et al.* (2007), the main zeolite band associated with the T-O asymmetric stretching vibrations provides information on the degree of crystallinity of a sample. This can be confirmed by looking at the IR spectra of the anchor impeller (Figure 5.2 b). From these spectra, it was observed that the intensity of this band in the product synthesised using the anchor blade at 200 rpm was the lowest, signifying that the crystallinity of this product was low. This was also shown in the XRD results (Figure 5.1b, Table 5.1) above. In addition, the exact position of this band appears in slightly higher wavenumbers (centred at 970 cm^{-1}) than that of the products obtained at 150 and 300 rpm (centred at 950 cm^{-1}). This basically means that the Si/Al ratio of this product (anchor, 200 rpm) was higher than that of the other products (150 and 300 rpm) as this band is sensitive to Si/Al ratio. Thus, this confirms the results obtained from the XRD analysis of this product that fly ash did not completely dissolve, as some of the Al was still incorporated in the mullite phase leading to increased Si/Al of the product.

The IR spectra of the products synthesised using a 4 flat-blade impeller (Figure 5.2c) show that bands of the T-O vibrations at different speeds overlap from 880 to 1060 cm^{-1} (centred at 950 cm^{-1}) and this made it difficult to interpret. However, this may be due to the Si/Al ratio and the concentration of these zeolite products being the same. Based on this results, it can be said that under these conditions (4-blade- 150 , 200 and 300 rpm) fly ash was completely dissolved liberating all the Si^{4+} and Al^{3+} from the solid phase (FA) into the solution (NaOH), leading to similar Si/Al of the zeolite products. These results were in good agreement with the results of the XRD analysis discussed previously. It can also be seen that with the screw impeller (Figure 5.2d), there was also complete dissolution of fly ash. The T-O asymmetric stretching vibrational bands of all the products obtained with the screw impeller lie in the region of 850 to 1160 cm^{-1} wavenumbers with its centre at approximately 950 cm^{-1} . Thus, these products possess similar Si/Al ratio. Based on these observations, it can be said that

FTIR is a good complementary technique for XRD, confirming phase purity and the crystallinity of the zeolite product.

5.3.1.3. Morphological characterisation by SEM

Scanning Electron Microscopy analyses were carried out only on the most crystalline zeolite Na-P1 product following the procedure outlined in Chapter 3, section C. The zeolite product obtained with the use of a 4 flat-blade impeller at 200 rpm was identified as the most crystalline zeolite product (100 % crystallinity) based on the XRD and FTIR analysis.

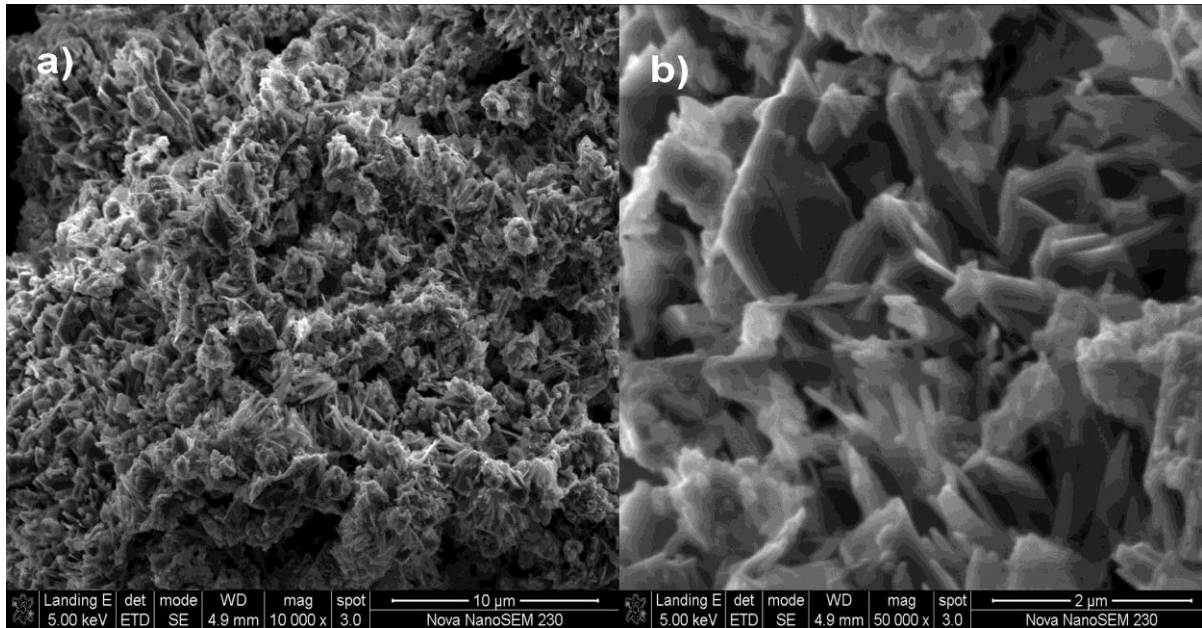


Figure 5-3: SEM images of zeolite Na-P1 synthesised with the 4 flat-blade impeller at 200 rpm. a) and b) both show zeolite Na-P1

The SEM images of the surface of the synthesised zeolites revealed a clear transformation of the spherical particles characteristic of the fly ash (Figure 4.4) into needle-like crystalline structures. These needle-like structures were identified from XRD analysis as zeolite Na-P1. According to the literature, this morphology has been shown to be a typical morphology for zeolite Na-P1 (Lee and Jo, 2010; Moutsatsou *et al.*, 2006; Garcia-Martinez *et al.*, 2002). The spherical ash particles were dissolved in an aqueous alkali solution and recrystallised to form the irregularly shaped zeolite as shown in Figure 5.3.

5.3.1.4. Summary

A pure phase of zeolite Na-P1 was successfully synthesised with the use of different impellers at different speeds during the aging step. In some cases, zeolite formation was assessed to be fairly unsuccessful, taking into account that the synthesis products contained a small percentage of hydroxysodalite ($\pm 30\%$) or mullite ($\pm 40\%$). SEM images showed that zeolite Na-P1 prepared in this study had a needle-like morphology. Based on the

experimental results, it was observed that the 4 flat-blade impeller was the optimum design of impeller that can be used for agitation during the aging step of the zeolite synthesis in a scaled-up process. Therefore, the 4 flat-blade impeller was used for agitation at 200 rpm during the aging step for all the experiments that were conducted from here on.

5.3.2. Effect of fly ash composition on the synthesis of zeolite Na-P1

As aforementioned in Chapter 2, fly ash differs from sample to sample depending on the coal source, type of coal burned, the boiler and its operating conditions and the process undergone by coal before combustion. Studies by Inada *et al.* (2005) showed that the chemical and mineralogical composition of the fly ash is one of the crucial factors influencing the zeolite synthesis outcome. For a large scale production of zeolites, the zeolite synthesis process must be optimised such that the conditions developed are suitable for any type of South African fly ash or fly ash source. Therefore, this section investigates the effects of the chemical and mineralogical compositions of two fly ash samples from the same power station on the synthesis of zeolite Na-P1.

5.3.2.1. Mineralogical and physical characterization

Experimental procedure and conditions for this part of the study were previously explained in section A of Chapter 3. The chemical and mineralogical compositions of the two batches of Arnot fly ash has been given and discussed previously in Chapter 4. Two batches of fly ash (FA) from the same power station, Arnot, were treated under the same synthesis conditions but yielded different zeolitic products. The main zeolites obtained from these experiments were zeolite Na-P1 and Analcime. Figure 5.4 illustrates the zeolitic products obtained when two batches of Arnot fly ash were used as starting materials for the synthesis of zeolite Na-P1 using the modified optimum conditions reported by Musyoka (2009).

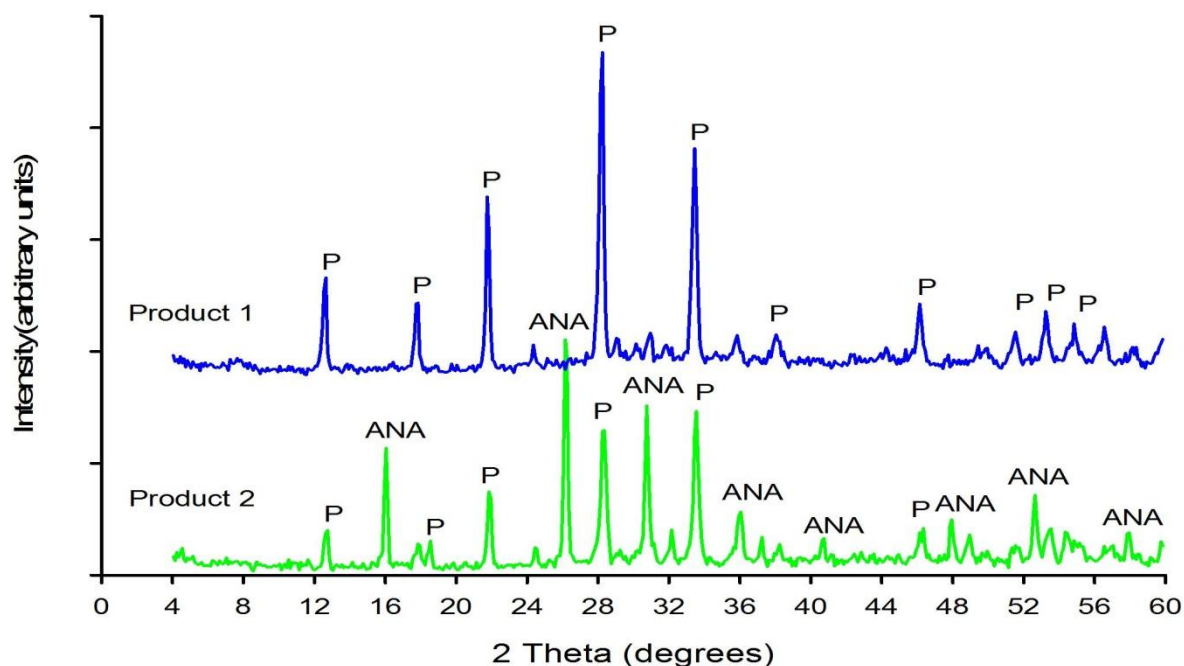


Figure 5-4: XRD spectra of the zeolites synthesised with the use of two batches of Arnot FA. Product 1 and 2-zeolites synthesised using Arnot batch 1 and batch 2 fly ashes respectively, P-Na-P1 and ANA-Analcime.

When batch 1 of Arnot FA was used as the starting material (product 1), a pure phase of zeolite Na-P1 was obtained, whereas analcime coexisted with zeolite Na-P1 when batch 2 of this ash was used (product 2). In product 2, analcime was the most dominant zeolite phase, with zeolite Na-P1 appearing in lower amounts. Phase quantification of the zeolites synthesised was determined following the procedure and equation 3.2 outlined in section C of Chapter 3. It was found that analcime amounted to 56.0 % of product 2 with Na-P1 being 44 %. In this case, analcime was considered as a contaminant since it was not the targeted zeolite. However, it must be recalled that ANA is a denser mineral phase, illustrating an Ostwald ripening.

A previous study has reported optimum conditions for the synthesis of a pure phase of zeolite Na-P1 using Arnot FA as a starting material (Musyoka, 2009). However, based on these results it can be said that these conditions are not optimised for fly ashes that vary in mineralogical composition. Although products 1 and 2 were synthesised using FA from the same Arnot power station under the same synthesis conditions, the mineralogical composition of these products was different. As previously mentioned in Chapter 2, one parameter that has been reported to have a significant effect on the zeolitisation process and consequently the type of zeolite synthesised is the $\text{SiO}_2/\text{Al}_2\text{O}_3$ ratio of the starting materials. The $\text{SiO}_2/\text{Al}_2\text{O}_3$ ratio of batch 1 and batch 2 of Arnot FA was 1.99 and 1.76 respectively. Although the $\text{SiO}_2/\text{Al}_2\text{O}_3$ ratios of the two batches of FA were similar, Querol *et al.* (2002)

mentioned that different zeolite synthesis behaviour may be obtained while using the same activation conditions for a similar $\text{SiO}_2/\text{Al}_2\text{O}_3$ ratio of the fly ash.

The differences between these batches have been explained in detail in Chapter 4. However, it is important to mention that batch 1 of Arnot FA was found to be more reactive than batch 2. This is because batch 1 contained a large amount of the reactive amorphous glassy phase and a low content of the less reactive mullite and quartz phases compared to batch 2. As a study by Inada *et al.* (2005) has shown, the Si/Al ratio in the solution at an early stage is very important because it governs the type of zeolite to be synthesised from coal FA. In the same study, it was also observed that zeolite Na-P1 forms easily from a silica-rich FA. Therefore, the Si/Al ratio of the amorphous glassy phase is very important and has a large influence on the type of zeolite to be produced. This explains the formation of analcime in product 2 since batch 2 of Arnot FA consisted of low contents of amorphous glass phase and silica. Thus, the difference in the composition of product 1 and product 2 can be attributed to the difference in the mineralogical compositions of the two batches of Arnot FA. The formation of analcime has been further explained in section 5.3.4.2.1 below. If one seeks to synthesise a pure phase of zeolite Na-P1 on a large scale, the Si/Al molar ratio of the synthesis gel would need to be monitored and may require some adjustment by adding either SiO_2 or Al_2O_3 from a supplementary source. Inada *et al.* (2005) observed that addition of SiO_2 promoted the formation of zeolite Na-P1 whereas the addition of Al_2O_3 prevented it.

Figure 5.5 illustrates the FT-IR spectra of the raw fly ash and the synthesised zeolitic products. The assignments of the FTIR spectra bands were done in accordance with the generally accepted practice for the silicate and zeolite families of compounds, as shown in Table 5.2.

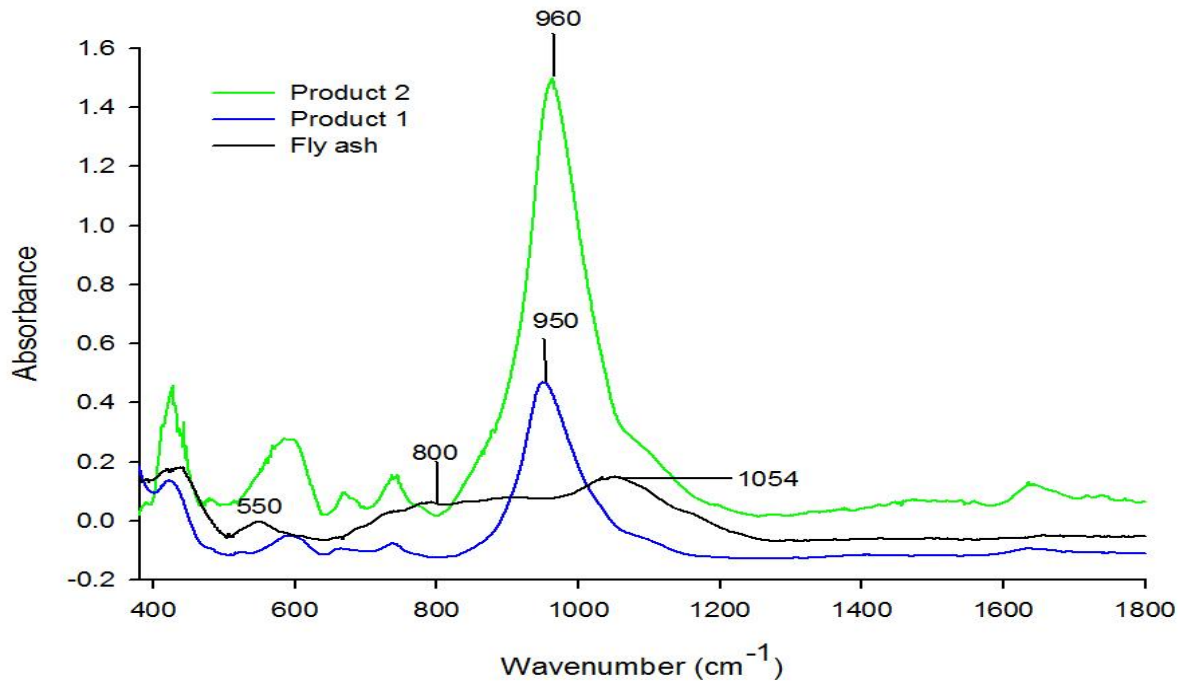


Figure 5-5: FTIR spectra of FA and the zeolitic products. Product 1 and 2-zeolites synthesised using Arnot batch 1 and batch 2 fly ashes respectively.

In the FTIR spectra of the synthesised zeolites (Figure 5.5), the characteristic vibration bands of FA disappeared, accompanied by the appearance of new peaks that reveal the occurrence of zeolites. The IR vibrations common to all zeolites are the asymmetric stretching modes, which appear in the region 950 to 1250 cm^{-1} (Musyoka, 2009; Breck, 1974). It can be seen that in the IR spectra of the synthesised zeolites, the T-O asymmetric stretching vibrations band at 1054 cm^{-1} of the original FA became sharper and shifted perceptibly to lower frequencies (around 850 to 1160 cm^{-1}) with its centre at approximately 950 cm^{-1} . This can be attributed to the increase in the number of tetrahedrally positioned Al atoms in the zeolite product as compared to the FA (Rees *et al.*, 2007; Fernandez-Jimenez and Palomo, 2005; Breck, 1974). In addition, the exact position of this band in product 2 appears at slightly higher wavenumbers (centred at 960 cm^{-1}) than that of the product 1 (centred at 950 cm^{-1}). This basically means that the Si/Al ratio of product 2 was higher than that of product 1, as this band is sensitive to Si/Al ratio. All these displacements denoted that the vitreous component of the FA reacted with NaOH to form zeolites.

Figure 5.6 shows SEM images of representative zeolitic products synthesised from the two batches of Arnot FA.

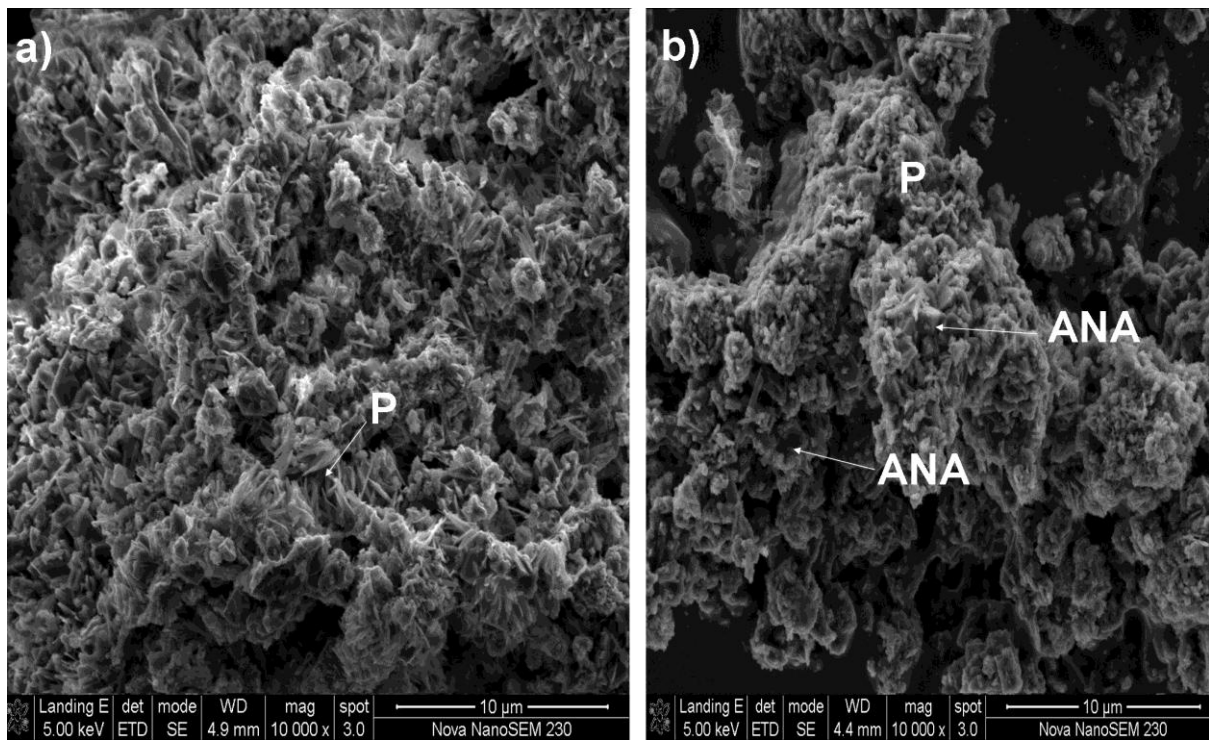


Figure 5-6: SEM images of fly ash and the synthesis products. (a) Pure phase of Na-P1. (b) Na-P1 and Analcime. (P-zeolite Na-P1 and ANA-Analcime).

The SEM images of the surface of the synthesised zeolites showed a clear transformation of the spherical particles of the fly ash into needle-like (Figure 5.6a) and trapezoidal-like (Figure 5.6b) crystalline structures. These needle-like and trapezoidal-like structures were identified from XRD analysis as zeolite Na-P1 and analcime respectively. The morphology of these zeolites was similar to that reported in literature (Lee and Jo, 2010; Taylor, 2007; Moutsatsou *et al.*, 2006; Garcia-Martinez *et al.*, 2002).

5.3.2.2. Synthesis of zeolite Na-P1 from other South African coal fly ashes

Since Hendrina and batch 2 of Arnot fly ash had similar mineralogical compositions (as shown in Table 4.3), Hendrina FA was used as a feedstock for the synthesis of zeolite Na-P1. Hendrina FA and Arnot batch 2 FA had the lowest content of the amorphous glassy phase compared to all the fly ashes evaluated. The same activation conditions as those that were used for batch 2 of Arnot FA were applied. The XRD results (Figure 5.7) confirmed that the content of the amorphous glassy phase is very important for zeolite synthesis. Similar results as those obtained with batch 2 of Arnot FA were observed.

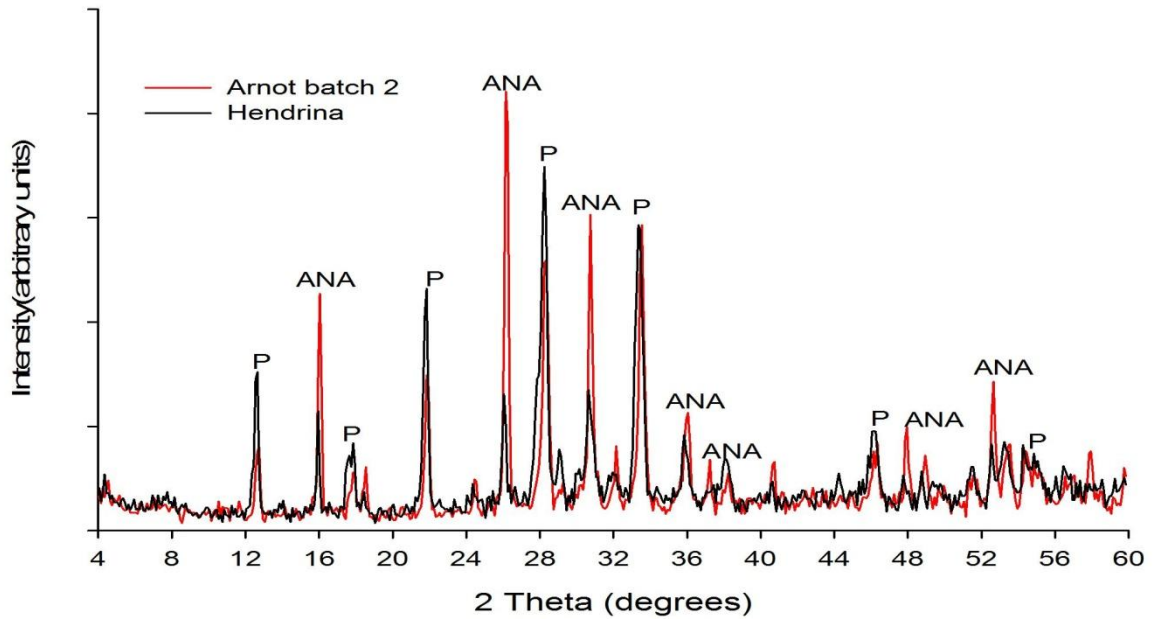


Figure 5-7: Zeolitic products synthesised using Arnot batch 2 and Hendrina fly ashes. (ANA-Analcime and P-zeolite Na-P1)

The major difference observed in the XRD analysis of Arnot batch 2 and Hendrina feedstock products was that the peaks of analcime in the product obtained with Arnot (batch 2) FA were more intense than those in the product obtained with Hendrina FA. Despite that, the mineralogical composition of the two products was the same, as both products contained zeolite Na-P1 and Analcime only, according to XRD results presented above.

Musyoka (2009) used fly ash from Duvha power station (Eskom's power station located in Mpumalanga, South Africa) to synthesise zeolite Na-P1 under the same conditions as those used for Arnot and Hendrina ashes. The only difference in the synthesis conditions was that Musyoka (2009) used a magnetic stirrer at 800 rpm to induce agitation during the aging step whereas a 4 flat-blade impeller was used at 200 rpm in this study. The mineralogical composition of Duvha fly ash was similar to that of the two ashes under discussion (Arnot batch 2 and Hendrina). The author observed that a pure phase of zeolite Na-P1 could not be obtained. In this case, the product obtained was a mixture of mullite and zeolite Na-P1 confirming the results found using Hendrina and Arnot batch 2 ashes. The presence of mullite in his product can be explained by the fact that a magnetic stirrer used for agitation during aging did not produce enough shearing to enhance the dissolution of this FA phase (mullite), although it was used at a higher agitation speed (800 rpm). This study, thus, proved that a pure phase of zeolite Na-P1 could not be obtained from fly ash with low amorphous phase content under the synthesis conditions studied.

A study on the use of other South African fly ashes, i.e. Tutuka, Lethabo and Matla, for the synthesis of zeolite Na-P1 was conducted by Molapo (2010). The chemical and mineralogical compositions of these ashes have been previously discussed in Chapter 4. Molapo (2010) observed that it was possible to synthesise zeolite Na-P1 from these ashes after 48 hours of aging at 47 °C under magnetic stirring and 48 hours of hydrothermal treatment at 140 °C under static conditions. Although these were high amorphous phase fly ashes, 100 % pure zeolite Na-P1 could not be obtained since traces of undissolved mullite, quartz and magnetite were observed in the products obtained with Lethabo and Matla fly ash. A pure phase of zeolite Na-P1 was only obtained from Tutuka FA in her study. This may be due to the fact that Tutuka FA had the same Si/Al ratio and similar mineralogical composition as Arnot batch 1 FA (Table 4.1 and 4.3), which (Arnot batch 1 FA) produced a pure phase of zeolite Na-P1 in the current study. The two ashes sourced from Lethabo and Matla power stations had lower Si/Al ratios when compared to Arnot batch 1 and Tutuka ashes, which may have influenced the desired outcome, as the amorphous glass content in these ashes was high. This makes the Si/Al ratio and the mineralogical composition of fly ash very important for the synthesis of zeolite Na-P1.

5.3.2.3. Summary

The effect of FA composition and mineralogical phase content on the phase purity of zeolite Na-P1 produced was investigated. This was achieved by treating two fly ash samples from the same power station (Arnot) under the same synthesis conditions. The main zeolites obtained from these experiments were zeolite Na-P1 and analcime. A pure phase of zeolite Na-P1 was successfully synthesised from the fly ash with higher amorphous glass phase content, whereas a mixture of zeolite Na-P1 and analcime was obtained from a low amorphous glass phase content fly ash. The results demonstrated that the efficiency in the conversion of FA into zeolites is affected by the contents of non-reactive FA phases (mainly mullite and quartz) as well as the amorphous glass phase content. This was confirmed by a study on Hendrina FA, which is also low in amorphous glass phase. The content of the amorphous glass phase was found to be crucial for the formation of zeolite Na-P1 since it easily dissolves into the alkaline solution. The scale-up synthesis of a pure phase of zeolite Na-P1 from various FA sources would be problematic, since this zeolite seemed to be sensitive to the $\text{SiO}_2/\text{Al}_2\text{O}_3$ ratio and the mineralogy of the fly ash. Adjustment of the Si/Al molar ratio of the synthesis gel by adding either SiO_2 or Al_2O_3 from a supplementary source may be necessary if a pure phase of zeolite Na-P1 is targeted. In order to produce a pure phase of zeolite Na-P1 from low amorphous glass content FA, further optimisation of the synthesis conditions would be required.

5.3.3. The use of different water sources for synthesis of zeolite Na-P1

As aforementioned, most of the studies on zeolites have been performed with the use of ultrapure water as a solvent to avoid the complicating effects of ions such as calcium (Caschi, 2005). However, the use of ultrapure water on an industrial scale would have serious implications on the production costs. Therefore, there is a need to investigate the synthesis of zeolite Na-P1 using different sources of water such as municipal tap water, acid mine drainage (AMD) and distilled water. The utilisation of these water sources as an alternative to ultrapure water would reduce the costs of utilities during synthesis of zeolites on a large scale. The use of AMD to synthesise zeolites would also help reduce the pollution caused by the disposal of this raw AMD water. The main aim of this investigation was to assess the possibility of synthesising zeolite Na-P1 from different water sources with the view of establishing a benchmark for the scale-up operation. In this set of experiments, batch 2 of Arnot FA was used as the feedstock for the synthesis of zeolite Na-P1 under the following conditions; aging at 47 °C for 48 hours under magnetic stirring and 48 hours of hydrothermal treatment at 140 °C under static conditions.

5.3.3.1. Characterisation of the acid mine drainage

As stated earlier, the acid mine drainage used in this study was collected from a uranium mine situated in Gauteng, South Africa. Table 5.3 summarises the pH, EC and the chemical composition of the AMD. The analyses for anions and cations were done using ion chromatography (IC) and inductively-coupled plasma (atomic emission and mass) spectroscopy (ICP-AES/MS) respectively. The table below only presents the concentration of the major elements that were observed in the AMD water. Nonetheless, minor elements such as Ba, Pb, K, Na, B, Zr, Zn, Y, Cu and Sr were found to exist in concentrations between 0 to 1 ppm.

Table 5-3: Composition of the AMD

Element	Concentration (ppm)
Mg	96.75 ± 4.67
Fe	294.81 ± 16.75
Ca	24.00 ± 1.52
Mn	22.54 ± 0.759
Cr	3.09 ± 0.323
Al	3.98 ± 0.630
SO ₄ ²⁻	4045.56 ± 68.86
NO ₃ ⁻	1231.41 ± 23.79
Cl ⁻	62.38 ± 2.28
pH	3.49 ± 0.49
EC (mS/cm)	3.37 ± 0.16

It can be inferred from the table above that the water (AMD) used in this study was characterised by high concentrations of Mg, Ca, Mn and Fe. This water was also found to contain high concentrations of SO₄²⁻, NO₃⁻ and Cl⁻ as shown in Table 5.3. The water (AMD) used in this study was acidic as indicated by the pH (pH=3.49). The acidic characteristic of the AMD results from the percolation of water through sulphide minerals, generally pyrite, which oxidises and dissociates when in contact with air and water. Thus, Fe²⁺ is released and rapidly oxidised to Fe³⁺, which precipitates as hydroxides. After the onset of the reaction, a cyclic series of events takes place, starting with the oxidation of Fe²⁺ to Fe³⁺, which is subsequently reduced by pyrite, releasing Fe²⁺ which increases the solution's acidity (Reyes, 2008; Snoeyink and Jenkins, 1980). This AMD had an orange-brown colour due to the very high concentrations of ferric iron in solution.

The AMD contained significant amounts of Fe, Mg and Ca i.e. 294.81, 96.75 and 24 ppm respectively. As aforementioned in Chapter 4, these elements have been reported to interfere with the zeolite crystallisation process. Ca²⁺ and Mg²⁺ were reported to act as competing ions during zeolite synthesis. Ca²⁺ was also reported to have structure-breaking

properties which lead to interference with the zeolite crystallisation process (Catalfamo *et al.*, 1993). It was also reported that Ca-bearing phases can act as an inhibitor for the synthesis of zeolites through the formation of calcium silicate (Ríos *et al.*, 2009; Juan *et al.*, 2007). Fe-bearing minerals were also found to show an inert behaviour during zeolite synthesis (Juan *et al.*, 2007). Thus, the lower the content of Ca, Mg and Fe, the less the interference during the crystallisation of zeolites. Since this water had high amounts of the Ca, Mg and Fe, possible interference during the zeolite formation process was expected.

5.3.3.2. Characterisation of tap and distilled water

Table 5.4 summarises the chemical composition of tap and distilled water used in this study. The analyses were done using inductively-coupled plasma (atomic emission and mass) spectroscopy.

Table 5-4: Composition of tap and distilled water

Element	Concentration (ppm)	
	Tap water	Distilled water
Al	9.01	0.0024
Ba	0.72	<0.001
Ca	29.76	0.0063
Cr	0.31	<0.001
Fe	2.78	<0.001
K	0.92	<0.001
Mg	10.11	0.0049
Na	21.94	0.24
Ni	1.91	<0.001
Zn	0.37	ND

*ND-Not detected

Tap water was found to contain higher amounts of Al, Ba, Ca, Cr, Fe, K, Mg, Na and Ni when compared to distilled water. All these metals occurred in concentrations between 0-1 ppm in the distilled water. Therefore, this water (distilled) was expected to have little to no interference in the crystallisation of zeolites, since all metals occurred in low concentrations. As stated earlier, in section 5.3.3.1, Ca²⁺ and Mg²⁺ were reported to act as competing ions during zeolite synthesis. These cations (Ca and Mg) compete with sodium (Na) in zeolite structure formation as charge-balancing cations. The concentration of these metals was slightly high in the tap water, i.e. Ca=29.76 ppm and Mg=10.11 ppm. However, at these concentrations, little to no interference was expected from these metals, since the Na used during the synthesis of zeolites was in much higher concentration than Ca and Mg in this water. During zeolite synthesis, Na is introduced in the form of NaOH as a charge balancing cation. In the tap water, Na concentration was also found to be high (i.e. 21.94 ppm). Other

metals such as Zn, Fe, Ba, K and Ni were found to exist in these waters, although their concentration was low.

5.3.3.3. Mineralogical and physical analysis of the synthesis products

The mineralogical compositions of the products obtained with the use of tap, distilled and AMD water were compared to that of the product obtained when ultrapure water was used as a solvent. Figure 5.8 illustrates the XRD spectra of the reaction products obtained when different waters were used under the conditions mentioned above.

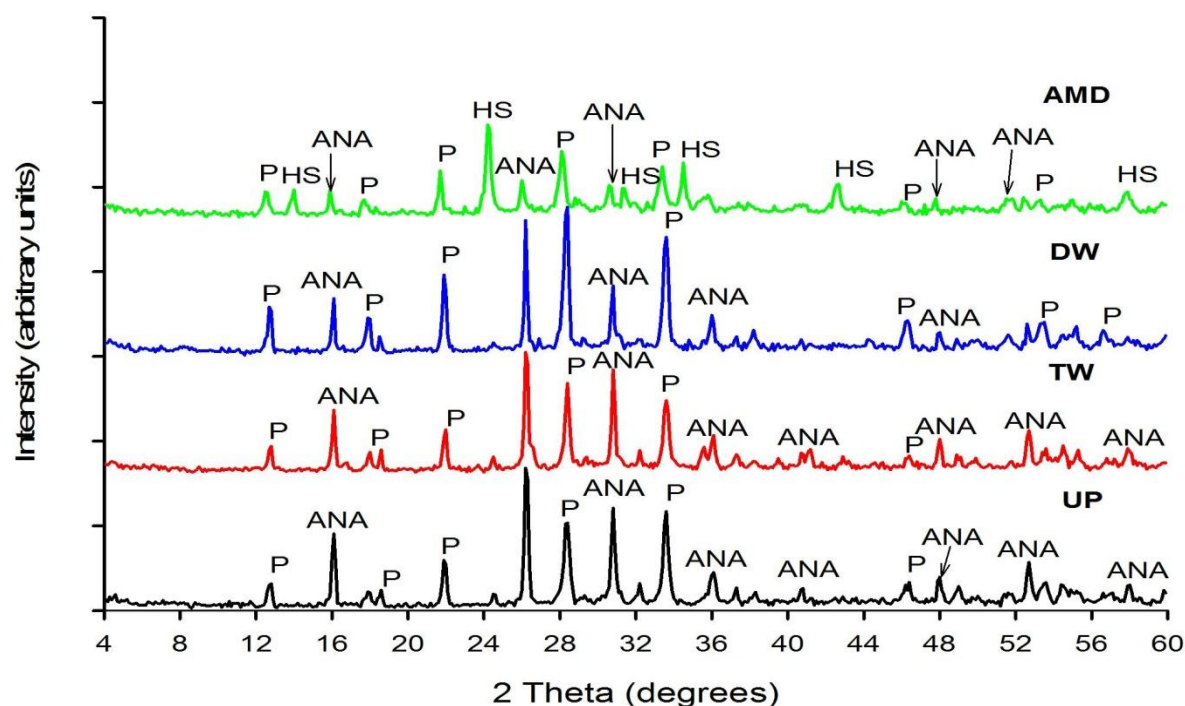


Figure 5-8: XRD patterns of the synthesis products obtained when different waters were used as solvents. (UP-Ultrapure water, TW-Tap water, DW-Distilled water, AMD-Acid mine drainage, P-zeolite Na-P1, ANA-Analcime and HS-Hydroxysodalite)

In this set of experiments, XRD (Figure 5.8) illustrated that zeolite Na-P1, analcime and hydroxysodalite were the main zeolite phases obtained when water from different sources was used as a solvent during zeolite synthesis. The main zeolite phases obtained when UP was used as a solvent were zeolite Na-P1 and analcime. As aforementioned in Chapter 3, batch 2 of Arnot fly ash was used as a starting material for these investigations. The difficulties associated with synthesising a pure phase of zeolite Na-P1 using this ash under the investigated synthesis conditions have been discussed in section 5.3.2 earlier. Nonetheless, the results obtained with UP were used as the basis for these investigations. The XRD patterns obtained when tap (TW) and distilled water (DW) were used for the synthesis of zeolites compared to those obtained when ultrapure water (UP) was used do not

show a significant difference. These patterns show complete dissolution of the fly ash phases (mullite and quartz) with zeolite Na-P1 and analcime being the only products observed when the three waters were used (TW, DW and UP). The only noticeable difference between these products was the decrease in the intensity of analcime peaks observed when distilled water was used. XRD patterns of the zeolitic products obtained when TW and UP were used were identical, as shown in Figure 5.8. This signifies the similarity of the products. Based on these results, it can be inferred that the presence of extra elements in the TW and DW had little to no influence on the zeolite products obtained, since the same zeolites (zeolite Na-P1 and analcime) obtained with UP water were obtained with these waters (TW and DW).

On the other hand, when AMD was used as a solvent, a new zeolite phase (hydroxysodalite) was observed, together with zeolite Na-P1 and analcime, as shown in Figure 5.8. In this set of experiments, zeolite Na-P1 and hydroxysodalite appeared to be the most dominant zeolite phases, with analcime occurring in trace amounts. In this case, hydroxysodalite can be regarded as a contaminant. Hydroxysodalite like analcime exhibits low cation exchange capacity, resulting in low potential industrial application. The formation of hydroxysodalite, in this case, can be attributed to several factors; the presence of Ca, Mg and Fe in higher concentrations, which might have interfered with the zeolite crystallisation process, as well as the low pH of the alkaline solution resulting from the mixing of AMD and NaOH. The effect of solution pH that might have resulted in the formation of hydroxysodalite is briefly explained below.

In this set of experiments, the AMD was mixed with NaOH pellets to make up a 5 M NaOH solution. Prior addition of NaOH pellets to the AMD, the pH of AMD was 3.49 as it has been discussed earlier. After the addition of NaOH to the AMD, the pH was found to be 5.38, which was still low for the synthesis of zeolites from the fly ash. Most studies on the synthesis of zeolites have been performed under basic conditions ($\text{pH} > 12$). This is because basic conditions facilitate the dissolution of Si and Al from the fly ash into the alkaline solution. Studies have shown that as the pH increases the rate of Si and Al dissolution also increases (Andini *et al.*, 2008; Pacheco-Torgal *et al.*, 2008; Fernández-Jiménez and Palomo, 2005; Inada *et al.*, 2005). In this case, the pH of the solution was low, which might have resulted in slow Si and Al dissolution kinetics leading to different Si/Al ratio in the solution, which might have favoured the formation of hydroxysodalite. Musyoka *et al.* (2011) used circumneutral mine water ($\text{pH} = 6.5$) and AMD ($\text{pH} = 2.5$) to synthesise zeolite A from coal fly ash. In that study, it was observed that when circumneutral mine water was used, a pure phase of zeolite A was observed. However, when the AMD was used, hydroxysodalite was observed to coexist with zeolite A. Based on these results it can be inferred that the chemical composition and the pH of the AMD had a significant influence on the type of zeolite produced.

SEM images of the zeolite products obtained with use of different water sources revealed interesting morphologies and are illustrated in Figure 5.9.

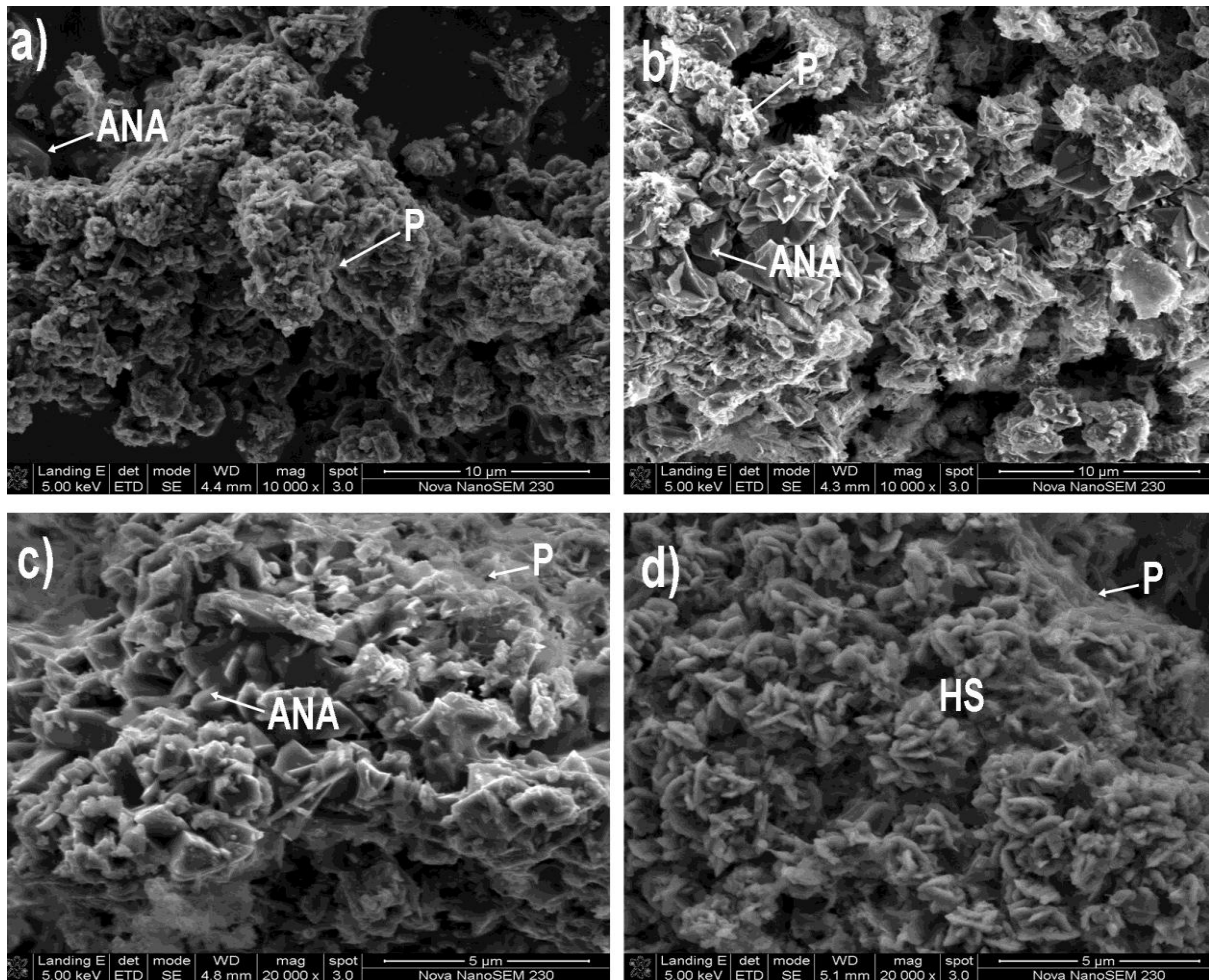


Figure 5-9: SEM images showing morphological aspects in the zeolitic products obtained when waters from different sources were used as solvents. a) UP b) TW c) DW d) AMD (P-Zeolite Na-P1, ANA-Analcime and HS-Hydroxysodalite)

Figure 5.9a to 5.9d illustrates SEM micrographs of the occurrence of typical morphologies for zeolite Na-P1, analcime and hydroxysodalite (HS) as had been identified by XRD. As denoted by the XRD patterns, the only zeolites that crystallised when UP, TW and DW were used were zeolite Na-P1 and analcime. These zeolites (zeolite Na-P1 and analcime) appeared as aggregates of randomly oriented needle-like and trapezoidal-like crystals respectively, as shown in Figure 5.9a to 5.9c. As aforementioned, similar morphologies were reported by Garcia-Martinez *et al.* (2002), Lee and Jo (2010), Moutsatsou *et al.* (2006), and Taylor (2007). The blade-shaped crystals in Figure 5.9d were identified as HS by XRD. In Figure 5.9d, analcime appears to be covered by HS and zeolite Na-P1 since it could not be recognised. These observations confirm the XRD results that when AMD was used (Figure 5.8), analcime appeared in small quantities as only a few weak peaks were identified.

5.3.3.4. Summary

The main aim of performing these experiments was to assess the possibility of synthesising zeolites (mainly zeolite Na-P1) from FA using different water sources. The results demonstrated that it is possible to synthesise zeolites using TW, DW and AMD. Zeolite Na-P1, analcime and hydroxysodalite were the main zeolite phases obtained. The extra elements present in the TW and DW did not influence the type of zeolite obtained, since the same zeolite phases obtained with UP water were obtained with these waters. In the case of AMD, zeolite formation was assessed to be fairly unsuccessful, taking into account that the synthesis product contained a substantial amount of HS, while a smaller fraction of the desired zeolitic phase was observed. Based on these results, it can be concluded that with further optimisation of the synthesis conditions, TW and DW can be used as a replacement for ultrapure water to synthesise a pure phase of zeolite Na-P1 on a large scale. However, AMD was not a suitable solvent for the synthesis of a pure phase of zeolite Na-P1.

5.3.4. Effects of hydrothermal reaction time

Failure to obtain a pure phase of zeolite Na-P1 from the low amorphous glass phase batch 2 of Arnot FA prompted further experiments to be conducted at different hydrothermal reaction times. The hydrothermal reaction time influences the phase, crystallinity and the morphology of the zeolitic products synthesised. The effects of this parameter were studied by varying the aging and the hydrothermal treatment time as described in Chapter 3, section 3.1.5.5. A mixture of batch 2 of Arnot FA and sodium hydroxide solution (reaction mixture) was aged at 47 °C for 12 to 48 hours under 200 rpm of stirring with a 4 flat-blade impeller and hydrothermally treated at 140 °C for 12 to 48 hours under static conditions. The experimental conditions are illustrated in Table 3.3. The main aim of conducting these experiments was to establish optimum conditions for the synthesis of a pure phase of zeolite Na-P1 from a low amorphous phase fly ash. As mentioned above, batch 2 of Arnot FA was used for these experiments since it contained low amorphous glass phase content.

5.3.4.1. Variation of aging time

Aging time is very important in this synthesis process owing to difficulties associated with the dissolution of the fly ash crystalline phases such as mullite and quartz, which in most cases appear as secondary products. The aging period permits the dissolution of fly ash (mostly the amorphous phase) while promoting the formation of nuclei, which are the building blocks of the final crystals. After aging, the subsequent crystallisation of zeolites at elevated temperatures proceeds more quickly than in non-aged cases.

5.3.4.1.1. Mineralogical analysis by XRD

The XRD patterns of the reaction mixture aged at different aging periods and hydrothermally treated for 12 hours are presented in Figure 5.10.

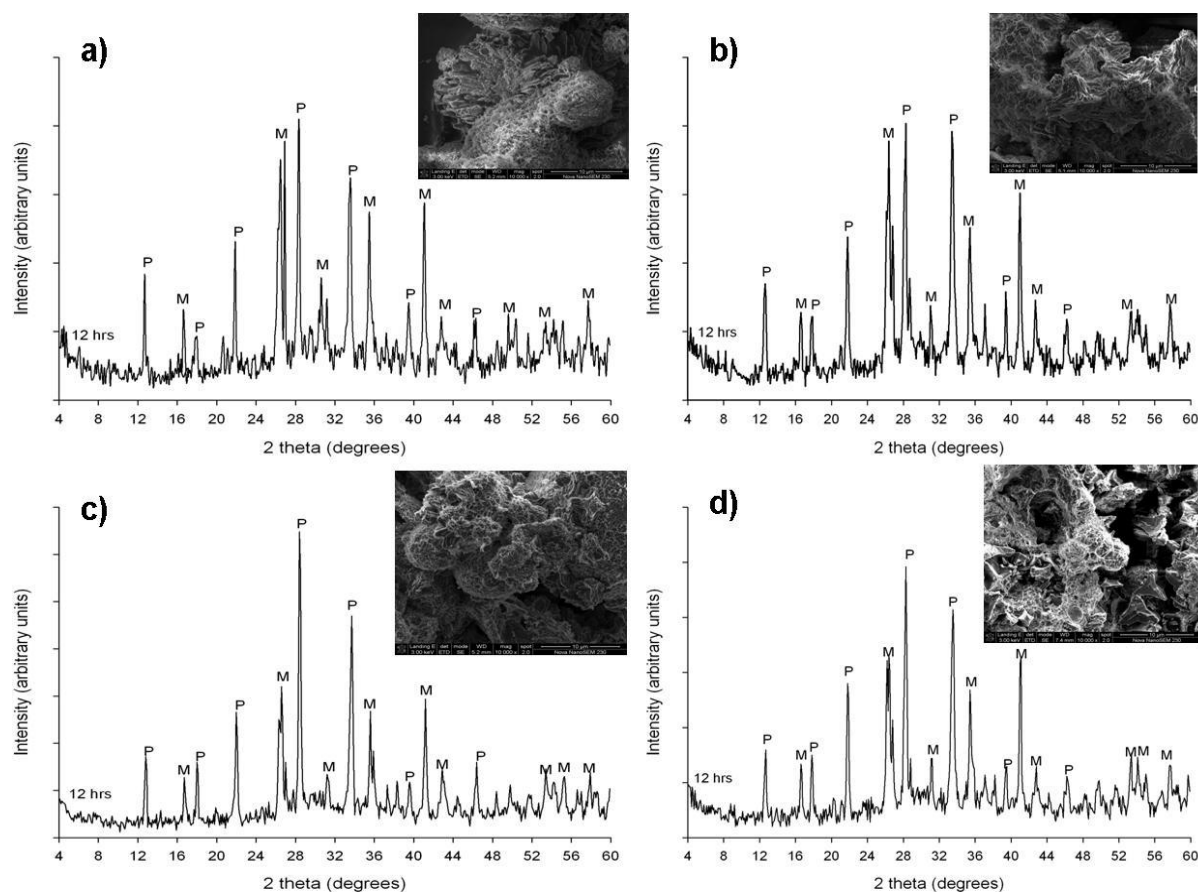


Figure 5-10: XRD patterns and SEM images of the synthesis products obtained after 12 hours of hydrothermal treatment at 140 °C and variation of aging period. a) 12 b) 24 c) 36 and d) 48 hours of aging. (M-Mullite and P-zeolite Na-P1).

The main synthesis products obtained after aging for different periods followed by crystallisation for 12 hours at 140 °C were mullite and zeolite Na-P1. Figure 5.10 shows a progressive decrease in the amorphous glassy phase (hump in the region between 18 and 44° 2 θ) as a function of time. Although quantification of the amorphous glassy phase was not done for the products shown in Figure 5.10, it can be observed in this figure that an increase in the aging time increased the dissolution of the amorphous glassy phase. This is denoted by the decrease in the hump (between 18 and 44° 2 θ) in the sample aged at 47 °C for 48 hours under 200 rpm of stirring. As aforementioned, the decrease or disappearance of this hump signifies that the amorphous glassy phase has been dissolved from the FA into the solution and subsequently consumed during zeolitisation.

5.3.4.1.2. Crystallinity

The effects of aging time were also determined by monitoring the crystallinity of mullite, zeolite Na-P1 and the Si/Al ratio of the synthesis solution after each aging period. The crystallinity of mullite and zeolite Na-P1 were calculated using equation 3.1. The sum of the area under four major peaks of mullite (around $2\theta=16, 26, 35$ and 41 degrees) and zeolite Na-P1 (around $2\theta= 12, 22, 28$ and 33 degrees) was used to calculate the crystallinity of each phase. The sum of the area under the same four major peaks of mullite in the raw fly ash was used as standard for the purpose of these calculations. The standard for zeolite Na-P1 used was the sum of the area under the same major peaks in the product synthesised at 36 hours of aging and 48 hours of hydrothermal treatment (Figure 5.14). The product was selected as the standard because its XRD spectra showed the highest intensity for the major peaks of zeolite Na-P1. This method was adopted from Gosh *et al.* (1994).

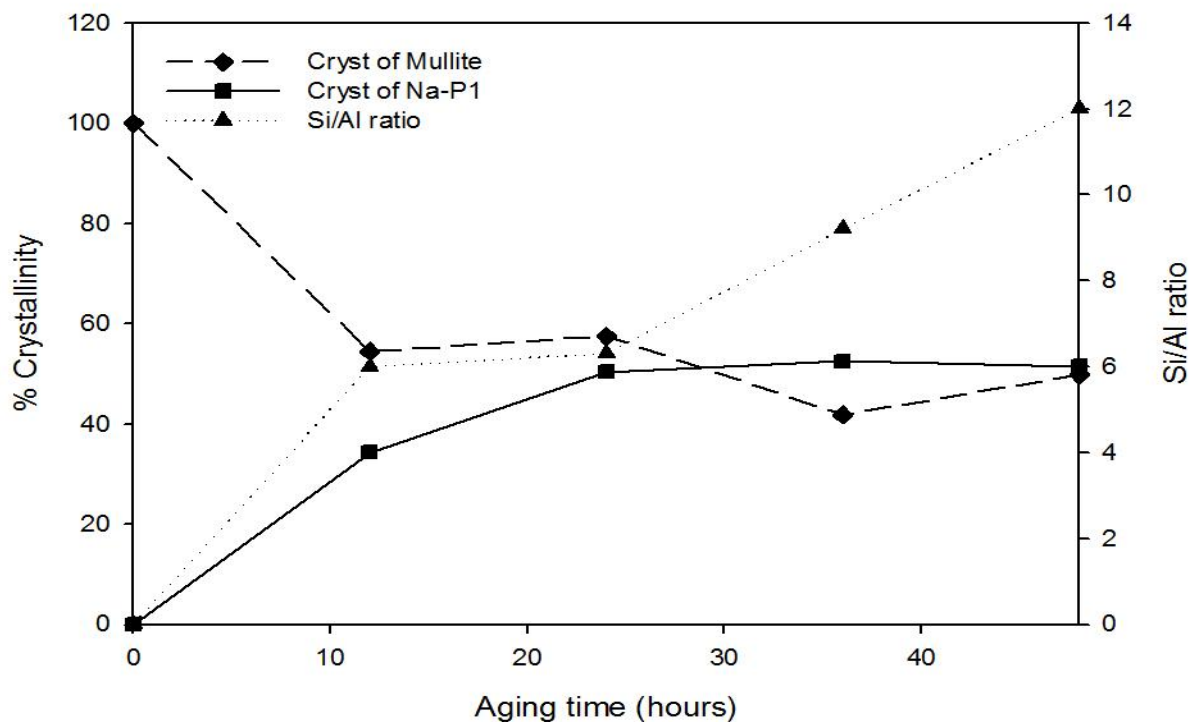


Figure 5-11: Percentage crystallinity of mullite and zeolite Na-P1 together with the Si/Al ratio of the synthesis solution as a function of the aging time.

The crystallinity of mullite and zeolite Na-P1 presented in Figure 5.11 was determined after aging for different periods followed by crystallisation for 12 hours at $140\text{ }^{\circ}\text{C}$ and these results are discussed below.

5.3.4.1.3. Si/Al ratio of the synthesis solution

It should be recalled that the Si/Al ratio in the synthesis solution at an early stage is important for deciding the type of zeolite to be synthesised (Inada *et al.*, 2005). The changes in the Si/Al ratio of the synthesis solution have been illustrated in Figure 5.11. Samples were taken after each aging period, filtered and analysed for major cations in the synthesis solution using ICP-AES/MS in order to determine the Si/Al ratio of the synthesis solution. As expected, the Si/Al ratio of the synthesis solution increased (0 to 12) with an increase in aging time. From 24 to 48 hours of aging, it was observed that there was a gradual increase in the dissolution of silicon from the solid phase into the liquid phase, leading to an increased Si/Al ratio. This high increase in the Si/Al ratio has been explained by Criado *et al.* (2010) as a result of the formation of the Al-rich aluminosilicate gel that occurs at an early stage of the aging step that further changes into a Si-rich gel as the reaction proceeds. In detail, the study explained that the formation of this Al³⁺ gel may be attributed to the fact that the Al-O bonds are weaker and can therefore be readily severed than the Si-O bonds, making reactive aluminium atoms readily soluble than silicon. As the reaction progresses, more Si-O groups in the solid particles dissolve, raising the silicate concentration in the medium. This gel gradually becomes richer in silicon (Criado *et al.*, 2010), hence increasing the Si/Al ratio. The maximum Si/Al ratio was about 12, obtained after 48 hours of aging. Since mullite was still present in high quantities after 48 hours of aging, it can be said that the silicon and aluminium in solution were from the amorphous and quartz phases of the feedstock. Studies by Inada *et al.* (2005) showed that high-Si concentration and low-Al concentration are the factors promoting the formation of zeolite Na-P1.

5.3.4.1.4. Crystallinity of mullite and zeolite Na-P1

The variation in crystallinity of mullite and zeolite Na-P1 with respect to aging time is also shown in Figure 5.11. The crystallinity of mullite decreased with increasing aging time until 36 hours (from 100 % in the fly ash to 41.8 %) and then increased slightly after 48 hours of aging (from 41.8 % after 36 hours to 49.8 % after 48 hours). The slight increase in the crystallinity of mullite from 36 to 48 hours may be due to several reasons. As can be seen in Figure 5.11, at 48 hours of aging the synthesis solution was concentrated with silicon, which might have led to the super-saturation of the solution, resulting in a decreased rate of mullite dissolution. As silicon and aluminium are being liberated from the solid phase into the solution, they react to form a viscous amorphous gel which tends to cover the surface of the fly ash particles, making it difficult for fly ash to dissolve. On the other hand, the crystallinity of Na-P1 increased with aging time until 36 hours of aging (from 0 to 52.6 % after 36 hours) and remained almost constant around 53 % until 48 hours of aging. Based on these results, it can be concluded that the aging time significantly affects the Si/Al ratio of the synthesis

solution, which in turn affects the type of zeolite to be produced. Figure 5.11 demonstrates that aging for 36 hours may be suitable. This is due to the fact that during this period low content of mullite was observed together with high Si/Al ratio and crystallinity of Na-P1.

5.3.4.2. Variation of Hydrothermal treatment (HT) time

The hydrothermal treatment of the reaction mixture is very important, since it increases the dissolution of the fly ash phase (especially mullite) that did not dissolve during aging and further increases the yield of zeolites. In the previous chapter (Chapter 4), it was mentioned that the dissolution of the fly ash phases follows the following sequence; amorphous glassy phase, followed by quartz and lastly mullite. Thus, it is not surprising that mullite was still present as a secondary product, although the reaction mixture was aged for longer periods and hydrothermally treated for 48 hours.

5.3.4.2.1. Zeolite synthesis at 12 hours of aging with a variation of HT time

Figure 5.12 shows XRD spectra of the transformation of fly ash phases into zeolitic products as a function of hydrothermal treatment time after 12 hours of aging at 47 °C under 200 rpm of stirring with a 4 flat-blade impeller.

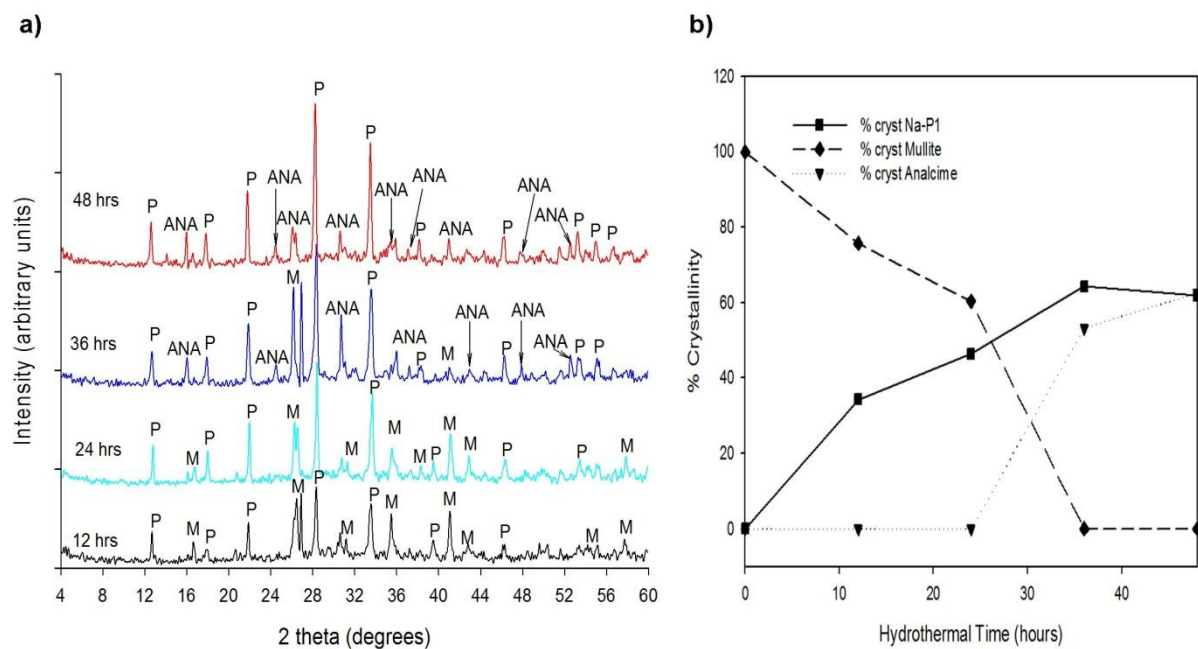


Figure 5-12: XRD patterns of the synthesis products obtained after 12 hours aging followed by variation of hydrothermal treatment time. a) XRD spectra and b) percentage crystallinity of different phases. (M-Mullite, P-Zeolite Na-P1 and ANA-Analcime).

The XRD patterns (Figure 5.12) indicate that zeolite Na-P1 was the only zeolite phase that crystallised over a 12 to 24 hour period with mullite appearing as a contaminant from undissolved FA. However, characteristic XRD peaks of analcime started appearing after 36

hours of HT. Over 36 to 48 hours of HT period, zeolite Na-P1 and analcime were the only products observed. At this stage, only a very small content of mullite was observed after 36 hours of HT. The mineralogical study demonstrated that the aluminosilicate glass and quartz were the most reactive fly ash phases, since mullite was still present after 24 hours of hydrothermal treatment (HT). The formation of zeolite Na-P1 after shorter reaction time, i.e. 12 hours of HT, occurs as a result of partial dissolution of the amorphous glass phase. As the reaction progresses, the amorphous phase continues to dissolve simultaneously with quartz and mullite. The dissolution of these Si-rich phases results in the increase in the Si/Al ratio in the synthesis solution. Consequently, nucleation and crystal growth of high-crystalline zeolites such as analcime as new mineral phases occurs (Querol *et al.*, 1996). Analcime exhibits low cation exchange capacity which makes it have low industrial application potential (Querol *et al.*, 2001). In this case, analcime is considered a contaminant since a pure phase of Na-P1 was targeted.

Figure 5.12b reveals that mullite decreased continuously until it was completely dissolved after 36 to 48 hours of HT. On the other hand, zeolite Na-P1 showed a progressive increase until 36 hours of HT and decreased after 48 hours. The decrease in the crystallinity of zeolite Na-P1 may be due to the formation or increase in the analcime content, as can be seen in Figure 5.12b. Querol *et al.* (1996) observed that the content of zeolite Na-P1 started decreasing as a result of the formation of other zeolite products such as Na-P derivatives, analcime, gmelinite and nepheline hydrate. The maximum crystallinity of Na-P1 reached in this set of experiments was 64.3 % after 36 hours of HT. Analcime, on the other hand, reached a maximum crystallinity of 62.8 % after 48 hours of HT.

5.3.4.2.2. Zeolite synthesis at 24 hours of aging with a variation of HT time

Failure to obtain a pure phase of zeolite Na-P1 led to further set of experiments during which the reaction mixture was aged for 24 hours at 47 °C under 200 rpm of stirring with a 4 flat-blade impeller and hydrothermally treated at 140 °C for different periods under static conditions. Figure 5.13 illustrates the XRD patterns of the reaction products synthesised after 24 hours of aging with variation of HT time. In this case, similar results as those obtained after 12 hours of aging were obtained. However, the major difference was that in this set of experiments, a significant amount of mullite was still present even after 36 and 48 hours of HT.

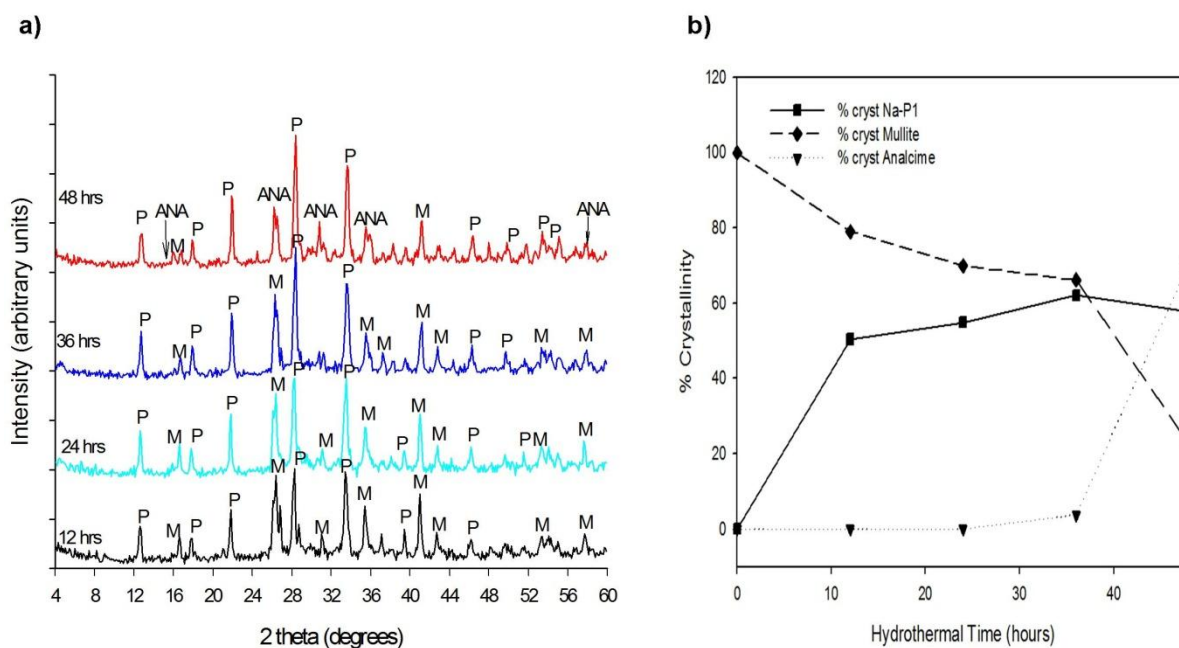


Figure 5-13: XRD patterns of the synthesis products obtained after 24 hours aging with variation of hydrothermal treatment time. a) XRD spectra and b) percentage crystallinity of different phases. (M-Mullite, P-Zeolite Na-P1 and ANA-Analcime).

In this set of experiments, analcime was only observed after 48 hours of HT. This confirms the findings above that analcime formed as result of the slow dissolution of SiO_2 and Al_2O_3 from the mullite phase. The maximum crystallinity of zeolite Na-P1 obtained in this experiment was 62.0 % (after 24 hours of aging and 36 hours of HT) which was lower than that obtained after 12 hours of aging and 36 hours of HT. This was attributed to the presence of mullite as a secondary contaminant after 36 of HT. It can be seen in Figure 5.13b that the crystallinity of zeolite Na-P1 decreased towards 48 hours of HT as a result of an increase in the content of analcime, which was 70.8 % after 48 hours. From these results, the aging time applied was deemed to have minimal influence on the quality of the zeolite products obtained, since these results were similar to those obtained at 12 hours of aging. These results prompted trials at 36 hours of aging.

5.3.4.2.3. Zeolite synthesis at 36 hours of aging with a variation of HT time

Figure 5.14 shows the XRD spectra of the representative synthesis products obtained after 36 hours of aging at 47 °C under 200 rpm of stirring with a 4 flat-blade impeller as a function of HT time. XRD revealed that poorly crystallised zeolite Na-P1 with un-reacted mullite were the main synthesis products after 12 hours of HT. However, as the HT time was increased to 24 h, increased mullite digestion was observed, with weak peaks of analcime starting to appear. After 24 hours of HT, mullite showed a drastic decrease from 68.6 % (at 12 hours HT) to 24.6 % (at 24 hours HT).

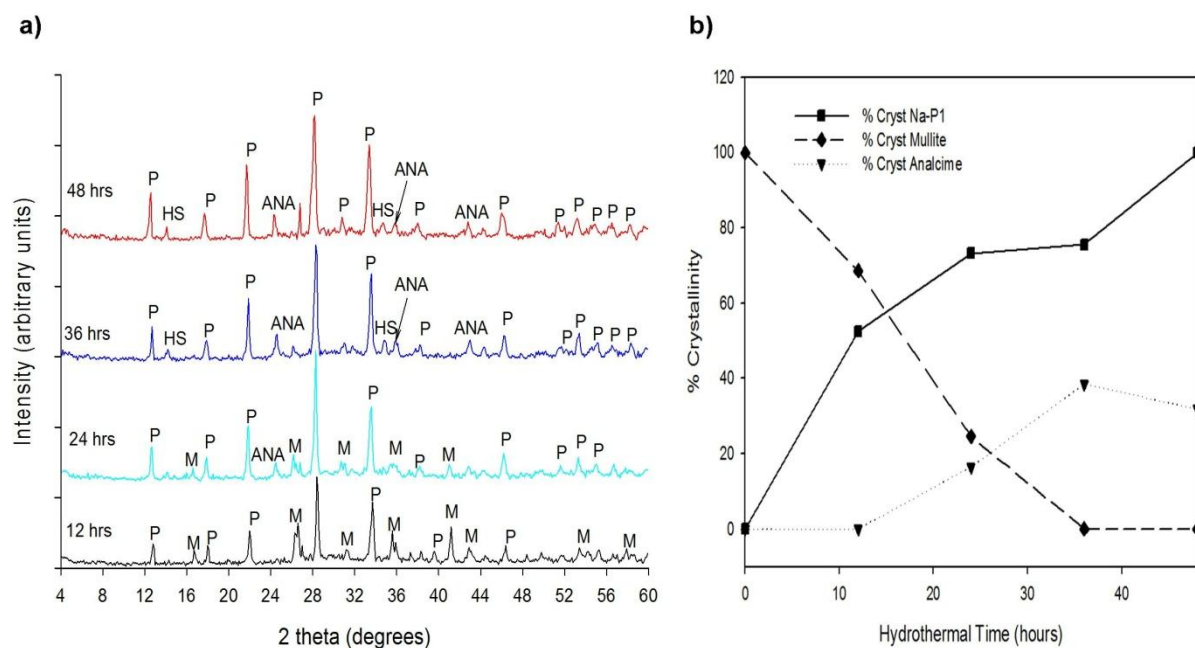


Figure 5-14: XRD patterns of the synthesis products obtained after 36 hours aging with variation of hydrothermal treatment time. a) XRD spectra and b) percentage crystallinity of different phases. (M-Mullite, P-Zeolite Na-P1 and ANA-Analcime).

As the hydrothermal reaction progressed from 24 to 36 hours, analcime peaks became slightly stronger. During this period, analcime reached its maximum crystallinity of 38.5 %, which was significantly lower when compared to the other products obtained after 36 hours of HT with 12 and 24 hours of aging. At this point, the crystallinity of zeolite Na-P1 was considerable higher (at 75.6 %). However, trace amounts of hydroxysodalite were also identified by XRD as shown in Figure 5.14a. Hydroxysodalite is one of the fly ash zeolites with low industrial application potential as indicated by Querol *et al.* (2001). Thus, hydroxysodalite was also considered as a contaminant.

After 48 hours of HT, analcime showed a decrease in crystallinity from 38.5 % (at 36 hours) to 31.9 % (at 48 hours). No mullite was detected (by XRD) at this point. Although traces of hydroxysodalite were still detected, zeolite Na-P1 occurred in nearly pure phase with high XRD reflection intensities of its characteristic peaks. As a result, this product was used as a standard in crystallinity calculations for zeolite Na-P1, as aforementioned. The crystallinity of Na-P1 in this product was considered to be 100 %. Further experiments were conducted at 48 hours of aging since the reported optimum conditions for the synthesis of a pure phase of zeolite Na-P1 from South African fly ash were 48 hours of aging at 47 °C and 48 hours of HT at 140 °C under static conditions (Musyoka, 2009).

5.3.4.2.4. Zeolite synthesis at 48 hours of aging with a variation of HT time

When the synthesis was conducted at 48 hours of aging, not much difference was observed. The main zeolitic products obtained were still zeolite Na-P1 and analcime as shown in Figure 5.15.

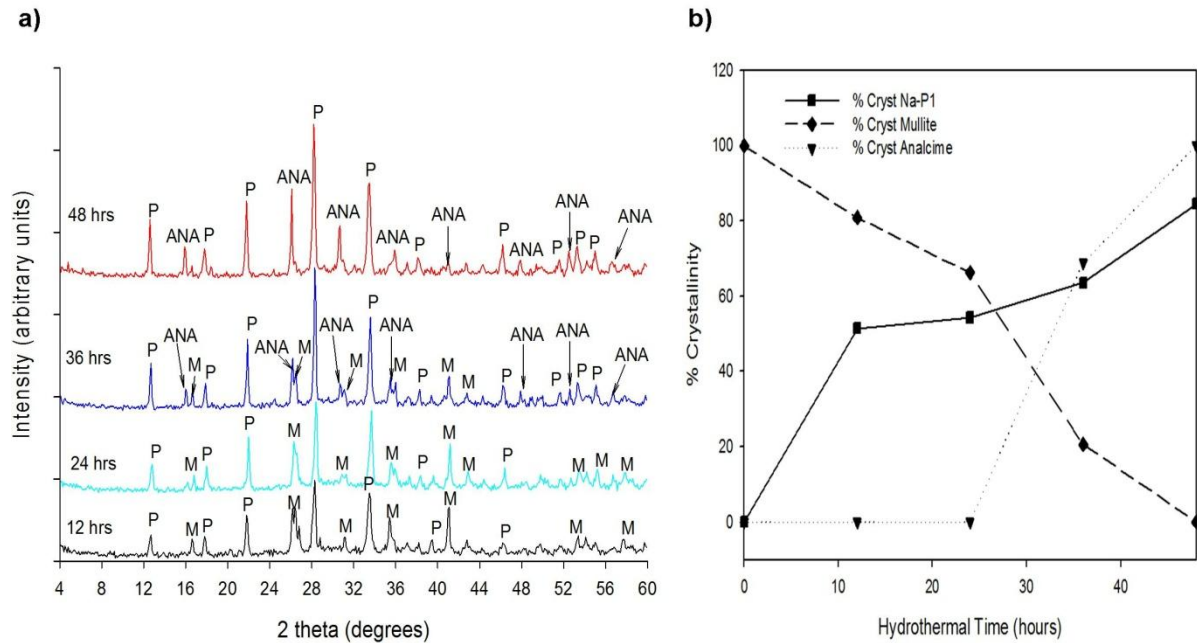


Figure 5-15: XRD patterns of the synthesis products obtained after 48 hours aging with variation of hydrothermal treatment time. a) XRD spectra and b) percentage crystallinity of different phases. (M-Mullite, P-Zeolite Na-P1 and ANA-Analcime).

However, in this set of experiments, mullite was observed together with Na-P1 and analcime after 36 hours of HT. When comparing the product obtained after 36 hours of HT in this case to that obtained after the same HT time with 36 hours of aging, it was observed that the crystallinity of analcime had drastically increased from 38.5 % (at 36 hours of aging) to 68.8 % (at 48 hours of aging). On the other hand, the crystallinity of Na-P1 had decreased from 75.6 % (at 36 hours of aging) to 63.6 % (at 48 hours of aging). As the reaction progressed to 48 hours of HT, analcime increased to reach its maximum crystallinity of 100 %. This product was used as a standard for crystallinity calculations of analcime. Based on these results, it was observed that the results obtained with 36 hours of aging were better than those obtained with 48 hours of aging.

Therefore, it can be concluded that the best synthesis conditions to achieve a pure phase of zeolite Na-P1 from batch 2 of Arnot fly ash were; aging at 47 °C for 36 hours with 200 rpm of stirring with a 4 flat-blade impeller and hydrothermal treatment at 140 °C for 48 hours under static conditions, although traces of analcime and hydroxysodalite were present. In order to

confirm and demonstrate the reproducibility of this data (36 hours of aging and 48 hours of HT), another experiment was conducted and the XRD patterns are depicted in Figure 5.16.

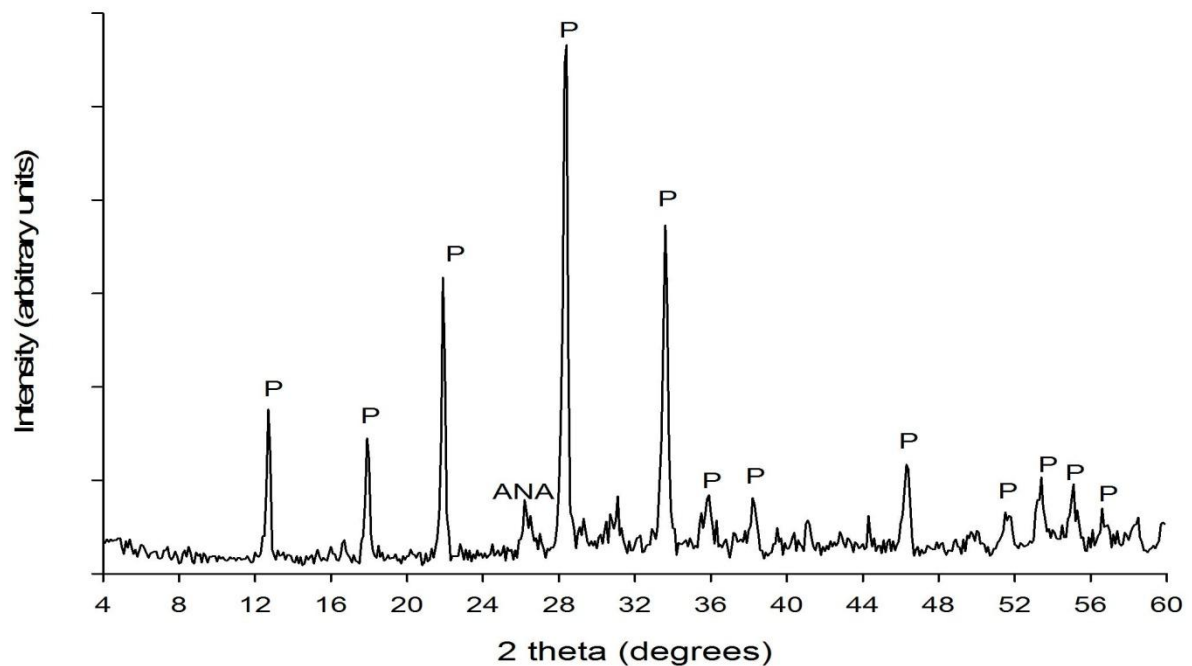


Figure 5-16: XRD patterns and SEM image of the zeolite products synthesised at 36 hours of aging and 48 hours of HT. (ANA-Analcime and P-zeolite Na-P1).

It can be seen from Figure 5.16 that under these conditions (aging at 47 °C for 36 hours under 200 rpm of stirring and hydrothermal treatment at 140 °C for 48 hours under static conditions), a pure phase of zeolite Na-P1 can be obtained. In this case, hydroxysodalite was not detected and only one peak of analcime was observed. As a result, this product can be considered to be essentially pure. This indicated that these conditions are suitable for the synthesis of zeolite Na-P1 from the fly ash used in these experiments. This product was compared to the one obtained with batch 1 of Arnot fly ash and the XRD spectra are illustrated in Figure 5.17.

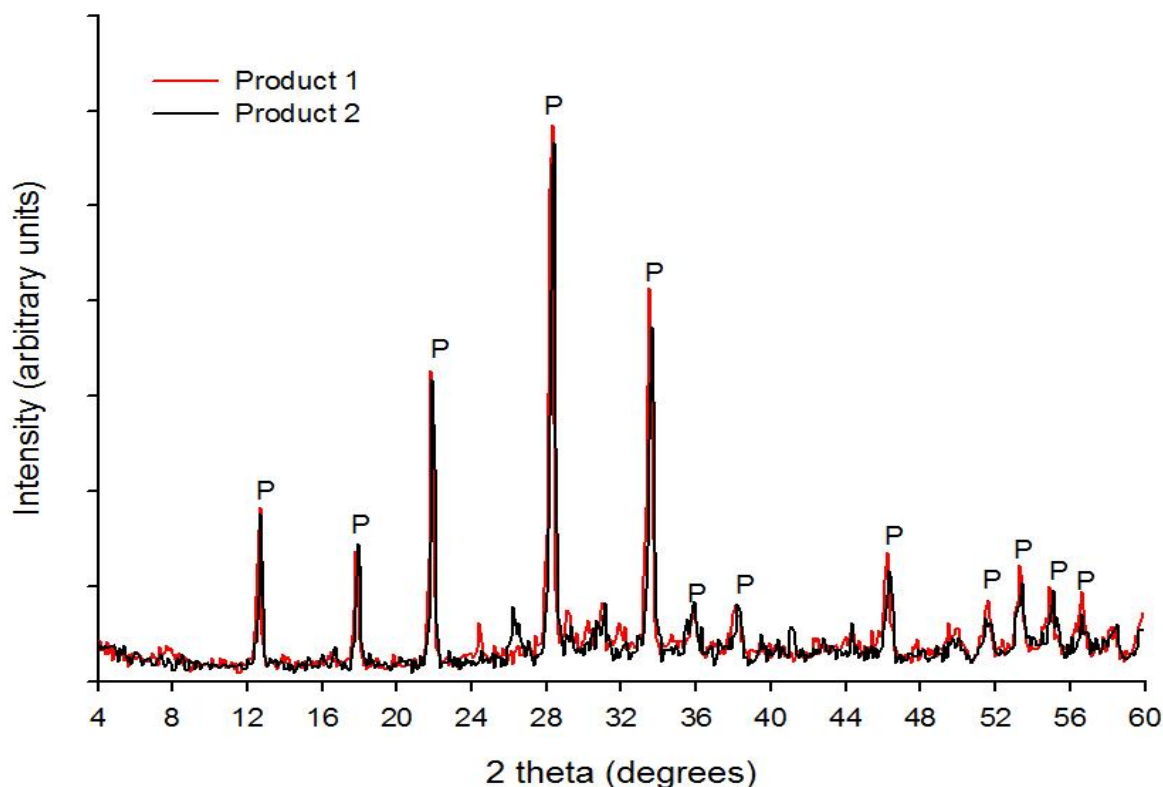


Figure 5-17: XRD spectra of zeolite Na-P1. (Product 1 (red) and 2 (black) are zeolite Na-P1 synthesised using batch 1 and batch 2 of Arnot fly ash respectively).

As aforementioned, the most crystalline zeolite Na-P1 product obtained with batch 1 of Arnot FA was synthesised under the following conditions; aging at 47 °C for 48 hours under stirring at 200 rpm with a 4 flat-blade impeller and hydrothermal treatment at 140 °C for 48 hours under static conditions. This product was compared to the one synthesised using batch 2 of Arnot fly ash (aging at 47 °C for 36 hours under stirring at 200 rpm with a 4 flat-blade impeller and hydrothermal treatment at 140 °C for 48 hours under static conditions) and the two zeolite Na-P1 products were found to be similar, as shown in Figure 5.17. The crystallinity of both these products was considered to be 100 %. Although the two batches of fly ash were sourced from the same power station, the synthesis conditions to achieve a pure phase of zeolite Na-P1 were different. This was due to the difference in the mineralogical compositions of the two batches of ash. This study has shown that although FA mineralogical variability may influence the mineralogical composition of the zeolitic product, adjustment of the aging synthesis conditions can be used to overcome this problem quite simply by monitoring the Si/Al ratio and adjusting the aging step accordingly.

5.3.4.2.5. Summary

Aging and hydrothermal reaction time can be adjusted to tailor the type and quality of the zeolite produced. The quality of the zeolite synthesised was subject to perturbations caused by the changes in the hydrothermal reaction time. Aging time significantly influenced the Si/Al ratio of the synthesis solution, which in turn affected the outcome of the zeolitisation process. Increased aging time resulted in increased Si/Al ratio. In these experiments, the main zeolites produced were zeolite Na-P1 and analcime, with traces of HS in some cases. The experimental results demonstrated that an increase in HT time results in a high zeolite yield. Mullite was found to be the last FA phase to dissolve into the alkaline solution, since it appeared as a secondary product, although the reaction mixture was treated for longer aging and hydrothermal reaction times. Variation of the reaction time resulted in the synthesis of a pure phase of zeolite Na-P1 from low amorphous phase FA, with the synthesis conditions being; aging at 47 °C for 36 hours under stirring at 200 rpm with a 4 flat-blade impeller and hydrothermal treatment at 140 °C for 48 hours under static conditions. The results also prove that FA samples sourced from the same power station may require different synthesis conditions in order to synthesise a pure phase of zeolite Na-P1. This study has also shown that although FA mineralogical variability may influence the mineralogical composition of the zeolitic product, adjustment of the aging synthesis conditions can be used to overcome this problem quite simply by monitoring the Si/Al ratio and adjusting the hydrothermal reaction time accordingly.

5.4. Conclusions to Chapter 5

The main objective of this study was to evaluate the effects of some parameters that may affect the scale-up synthesis of zeolite Na-P1. In this study, the experiments were conducted on a laboratory scale and zeolite Na-P1 was synthesised, thereafter characterised in terms of phase purity and morphology. Although this study was conducted on a laboratory scale, it gave an insight of what to expect on a large scale synthesis process. A pure phase of zeolite Na-P1 was successfully synthesised via a two-stage hydrothermal treatment method, using Arnot FA as the starting material. In some cases, zeolite formation was assessed as fairly unsuccessful, taking into account that the synthesis products contained a substantial amount of the unwanted zeolites (analcime and HS) and/or un-reacted FA phases (mullite or quartz). During this investigation several variables were considered; impeller design and agitation, fly ash composition, use of different water sources during the synthesis process and reaction time.

Three types of impellers at three agitation speeds were investigated in this study and a pure phase of zeolite Na-P1 was successfully synthesised with the use of these impellers at different speeds. In some cases, a pure phase could not be obtained. Based on the

experimental results, it was observed that a 4 flat-blade impeller was the optimum design of impeller that can be used for agitation during the aging step of the zeolite synthesis in a scaled-up process. A high crystalline zeolite Na-P1 product was obtained when this impeller was used at 200 rpm. These investigations also proved for the first time that different impeller designs and agitation during the aging step can have a profound impact on the zeolitic product quality. Therefore, it is not only the hydrothermal synthesis conditions and the molar regime but also the dissolution kinetics of the feedstock that influence the outcome of the zeolite synthesis process.

The effect of fly ash composition and mineralogical phase content on the phase purity of zeolite Na-P1 was also studied and it was observed that two fly ash samples from the same power station (Arnot) with similar chemical compositions but different mineralogical composition yielded different zeolitic products when treated under the same synthesis conditions. A pure phase of zeolite Na-P1 was successfully synthesised from the fly ash with higher amorphous glass phase content whereas mixture of zeolite Na-P1 and analcime was obtained from low amorphous glass phase content fly ash. The results also demonstrated that the efficiency in the conversion of FA into zeolites is affected by the contents of non-reactive FA phases (mainly mullite and quartz) as well as the amorphous glass phase content. This was confirmed by a study using Hendrina FA, which also had a low amorphous glass phase content. The content of the amorphous glass phase was found to be crucial for the formation of zeolite Na-P1 since it easily dissolves into the alkaline solution.

The use of tap and distilled water as well as acid mine drainage during the synthesis of zeolite Na-P1 as a substitute for ultrapure water was investigated. It was found that it is possible to synthesise zeolites using TW, DW and AMD. The zeolitic products obtained when TW and DW was used were similar to those obtained with ultrapure water, meaning that the elemental species present in these waters did not influence the type of zeolite obtained. However, in the case of AMD, the synthesis product obtained contained a substantial amount of HS, while a lower fraction of the desired zeolite Na-P1 was observed. Based on these results, it was concluded that with further optimisation of the synthesis conditions, TW and DW can be used as a replacement for ultrapure water to synthesise a pure phase of zeolite Na-P1 on a large scale. However, AMD was not a suitable solvent for the synthesis of zeolite Na-P1.

The effect of hydrothermal reaction time on the phase and purity of zeolite Na-P1 was also assessed, with the aim of establishing optimum synthesis conditions for the synthesis of a pure phase of zeolite Na-P1 from low amorphous phase fly ash. Aging and hydrothermal reaction time can be adjusted to tailor the type and quality of the zeolite produced. Aging time significantly influenced the Si/Al ratio of the synthesis solution, which in turn affected the

outcome of the zeolite synthesis process. The experimental results demonstrated that an increase in HT time results in a yield of high crystalline zeolites. Variation of the reaction time resulted in the synthesis of a pure phase zeolite Na-P1 from low amorphous phase FA, with the synthesis conditions being; aging at 47 °C for 36 hours under stirring at 200 rpm with a 4 flat-blade impeller and hydrothermal treatment at 140 °C for 48 hours under static conditions. This study also showed that although FA mineralogical variability may influence the mineralogical composition of the zeolitic product, adjustment of the aging synthesis conditions can be used to overcome this problem simply by monitoring the Si/Al ratio and adjusting the aging step accordingly.

The synthesis conditions of zeolite Na-P1 on a large scale must be optimised such that the conditions developed are optimum for any type of South African fly ash or fly ash source in order to reduce capital, operational and production costs. The results obtained in this study demonstrated that the scale-up synthesis of a pure phase of zeolite Na-P1 from fly ash would require step-by-step optimisation of the synthesis conditions, since this zeolite seemed to be sensitive to the $\text{SiO}_2/\text{Al}_2\text{O}_3$ ratio, agitation and the mineralogy of the fly ash. Further optimisation of the synthesis conditions and adjustment of the Si/Al molar ratio of the synthesis gel by adding either SiO_2 or Al_2O_3 from a supplementary source may be necessary if a pure phase of zeolite Na-P1 is targeted. As a consequence, this may have implications on the operating time and costs.

CHAPTER 6

6. SYNTHESIS OF ZEOLITE A

6.1. Introduction

It can be inferred from Chapter 5 that the scale-up of the synthesis of zeolite Na-P1 can be challenging, requiring step-by-step optimisation for each FA source. It would be necessary to consider the synthesis of an alternative zeolite type, with a view to avoid this challenge and possibly synthesise another valued product. This chapter focuses on the synthesis of zeolite A. This zeolite is one of the most widely used zeolites due to its unique molecular sieving and ion-exchange capabilities. A previous study by Musyoka *et al.* (2011) has shown that a pure phase of zeolite A can be synthesised under mild temperatures (i.e. under 100 °C) via the alkali fusion method in less than eight hours (i.e. 1.5 hours of fusion, 2 hours of extraction of soluble silicates, 1 hour of filtration and 2 hours of hydrothermal treatment).

This section of the study was conducted in order to investigate some of the parameters that were found to significantly affect the zeolitisation process. These parameters include fly ash composition and the effect of water chemistry. In Chapter 5 it was proved that fly ash composition and water chemistry affect the synthesis of zeolite Na-P1 significantly. Therefore, it is important to assess the effect of these parameters on the synthesis of zeolite A. This was conducted with the aim of establishing suitable conditions for the scale-up of zeolite A from South African fly ashes. In this chapter the results corresponding to the synthesis of zeolite A from different South African fly ashes are discussed.

6.2. Materials and Methods

6.2.1. Experimental procedure

Experimental procedure and conditions together with the experiments conducted for this part of the study were previously explained in section B of Chapter 3.

6.2.2. Analytical techniques

The analytical techniques used for this part of the study were previously explained in section C of Chapter 3.

6.3. Results and discussion

6.3.1. Alkaline fusion of fly ash

Alkali fusion is a conventional method used for decomposing materials containing silicon and/or aluminium. As reported previously (Chapter 3), during fusion, FA is mixed with powdered NaOH. The sodium hydroxide present in the reaction mixture acts as an activator during fusion at high temperatures to form soluble silicate and aluminate salts, which further takes part in zeolite formation during hydrothermal process. (Ojha *et al.*, 2004). As stated in Chapter 3, an alkaline fusion step was introduced prior to the hydrothermal treatment, because it plays an important role in enhancing the dissolution of precursors needed for hydrothermal conversion in zeolite synthesis. On the other hand, this approach was adopted in this study because larger amounts of aluminosilicates can be dissolved employing this method. During fusion, FA is converted into sodium silicate and sodium aluminate, both of which are soluble in water. The fusion method has high fly ash conversion efficiency and can be directed towards certain types of zeolites by adjusting the hydrothermal synthesis conditions. However, the use of a high temperature fusion step makes this method very energy-intensive. Figure 6.1 illustrates the difference between the mineralogy and the morphology of the original FA and the fused FA.

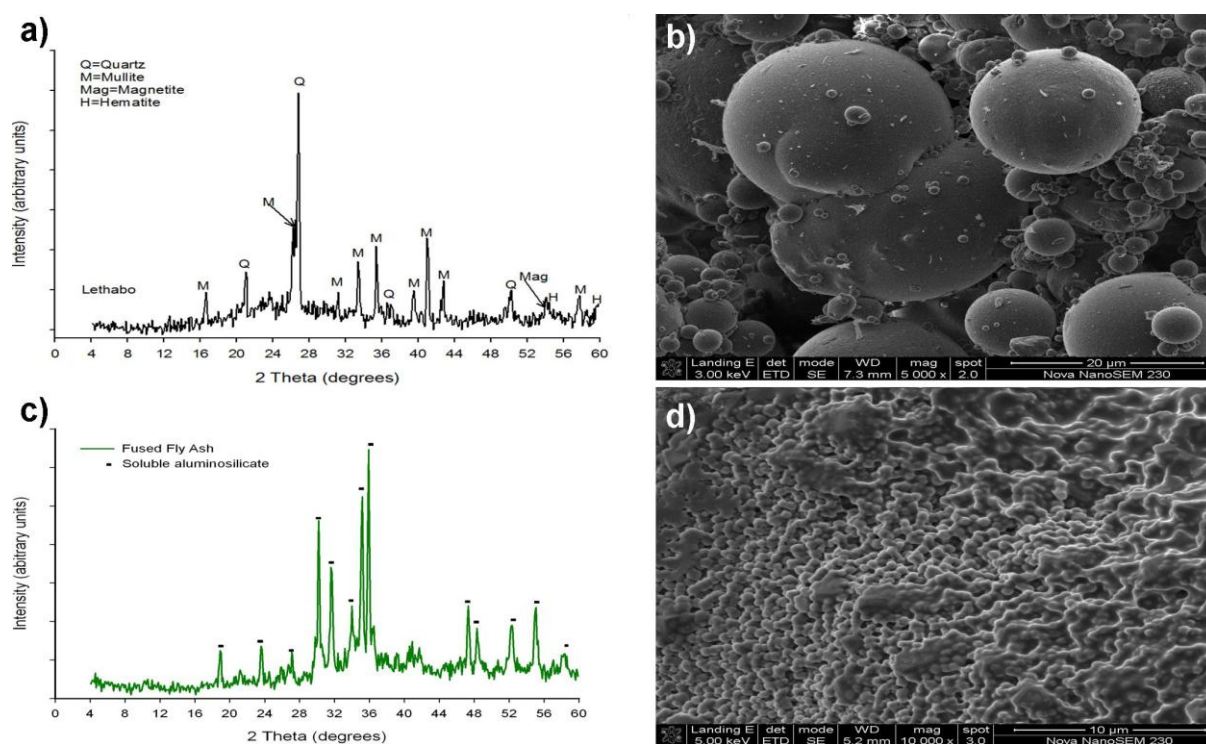


Figure 6-1: XRD patterns and SEM images of the original FA and fused FA. a) XRD patterns of the original FA. b) SEM image revealing the morphology of the original FA. c) XRD patterns of fused FA. d) SEM image of fused FA.

As stated earlier in Chapter 4, the major crystalline phases of FA are quartz, mullite, hematite and magnetite. Aluminosilicate glass exists as an amorphous phase indicated by the hump between 18 to 32 degrees 2θ (Figure 6.1a). On the other hand, a large amount of sodium aluminosilicates exist in the fused FA, which implies that fusion was effective in extracting silicon and aluminium from the FA phases (Figure 6.1c). The FA phases (mainly mullite and quartz) reacted with NaOH and resulted in the disappearance of their characteristic XRD peaks in FA (Figure 6.1c). As previously discussed, the original FA particles are spherical in shape with a relatively smooth surface (Figure 6.1b). On the other hand, fused FA exhibited no evidence of the original FA morphology or mineralogy.

6.3.2. Effect of water sources on the synthesis of a zeolite A

As mentioned in Chapter 3, the synthesis conditions for a pure phase of zeolite A were optimised by Musyoka *et al.* (2011) using Arnot fly ash. His conditions were adopted in this study in order to demonstrate the reproducibility of his data for different FA sources and solvents (i.e. fusion at 550 °C for 1.5 hours followed by extraction at room temperature for 2 hours under stirring at 1400 rpm. After the extraction step the solids were filtered and the clear solution was used for the crystallisation (at 100 °C) of zeolite A after adjusting the molar regime with an aluminate solution). Circumneutral mine water (CMW) was used as a substitute for ultrapure water (UP) during the synthesis process in order to test the validity of the synthesis conditions and the possibility of synthesising zeolite A from mine water. The CMW used in this study was obtained from a coal mine in Mpumalanga, South Africa.

6.3.2.1. Characterisation of the circumneutral mine water

As aforementioned, the circumneutral mine water (CMW) used in this study was collected from Middleburg coal mine in Mpumalanga, South Africa. Table 6.1 summarises the pH, EC and the chemical composition of the CMW. The analyses for anions and cations were done using ion chromatography (IC) and inductively-coupled plasma (atomic emission and mass) spectroscopy respectively. The table below only presents the concentration of the major elements that were observed in this water.

Table 6-1: Composition of the CMW

Element	Concentration (ppm)
Al	3.52 ± 0.33
Ca	535.55 ± 2.87
Fe	2.41 ± 0.071
K	29.19 ± 0.014
Mg	861.77 ± 15.51
Mn	24.96 ± 0.085
Na	20.12 ± 0.036
SO ₄ ²⁻	4603 ± 28.28
NO ₃ ⁻	35.69 ± 0.014
Cl ⁻	155 ± 8.49
pH	6.50 ± 0.49
EC (mS/cm)	5.02 ± 0.16

It can be seen from the table above that the water (CMW) used in this study was characterised by high concentrations of Mg and Ca. The concentrations of Mn and Na were also found to be high in this water. This water was also found to contain high concentrations of SO₄²⁻, NO₃⁻ and Cl⁻ as shown in Table 6.1. The water (CMW) used had a circumneutral pH (pH=6.50). The CNW contained small amounts of Fe and Al (2.41 and 3.52 ppm respectively). According to Uhlmann *et al.* (2004) and Jenke *et al.* (1983), at circumneutral pH Al and Fe precipitates out as hydroxides. Minor elements such as Cd, Cu, Mo, V, Zr, Zn, Y and Th were found to exist in concentrations between 0 and 1 ppm. As stated earlier in section 5.3.3.2, Ca²⁺ and Mg²⁺ were reported to act as competing ions during zeolite synthesis. These cations (Ca and Mg) compete with sodium (Na) in zeolite structure formation as charge balancing cations. The concentration of these metals was found to be high in the CMW used in this study. Therefore, interference during zeolite formation was expected.

6.3.2.2. Mineralogical analysis

Figure 6.2 depicts the XRD patterns obtained when Arnot FA, UP and CMW were used as the starting materials.

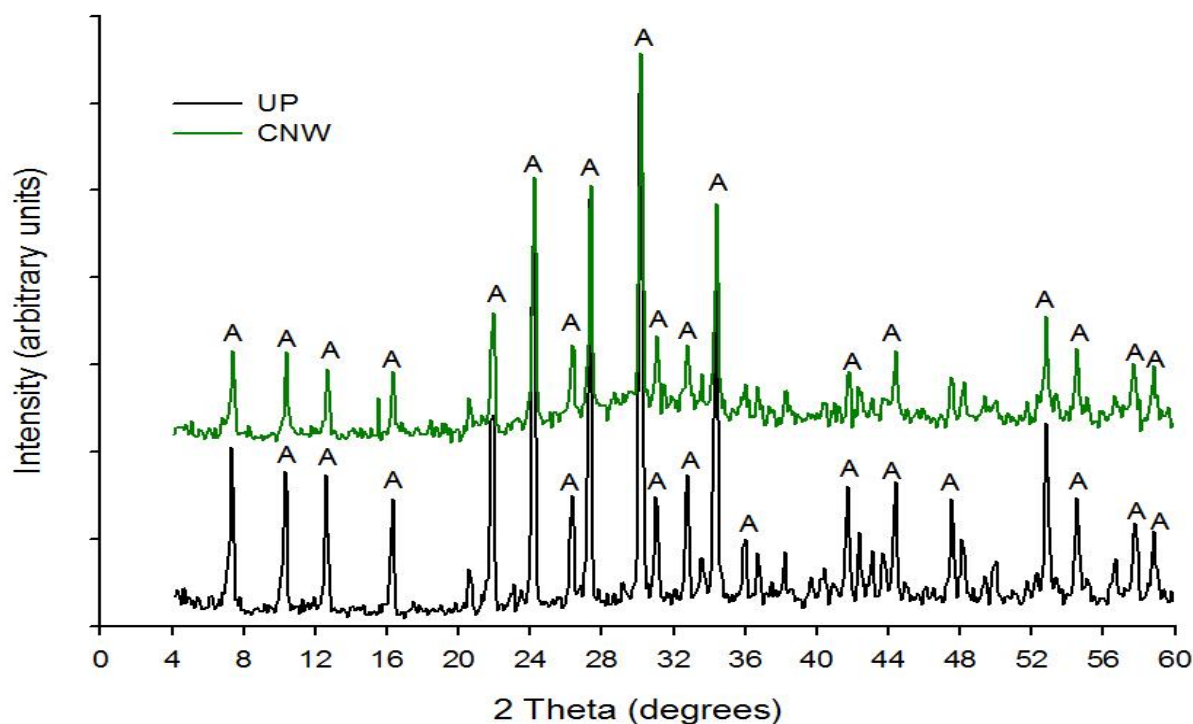


Figure 6-2: XRD patterns of zeolite A synthesised using Arnot FA, ultrapure and mine waters as the starting materials. (A-zeolite A, CMW-circumneutral mine water and UP-ultrapure water).

The most distinct changes in the XRD patterns of the fused fly ash when compared to those of the zeolitic products are the disappearance of the fused product's sodium aluminosilicates peaks and the appearance of a new crystalline phase. The major crystalline phase obtained after UP water and CMW were used during the synthesis process was zeolite A. The XRD pattern obtained when CMW was used for the synthesis of zeolites, compared to that obtained when ultrapure water (UP) was used, does not show a significant difference. These patterns show that zeolite A was the only product obtained after 2 hours of hydrothermal treatment at 100 °C. The only noticeable difference between these products was the lower crystallinity and presence of un-reacted amorphous material, giving rise to a hump in the region of 24 to 36 degrees 2θ observed in the XRD pattern of the product obtained with CMW. This implies that the presence of extra elements in the CMW had little to no influence on the synthesis products obtained, since the same zeolite phase obtained with UP water was obtained with CMW. The same observations were made by Musyoka *et al.* (2011) in his study. The results obtained demonstrated that synthesis conditions used for the synthesis of zeolite A from Arnot batch 2 FA were robust, since a pure phase was obtained even when mine water was used.

6.3.2.3. Morphological analysis

Scanning Electron Microscopy (SEM) was used to determine the morphology of the zeolite crystals. Figure 6.3a-b shows the typical crystals of the zeolite phase (zeolite A) obtained when ultrapure and mine waters were used as the starting materials during the synthesis process.

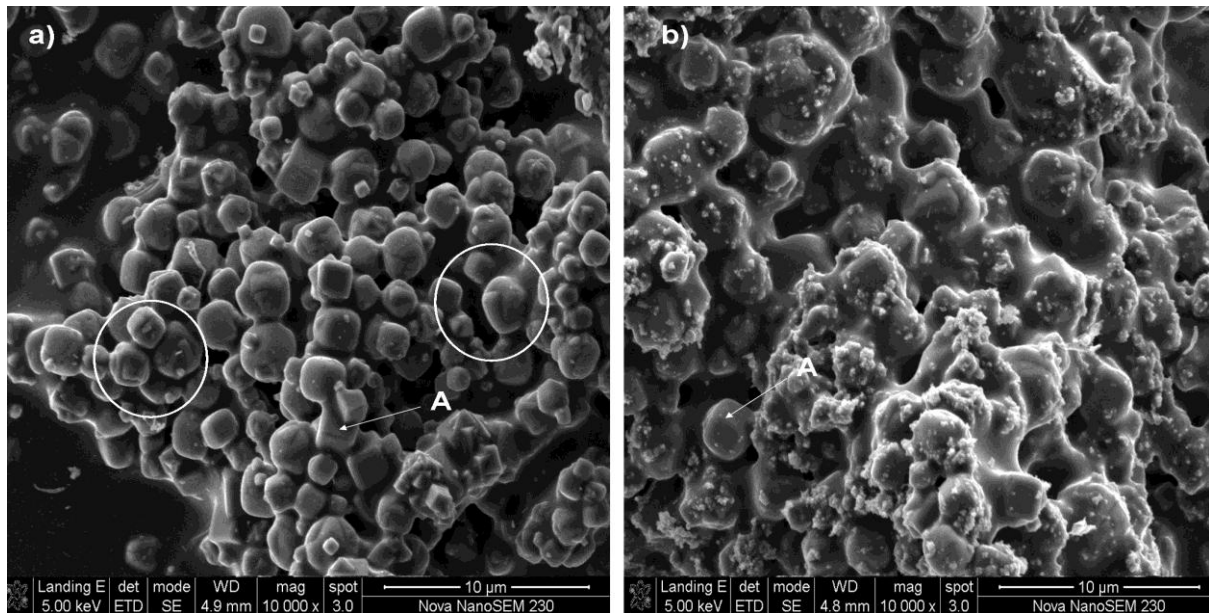


Figure 6-3: SEM images of zeolite A synthesised from Arnot fly ash using different solvents. a) Ultrapure water b) CMW.

The photomicrographs clearly showed the transformation of amorphous microparticles of aluminosilicate transforms into zeolite A. The morphology of single crystals of zeolite A looks well defined. Figure 6.3a shows that when ultrapure water was used; zeolite A crystals had a cubic morphology with truncated edges. This morphology is similar to that reported in literature (Jamil *et al.*, 2010; Rayalu *et al.*, 2001). These cubic crystals displayed occasionally intergrown twins as shown in the areas marked with circles in Figure 6.3a. In the case of CMW (Figure 6.3b), zeolite A had the same morphology (cubic). However, these cubes had smooth edges and were covered with unconverted amorphous materials. These results (Figure 6.3b) concur with XRD results reported earlier in Figure 6.2.

6.3.3. Effect of fly ash composition on the synthesis of zeolite A

In this set of experiments, four fly ash samples from different South African power stations (i.e. Hendrina, Matla, Tutuka and Lethabo fly ashes) were used to synthesise zeolite A. All these fly ashes were classified as class F type based on their $\text{SiO}_2 + \text{Al}_2\text{O}_3 + \text{Fe}_2\text{O}_3$ content that is greater than 70 %. The characterisation of these fly ashes (in terms of morphology, PSD, chemical and mineralogical compositions) has been presented in Chapter 4. The experimental conditions for this investigation have been clearly outlined in Chapter 3, section

3.2.4.2. The results obtained from these fly ashes were compared to that obtained when Arnot batch 2 FA was used as the starting material since it (Arnot batch 2 FA) was shown to produce a high crystalline zeolite A under the same conditions (Musyoka *et al.*, 2011). These products were compared in terms of mineralogical and chemical compositions, crystallinity and morphology. The main aim of these experiments was to investigate the effect of using South African FA from different sources with different mineralogical and chemical compositions on the zeolite A product characteristics.

6.3.3.1. Mineralogical analysis

The XRD patterns of the zeolitic products obtained are presented in Figure 6-4 and Figure 6-5. The XRD results reveal that a pure phase of zeolite A was obtained when all these fly ashes were used as starting materials. Although a pure phase was obtained, the crystallinity of these products was found to be different. The XRD patterns showed that the synthesis products obtained from Arnot batch 2, Hendrina and Matla fly ashes had quite similar reflection peak intensities. However, the zeolite A product obtained from Matla FA exhibited the highest peak intensities. As a consequence, this product was considered to be the most crystalline zeolite A product. The crystallinity of these products was calculated based on the procedure outlined below.

6.3.3.2. Crystallinity

The crystallinity of zeolite A was calculated using equation 3.1. The sum of the area under ten major peaks (centred at $2\theta=7.5, 10.4, 12.7, 16.4, 22, 24.3, 27.4, 30.2, 34.2$ and 52.9 degrees) was determined for each product. Since zeolite A from Matla FA was found to be most crystalline product, this sample was used as the standard (100 % crystallinity) for the purpose of these calculations. The results for the crystallinity calculations are summarised in Table 6.1.

Table 6-2: Crystallinity of the synthesis product

Fly ash sources	% crystallinity
Matla	100
Arnot batch 2	92.9
Hendrina	77.3
Tutuka	43.8
Lethabo	30.2

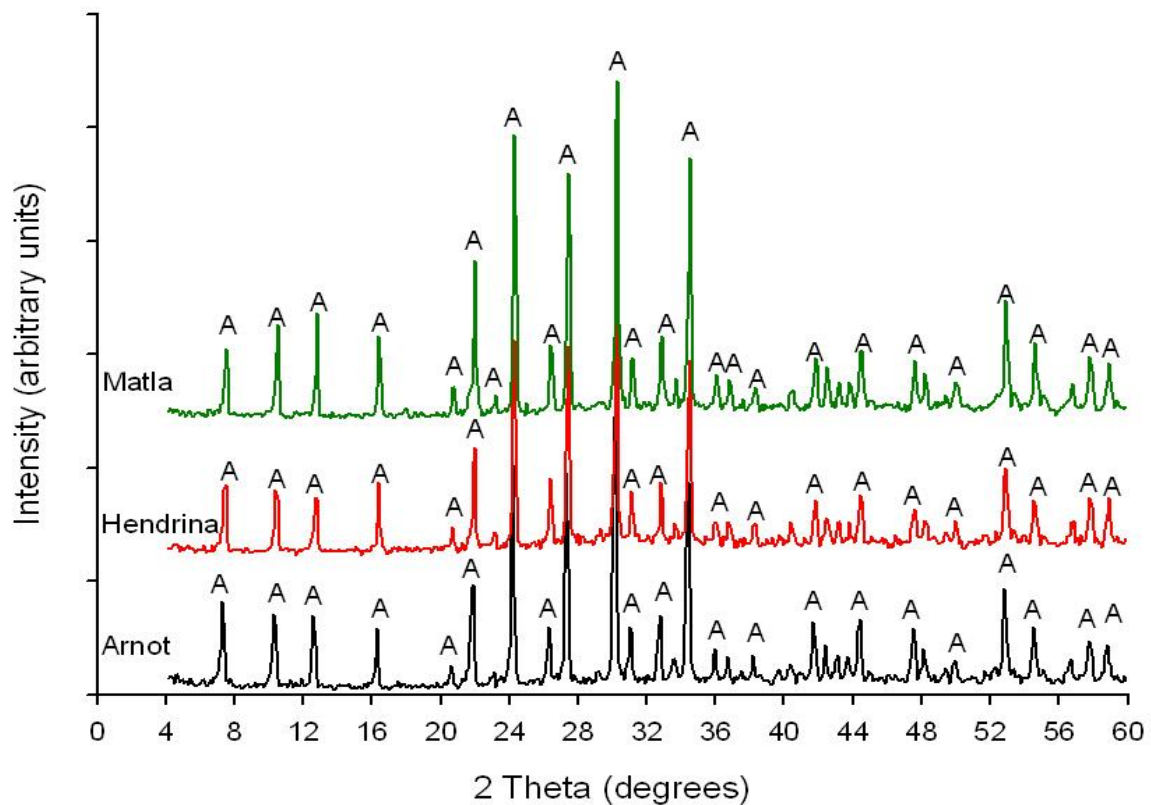


Figure 6-4: XRD patterns of zeolite A synthesised from Arnot, Hendrina and Matla fly ashes.(A-zeolite A)

Table 6-2 indicates that zeolite A synthesised from Arnot batch 2 FA had the second highest crystallinity after Matla FA zeolite followed by Hendrina FA zeolite. Lethabo and Tutuka fly ashes produced lower crystallinity zeolites as can be seen in Table 6-2 and Figure 6-5. The XRD spectra of the products obtained fly Lethabo and Tutuka fly ashes show that zeolite A was the only crystalline phase obtained (Figure 6.5). However, the products from these two ashes contained a large amount of unconverted amorphous materials, indicating that the synthesis time may have been too short. These amorphous materials are denoted by the hump in the region between 22 to 38 degrees 2θ as observed in the XRD spectra of these products (Figure 6-5). Matla, Tutuka and Lethabo fly ashes had similar mineralogical composition as shown in Table 4.3 and Figure 4.3. As stated in Chapter 4, these fly ashes were found to be very reactive, since they contained a high content of the amorphous glassy phase and a very low content of un-reactive mullite and quartz phases. However, under the same synthesis conditions, these fly ashes yielded products with different crystallinity. Zeolite A synthesised from Matla, Tutuka and Lethabo fly ashes exhibited percentage crystallinity of 100, 43.8 and 30.2 % respectively. The lower crystallinity observed in the zeolite A products from Tutuka and Lethabo ashes may due to the larger particle sizes of these ashes (Tutuka and Lethabo) when compared to the particle size of Matla ash (Chapter 4, section 4.5)..

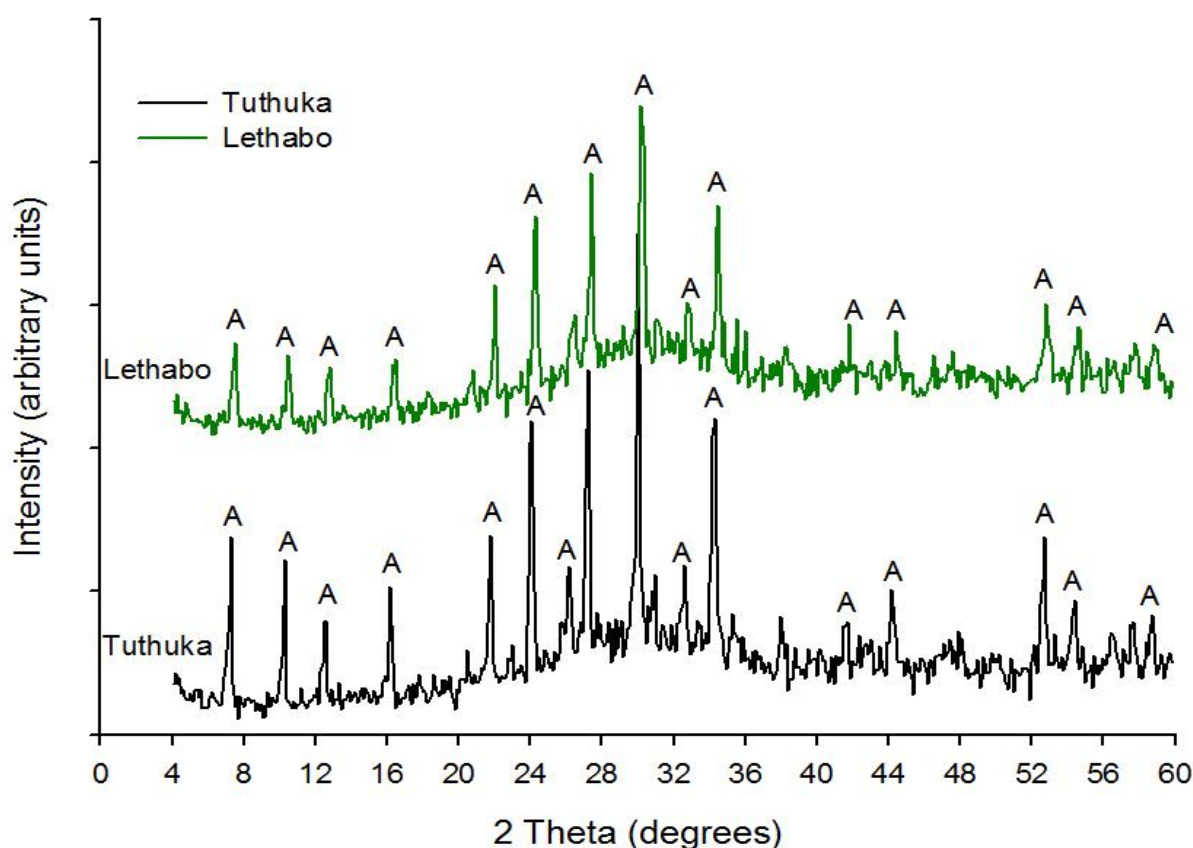


Figure 6-5: XRD patterns of zeolite A synthesised from Tutuka and Lethabo fly ashes. (A-zeolite A)

Based on these results, it can be inferred that the amorphous glassy phase of the fly ashes did not have a significant effect on the phase of the zeolite produced since zeolite A was the only zeolite obtained when all the fly ashes were used. However, the hydrothermal conditions may need to be adjusted in order to obtain a fully crystalline zeolite A material for different FA sources such as Tutuka and Lethabo power stations.

In these experiments, 100 g of FA was fused with 120 g of NaOH powder and from this only about 17 to 20 g of zeolite A was produced in each run. It can be seen that the yield of zeolites from this process was $\pm 20\%$, which is very low for such an energy-intensive synthesis process (alkali fusion method). The use of the clear solution process (i.e. filtration of solids after dissolution of the fused ash in water) on an industrial scale or pilot plant scale would have implications on the production cost as well as the environment, since large amounts of unused solids require disposal. As a consequence, the synthesis of a pure phase of zeolite A through the alkali fusion method with the solids must be investigated.

6.3.3.3. Elemental composition of the synthesised product

Table 6.2 illustrates the weight percentage of the major oxides present in zeolite A products obtained from different fly ashes. This table shows that the content of the major oxides in raw FA (Table 4.1) changed when FA was converted to zeolite A. The synthesised zeolite A products incorporated a significant amount of sodium (Na) compared with the raw FA. This is attributed to the fact that FA was activated with NaOH. Similar findings were obtained by Reyes (2008) and Maruyama *et al.* (2002). Maruyama *et al.* (2002) explained that the increase in the Na content is caused by the Na⁺ ions to neutralise the minus charge on aluminate in zeolite structure when a zeolite crystal is formed.

Table 6-3: Chemical composition (major oxides) of the representative zeolite A products synthesised from different fly ashes.

Major Oxides (Mean mass %)	Arnot	Hendrina	Lethabo	Matla	Tutuka
SiO ₂	35.35	35.46	35.55	35.48	34.90
TiO ₂	<0.01	<0.01	<0.01	<0.01	<0.01
Al ₂ O ₃	29.08	30.43	30.48	30.08	30.60
Fe ₂ O ₃	0.04	0.03	0.03	0.03	0.03
MnO	<0.01	<0.01	<0.01	<0.01	<0.01
MgO	<0.01	<0.01	<0.01	<0.01	<0.01
CaO	<0.01	<0.01	<0.01	<0.01	<0.01
Na ₂ O	19.19	17.81	19.65	17.32	19.83
K ₂ O	0.32	0.28	0.33	0.44	0.36
P ₂ O ₅	<0.01	<0.01	<0.01	<0.01	<0.01
Cr ₂ O ₃	<0.01	<0.01	<0.01	<0.01	0.01
NiO	0.01	0.01	0.01	0.01	0.02
V ₂ O ₅	<0.01	<0.01	<0.01	<0.01	<0.01
ZrO ₂	0.01	0.01	0.01	0.01	0.01
CuO	<0.01	<0.01	<0.01	<0.01	<0.01
LOI	16.39	16.24	14.09	17.13	14.86
Sum (%)	100.37	100.26	100.15	100.49	100.62
SiO ₂ /Al ₂ O ₃	1.22	1.17	1.17	1.18	1.14

Although the XRD results showed that the zeolite A products from Tutuka and Lethabo ashes contained unconverted amorphous material, the XRF results (Table 6.2) revealed that the chemical compositions of the zeolite A obtained from the different FA sources investigated in this study were similar. The $\text{SiO}_2/\text{Al}_2\text{O}_3$ ratio of the zeolite is a vital factor in determining its chemical and adsorptive properties such as hydrophilicity and hydrophobicity (Tsai *et al.*, 2009). As a consequence, it has a very significant impact on the zeolite performance in water treatment (Reyes, 2008). According to literature, a zeolite with a low $\text{SiO}_2/\text{Al}_2\text{O}_3$ ratio will tend to be hydrophilic, while a high silica zeolite (>2.00) will tend to be hydrophobic and organophilic (Tsai *et al.*, 2009; Reyes, 2008; Misak, 2000). According to Pfenninger (1999), the $\text{SiO}_2/\text{Al}_2\text{O}_3$ ratio of zeolite A fluctuates between 1.92 and 2.08. Pfenninger (1999) also reported that zeolite A products with higher $\text{SiO}_2/\text{Al}_2\text{O}_3$ ratio tend to be more thermally stable than those with a lower $\text{SiO}_2/\text{Al}_2\text{O}_3$ ratio. The zeolite products obtained in this study showed low $\text{SiO}_2/\text{Al}_2\text{O}_3$ ratios, ranging from 1.14 to 1.22. Reyes (2008) reported that when the fusion method was used, low $\text{SiO}_2/\text{Al}_2\text{O}_3$ ratio zeolites were obtained. Based on the information given above, zeolite A produced from all the fly ashes studied can be a suitable adsorbent during water treatment. The Fe_2O_3 content of the raw fly ashes was found to range from 3 to 5 wt % as discussed earlier in Chapter 4. However, the content of this oxide in the zeolite products obtained showed a drastic decrease to less than 0.05 wt %, meaning that Fe was not incorporated in the zeolite structure (Table 6.2). The content of other impurities such as TiO_2 , Cr_2O_3 , ZrO_2 , V_2O_5 , NiO , MnO , etc. in the zeolite A products also showed a drastic decrease to less than 0.01 compared to their (impurities) contents in the raw FA.

6.3.3.4. Morphological analysis

Figure 6.6 shows the SEM images of the representative zeolite A products synthesised from different fly ashes.

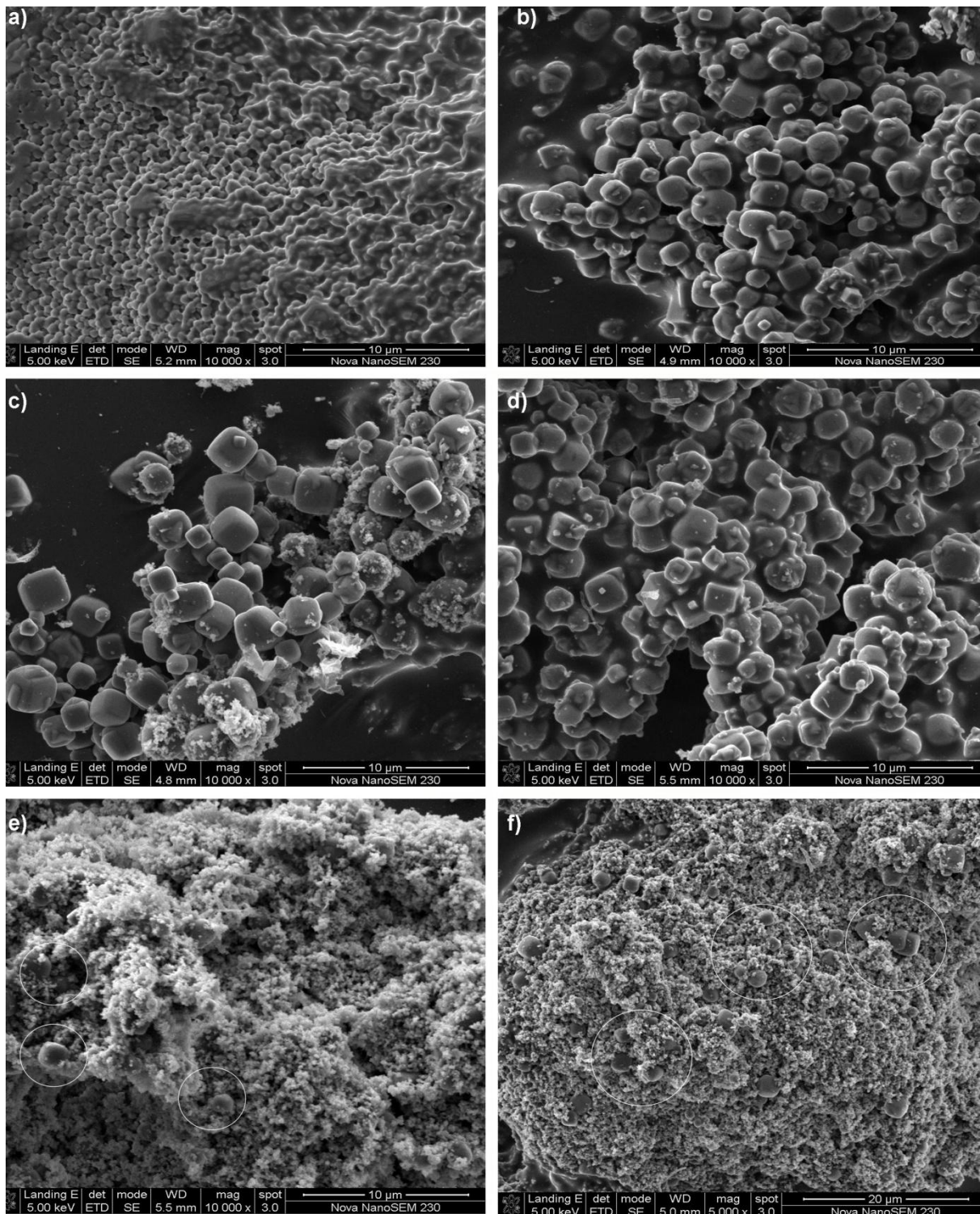


Figure 6-6: SEM images illustrating the transformation of fused fly ash into zeolite A using different fly ashes. a) fused fly ash b) Arnot c) Hendrina d) Matla e) Lethabo and f) Tutuka

The SEM images of the surface of the synthesised zeolites revealed a clear transformation of the small spherical particles of the fused fly ash (Figure 6.6a) into cubic crystalline structures. These cubic structures were identified by XRD as zeolite A. As stated earlier, this morphology is similar to that reported by Jamil *et al.* (2010) and Rayalu *et al.* (2001). In some cases, these cubic zeolite A crystals appeared to have truncated edges (Figure 6.6b and d)

while others had smooth edges (Figure 6.6b, e and f). Figure 6.6e and f represent the zeolite A products synthesised from Lethabo and Tutuka fly ashes respectively. It can be seen from these images (Figure 6.6e-f) that the zeolite A crystals were covered with unconverted amorphous material. These results concur with XRD results reported earlier in Figure 6.5.

6.4. Conclusion to Chapter 6

In this chapter, the possibility of synthesising zeolite A from different South African fly ash sources with different mineralogical and chemical compositions was investigated using the alkali fusion method. The use of circumneutral mine water (CMW) as a replacement for ultrapure water was also investigated in this chapter. The fusion step promoted the solid-state reaction between the NaOH powder and the crystalline phases of FA. As a result, a sodium aluminosilicate phase was formed at the fusion temperature. The fused product is generally dissolved in water more readily than quartz, mullite and hematite in FA. The only disadvantage of the fusion method is high energy requirements during the high temperature fusion step. The results showed that CMW can be used as a replacement for ultrapure water during the synthesis of zeolite A from FA using the fusion method. The presence of extra elements in the CMW had little to no influence on the synthesis products obtained since the same zeolite phase obtained with UP water was obtained with CMW. The results obtained when different South African fly ash sources were used demonstrated that zeolite A was the only zeolite phase that crystallised after 2 hours of hydrothermal treatment. However, low crystalline zeolite A products were obtained from Lethabo and Tutuka fly ashes. The lower crystallinity did not correlate with any of the compositional or mineralogical characteristics of Tutuka and Lethabo ashes.

CHAPTER 7

7. CONCLUSIONS AND RECOMMENDATIONS

In this chapter the specific aims of this study are reviewed to present an overview of the major findings of this study. Recommendations for further work are also given.

7.1. General conclusions

The main objective of this study was to investigate which parameters would have impact on the scale-up conditions for the synthesis of zeolite Na-P1 and zeolite A from South African coal fly ashes. In this study, the experiments were conducted on a laboratory scale and zeolites were synthesised and characterised in terms of phase purity, structure and morphology. Although this study was conducted on a laboratory scale, it gave an insight into what parameters should be controlled in a large scale synthesis process. Several characterisation techniques were used in this study. Each characterisation technique was used to probe a particular aspect of a specific material and therefore the use of a combination of methods was necessary to obtain a balanced description of the fly ash feedstock, as well as the zeolitic products obtained. Six fly ash samples sourced from five power stations (i.e. Arnot, Hendrina, Matla, Lethabo and Tutuka power stations) were used in this study. Fly ashes from all these power plants were classified as class F based on their CaO content as well as their $\text{SiO}_2 + \text{Al}_2\text{O}_3 + \text{Fe}_2\text{O}_3$ content. The major crystalline phases in these fly ashes were found to be quartz, mullite, magnetite, calcite and hematite. The chemical composition and particularly the $\text{SiO}_2/\text{Al}_2\text{O}_3$ ratio of the raw materials were deemed appropriated for the synthesis zeolite Na-P1. In certain instances, the $\text{SiO}_2/\text{Al}_2\text{O}_3$ ratio needed some adjustment with an additional sodium aluminate source in order to produce a pure phase of zeolite A.

During the synthesis of zeolite Na-P1, the impacts of several variables were considered; the effect of impeller design and agitation, fly ash composition, use of different water sources during the synthesis process and hydrothermal reaction time. Generally, the phase purity of the synthesised zeolites was strongly dependent on the mineralogical and chemical composition of the feedstock (fly ash), hydrothermal reaction time as well as the solvent (H_2O).

A two stage synthesis process, consisting of aging and hydrothermal treatment steps was followed for the synthesis of zeolite Na-P1. When the effect of impeller design and agitation

during the aging step was investigated, a pure phase of zeolite Na-P1 was successfully synthesised using Arnot fly ash as a feedstock. In some cases, zeolite formation was assessed as fairly unsuccessful, taking into account that the synthesis products contained a small amount of the unwanted zeolites (analcime and hydroxysodalite) and/or un-reacted fly ash phases (mullite or quartz). Based on the experimental results, it was observed that a 4 flat-blade impeller was the optimum design of impeller that can be used for agitation during the aging step of the zeolite synthesis in a scaled-up process. A high crystalline zeolite Na-P1 product was obtained when this impeller was used at 200 rpm during aging under the following conditions; aging at 47 °C for 48 hours and hydrothermal treatment at 140 °C for 48 hours under static conditions. The investigation of the effect of impeller design and agitation during the aging step proved for the first time that different impeller designs and agitation during the aging step can have a profound impact on the zeolitic product quality. Therefore, it is not only the hydrothermal synthesis conditions and the molar regime but also the dissolution kinetics of the feedstock that influence the outcome of the zeolite synthesis process.

The effect of FA composition and mineralogical phase content on the phase purity of zeolite Na-P1 produced was investigated. An important aspect of this study is the fact that the experimental data revealed the importance of chemical and mineralogical composition of fly ash during zeolite synthesis. The results of this study showed that two fly ash samples from the same power station (Arnot) may show different behaviour during zeolite synthesis and yield different zeolitic products when treated under the same synthesis conditions. This was found to be due to the versatile nature of fly ash (i.e. difference in chemical and mineralogical composition). A pure phase of zeolite Na-P1 was successfully synthesised from the fly ash with higher amorphous glass phase content, whereas a mixture of zeolite Na-P1 and analcime was obtained from low amorphous glass phase content fly ash. The results demonstrated that the efficiency in the conversion of fly ash into zeolites was affected by the contents of the non-reactive fly ash phases (mainly mullite and quartz) as well as the amorphous glass phase content. The content of the amorphous glass phase was found to be crucial for the formation of zeolite Na-P1 since it easily dissolves into the alkaline solution.

The use of ultrapure water for the synthesis of zeolites on an industrial scale may lead to production cost implications. However, this study revealed that ultrapure water can be replaced by tap and distilled water during the synthesis of a pure phase of zeolite Na-P1 on an industrial scale in order to reduce the cost associated with the processing of water to ultrapure water. This is because the zeolitic products obtained when tap and distilled water were used were similar to that obtained with ultrapure water, meaning that the extra elements present in these waters did not negatively influence the type of zeolite produced. This study also showed that acid mine drainage as a solvent can replace ultrapure water to

synthesise mixed phase zeolites from FA. The main zeolites obtained when acid mine drainage was used were zeolite Na-P1, analcime and hydroxysodalite. Therefore, acid mine drainage was not a suitable solvent for the synthesis of a pure phase of zeolite Na-P1 under the conditions investigated.

The effect of hydrothermal reaction time on the phase purity of zeolite Na-P1 was also assessed with the aim of establishing optimum synthesis conditions for the synthesis of a pure phase of zeolite Na-P1 from low amorphous phase fly ash. Aging time significantly influenced the Si/Al ratio of the synthesis solution, which in turn affects the outcome of the zeolite synthesis process. The experimental results demonstrated that an increase in hydrothermal treatment time resulted in high zeolite Na-P1 yield. Variation of the hydrothermal reaction time resulted in the synthesis of a pure phase zeolite Na-P1 from a low amorphous phase fly ash, with the synthesis conditions being; aging at 47 °C for 36 hours under 200 rpm of stirring with a 4 flat-blade impeller and hydrothermal treatment at 140 °C for 48 hours under static conditions. It is important to highlight that this study has also shown that aging and hydrothermal reaction time can be adjusted to tailor the type and quality of the zeolite produced.

This study has also shown for the first time that a pure phase of zeolite A can be synthesised from various sources of South African fly ash, containing different mineralogical and chemical compositions, via the alkali fusion method. Unlike in the case of zeolite Na-P1, a pure phase of zeolite A could be obtained when mine water was used as a replacement for ultrapure during the synthesis process. The experimental results also showed that the mineralogical composition of fly ash did not significantly affect the phase purity of the zeolite A product as much as it affected the zeolite Na-P1 product. This was due to the introduction of the alkali fusion step during the synthesis of zeolite A, which converted all the fly ash phases into sodium silicate and sodium aluminate, which are soluble in water. As a consequence, a pure phase of zeolite A was obtained with all the fly ashes used.

The results demonstrated that the scale-up synthesis of zeolite Na-P1 would require step-by-step optimisation of the synthesis conditions, since this zeolite was sensitive to the $\text{SiO}_2/\text{Al}_2\text{O}_3$ ratio, agitation and the mineralogy of the fly ash. Further optimisation of the synthesis conditions and adjustment of the Si/Al molar ratio of the synthesis gel by adding either SiO_2 or Al_2O_3 from a supplementary source may be necessary if a pure phase of zeolite Na-P1 targeted. As a consequence, this may have implications on the operating time and costs. The synthesis conditions for zeolite Na-P1 may vary based on the type or source of the FA samples. However, on a large scale, one set of the synthesis conditions of zeolite Na-P1 may not be adequate and a case by case optimisation approach is needed.

When comparing the synthesis process of zeolite A (i.e. alkali fusion method) and that of zeolite Na-P1, the zeolite A synthesis process is more robust and less rigorous to scale up. The synthesis process for zeolite A (alkali fusion, using a clear solution for the crystallisation of zeolite A) used in this study has several advantages over that of zeolite Na-P1. These advantages include; low reaction temperature (i.e. below 100 °C compared to 140 °C for zeolite Na-P1), shorter reaction times (i.e. less than 8 hours compared to 4 days for zeolite Na-P1) and complete dissolution of FA phases. This process of using the clear solution for the synthesis of zeolite A produces pure, high crystalline zeolite products with well-defined morphologies. The zeolite A products obtained from this process contained low amounts of impurities. On the other hand, this process (zeolite A process) causes a large wastage of the feedstock when compared to that of zeolite Na-P1, since the filtered solids (during zeolite A synthesis) were not being used further. Another disadvantage of the zeolite A synthesis period is that the high temperature fusion step makes this method energy-intensive. However, the short reaction time for zeolites A synthesis is preferable for efficient industrial production, because a longer reaction time for zeolite Na-P1 consumes more energy.

It is important to note that when the alkali fusion method was employed, low synthesis temperature and very short synthesis periods are used to synthesise a high crystalline pure zeolite product (e.g. zeolite A). When fusion is not introduced in the synthesis process, longer aging times and longer hydrothermal treatment times at high temperatures have to be employed (e.g. zeolite Na-P1 synthesis).

7.2. Recommendations and future work

This study evaluated parameters that could influence the scale-up conditions for both zeolite Na-P1 and zeolite A. This study showed that the scale-up of zeolite A may be easier than that of zeolite Na-P1. Therefore, pilot scale zeolite synthesis of zeolite A from South African fly ashes should be attempted to replicate the conditions applied at the bench scale. However, before this can commence, there are some aspects concerning the synthesis process which were not within the scope of this study that need to be investigated or optimised. These include;

- The investigation of a possible alternative method to substitute the high temperature fusion step in order to make the synthesis process cost effective.
- Mass balances should be done in order to determine the actual synthesis efficiency and mobility and fate of trace elements during the synthesis process.
- Environmental and HAZOP studies must be conducted before scale-up can commence, i.e. waste minimisation studies must be conducted in order to minimise or find an alternative use for the post-synthesis supernatant.

- The effect of agitation during the hydrothermal treatment/crystallisation step for both zeolite Na-P1 and zeolite A.

REFERENCES

- Adriano, D. C., Page, A. L., Elseewi, A. A., Chang, A. C. & Straughan, I. 1980. Utilization and disposal of fly ash and other coal residues in terrestrial ecosystems: A review. *Journal of Environmental Quality*, 9, 333-344.
- Ahmaruzzaman, M. 2010. A review on the utilization of fly ash. *Progress in Energy and Combustion Science* 36, 327–363.
- Alonso, J. L. & Wesche, K. 1991. Characterization of fly ash. In: WESCHE, K. (ed.) *Fly Ash in Concrete: Properties and Performance*. London: E & FN Spon.
- Amrhein, C., Haghnia, G. H., Kim, T. S., Mosher, P. A., Gagajena, R. C., Amanios, T. A. & De La Torre, L. 1996. Synthesis and Properties of Zeolites from Coal Fly Ash. *Environmental Science & Technology*, 30, 735-742.
- Andini, S., Cioffi, R., Colangelo, F., Grieco, T., Montagnaro, F. & Santoro, L. 2008. Coal fly ash as raw material for the manufacture of geopolymer-based products. *Waste management*, 28, 416-423.
- Auerbach, S. M., Carrado, K. A. & Dutta, P. K. 2003. *Handbook of zeolites science and technology*, New York, Basel, Marcel Dekke Inc.
- Baerlocher, C., Meier, W. M. & Olson, D. H. 2007. *Atlas of zeolite framework types*, Elsevier.
- Barrer, R. M. 2007. *Hydrothermal chemistry of zeolites*, London, Academic press.
- Bebon, C., Colson, D., Marrot, B., Klein, J. P. & Di Renzo, F. 2002. Synthesis of zeolites: study and application of a new process of homogenous shaking out of the medium to minimize the shear rate during the crystallization. *Microporous and Mesoporous Materials*, 53, 13-20.
- Belviso, C., Cavalcante, F. & Fiore, S. 2010. Synthesis of zeolite from Italian coal fly ash: differences in crystallization temperature using seawater instead of distilled water. *Waste management*, 30, 839–847.
- Berggaut, V. & Singer, A. 1996. High capacity cation exchanger by hydrothermal zeolitization of coal fly ash. *Applied Clay Science* 10, 369-378.
- Breck, D. W. 1974. *Zeolite Molecular Sieves*, New York, John Wiley & Sons

- Byrappa, K. & Yoshimura, M. 2001. *Handbook of Hydrothermal Technology: A Technology for Crystal Growth and Materials Processing*, Park Ridge, New Jersey, U.S.A, Noyes Publications.
- Cao, G. & Shah, M. J. 2007. In situ monitoring of zeolite crystallization by electrical conductivity measurement: New insight into zeolite crystallization mechanism. *Microporous and Mesoporous Materials*, 101, 19–23.
- Carlson, C. L. & Adriano, D. C. 1993. Environmental Impacts of Coal Combustion Residues. *Journal of Environmental Quality*, 22, 227-247.
- Casci, J. L. 2005. Zeolite molecular sieves: preparation and scale-up. *Microporous and Mesoporous Materials*, 82, 217-226.
- Catalfamo, P., Corigliano, F., Primerano, P. & Di Pasquale, S. 1993. Study of the pre-crystallization stage of hydrothermally treated amorphous aluminosilicates through the composition of the aqueous phase. *Journal of the Chemical Society, Faraday Transactions*, 89, 171-175.
- Chen, H. F., Fang, J. N., Lo, H. J., Song, S. R., Chung, S. H., Chen, Y. L., Lin, I. C. & Li, L. J. 2002. Synthesis of zeolites from the gismondine group. *Western Pacific Earth Sciences*, 2, 331-346.
- Criado, M., Fernández-Jiménez, A., De La Torre, A. G., Aranda, M. a. G. & Palomo, A. 2007. An XRD study of the effect of the SiO₂/Na₂O ratio on the alkali activation of fly ash. *Cement and Concrete Research*, 37, 671-679.
- Criado, M., Fernandez-Jimenez, A. & Palomo, A. 2007. Alkali activation of fly ash: Effect of the SiO₂/Na₂O ratio Part I: FTIR study. *Microporous and Mesoporous Materials*, 106, 180-191.
- Criado, M., Fernández-Jiménez, A. & Palomo, A. 2010. Alkali activation of fly ash. Part III: Effect of curing conditions on reaction and its graphical description. *Fuel*, 89, 3185-3192.
- Cundy, C. S. & Cox, P. A. 2005. The hydrothermal synthesis of zeolites: Precursors, intermediates and reaction mechanism. *Microporous and Mesoporous Materials*, 82, 1-78.
- Davis, M. E. & Raul, F. L. 1992. Zeolite and Molecular Sieve Synthesis. *Chemical Materials*, 4, 756-768.

- Dyer, A. 1988. *An Introduction to Zeolite Molecular Sieves*, John Wiley & Sons Inc.
- Elliot, A. D. 2006. *An Investigation into the Hydrothermal Processing of Coal Fly Ash to Produce Zeolite for Controlled Release Fertiliser Applications*. PhD Thesis, Curtin University of Technology.
- Elliot, A. D. & Zhang, D. 2005. Controlled Release Zeolite Fertilisers: A Value Added Product Produced from Fly Ash. *World of Coal Ash (WOCA)*. Lexington, Kentucky, USA.
- Endres, J. C. T., Ferret, L. S., Fernandez, I. D. & Hofmeister, L. C. Year. The Removal of Fe, Zn, Cu, and Pb from Wastewaters Using Chabazite Zeolites Produced from Southern Brazilian Coal Ashes. *In*, 2001. 820-826.
- Eskom 2009. Annual Report.
- Eskom 2011. Annual Report.
- Feijen, E. J. P., Martens, J. A. & Jacobs, P. A. 1994. Zeolites and their mechanism of synthesis. *In*: WEITKAMP, J., KARGE, H. G., PFEIFER, H. & HÖLDERICH, W. (eds.) *Zeolites and Related Microporous Materials: state of the art 1994*. Amsterdam: Elsevier.
- Fernandez-Jimenez, A. & Palomo, A. 2003. Characterisation of fly ashes. Potential reactivity as alkaline cements. *Fuel*, 82, 2259-2265.
- Fernandez-Jimenez, A. & Palomo, A. 2005. mid-infrared spectroscopic studies of alkali-activated fly ash structure. *Microporous and Mesoporous Materials*, 86, 207-214.
- Fernández-Jiménez, A. & Palomo, A. 2005. Composition and microstructure of alkali activated fly ash binder: Effect of the activator. *Cement and concrete research*, 35, 1984-1992.
- Fisher, G. L., Chang, D. & Brummer, M. 1976. Fly ash collected from electrostatic precipitators: microcrystalline structures and the mystery of the spheres. *Science*, 192, 553-555.
- Flanigien, E. M. 1991. Zeolite and molecular sieves: A historical perspective. *In*: VAN BEKKUM, H., FLANIGEN, E. M. & JANSEN, J. C. (eds.) *Introduction to zeolite science and practice*. Amsterdam: Elsevier.

- Garcia-Martinez, J., Cazorla-Amoros, D. & Linares-Solano, A. 2002. Selective synthesis of zeolite briquettes from conformed ashes. *Journal of Chemical Technology and Biotechnology*, 77, 287-291.
- Gitari, W. M., Petrik, L. F., Etchebers, O., Key, D. L. & Okujeni, C. 2008. Utilization of fly ash for treatment of coal mines wastewater: Solubility controls on major inorganic contaminants. *Fuel*, 87, 2450–2462.
- Goodarzi, F. 2006. Characteristics and composition of fly ash from Canadian coal-fired power plants. *Fuel*, 85, 1418-1427.
- Gosh, B., Agrawal, D. C. & Bhatia, S. 1994. Synthesis of zeolite A from calcined diatomaceous clay: Optimization studies. *Industrial & Engineering Chemistry Research*, 33, 2107-2110.
- Hedström, A. 2001. Ion-exchange of Ammonium in Zeolites: A Literature Review. *Journal of environmental engineering*, 127, 673-681.
- Hemrajani, R. R. & Tatterson, G. B. 2004. Mechanically Stirred Vessels *In: PAUL, E. L., ATIEMO-OBENG, V. A. & KRESTA, S. M. (eds.) Handbook of industrial mixing.* Hoboken, New Jersey: John Wiley & Sons, Inc.
- Holler, H. & Wirsching, U. 1985. Zeolite formation from fly ash. *Fortschritte der Mineralogie*, 63(1), 21-43.
- Hollman, G. G., Steenbruggen, G. & Janssen-Jurkovicova´ 1999. A two-step process for the synthesis of zeolites from coal fly ash. *Fuel*, 78, 1225-1230.
- Ibrahim, S. A. B. 2007. *Synthesis and Characterization of Zeolites from Sodium Aluminosilicate Solution.* Unpublished MSc Thesis, Universiti Sains Malaysia.
- Inada, M., Eguchi, Y., Enomoto, N. & Hojo, J. 2005. Synthesis of zeolite from coal fly ashes with different silica–alumina composition. *Fuel*, 84, 299-304.
- Inada, M., Tsujimoto, H., Eguchi, Y., Enomoto, N. & Hojo, J. 2005. Microwave-assisted zeolite synthesis from coal fly ash in hydrothermal process. *Fuel*, 84, 1482-1486.
- Iyer, R. S. & Scott, J. A. 2001. Power station fly ash-a review of value added utilization outside of the construction industry. *Resources, Conservation and Recycling*, 31, 217–228.

- Jamil, T. S., Ibrahim, H. S., Abd El-Maksoud, I. & El-Wakeel, S. 2010. Application of zeolite prepared from Egyptian kaolin for removal of heavy metals: I. Optimum conditions. *Desalination*, 258, 34-40.
- Jenke, D. R., Pagenkopf, G. K. & Diebold, F. E. 1983. Chemical changes in concentrated, acidic, metal-bearing wastewaters when treated with lime. *Environmental science & technology*, 17, 217-223.
- Juan, R., Hernandez, S., Andres, J. M. & Ruiz, C. 2007. Synthesis of granular zeolitic materials with high cation exchange capacity from agglomerated coal fly ash. *Fuel*, 86, 1811-1821.
- Kim, W., Jung, S. H. & Ahn, B. J. 1997. Synthesis of Na-P1 Zeolite from Coal Fly Ash. *Journal of Ind. & Eng. Chemistry*, 3, 185-190.
- Kitsopoulos, K. P. 1999. Cation-exchange capacity (CEC) of zeolitic volcanoclastic materials: applicability of the ammonium acetate saturation (AMAS) method. *Clays and clay minerals*, 47, 688-696.
- Kolousek, D., Seidl, V., Prochazkova, E., Obsasnikova, J., Kubelkova, L. & Svetlik, I. 1993. Ecological utilization of power-plant fly ashes by their alteration to phillipsite: Hydrothermal alteration, application. *Acta Universitatis Carolinae Geologica*, 1, 167-178.
- Koukouzas, N., Hämmäläinen, J., Papanikolaou, D., Tourunen, A. & Jäntti, T. 2007. Mineralogical and elemental composition of fly ash from pilot scale fluidised bed combustion of lignite, bituminous coal, wood chips and their blends. *Fuel*, 86, 2186-2193.
- Kruger, R. A. 1997. Fly ash beneficiation in South Africa: creating new opportunities in the market-place. *Fuel*, 76, 777-779.
- Kutchko, B. G. & Kim, A. G. 2006. Fly ash characterization by SEM-EDS. *Fuel*, 85, 2537-2544.
- Landman, A. A. 2003. *Aspects of solid-state chemistry of fly ash and ultramarine pigments*. PhD Thesis, University of Pretoria.
- Lee, K. M. & Jo, Y. M. 2010. Synthesis of zeolite from waste fly ash for adsorption of CO₂. *Journal of Materials Cycles and Waste Management*, 12, 212-219

References

- Lin, C. F. & Hsi, H. C. 1995. Resource recovery of waste fly ash: synthesis of zeolite-like materials. *Environmental science & technology*, 29, 1109-1117.
- Liu, G., Zhang, H., Gao, L., Zheng, L. & Peng, Z. 2004. Petrological and mineralogical characterizations and chemical composition of coal ashes from power plants in Yanzhou mining district, China. *Fuel Processing Technology*, 85, 1635-1646.
- Mantler, M. & Schreiner, M. 2000. X-ray fluorescence spectrometry in art and archeology. *Journal of x-ray spectrom*, 29, 3-17.
- Marrot, B., Bebon, C., Colson, D. & Klein, J. 2001. Influence of the shear rate during the synthesis of zeolites. *Crystal Research and Technology*, 36, 269-281.
- Misak, N. Z. 2000. Some aspects of the application of adsorption isotherms to ion exchange reactions. *Reactive and Functional Polymers*, 43, 153-164.
- Molapo, K. 2010. *Synthesis of zeolite Na-P1 from South African coal fly ashes*. Unpublished Honours Thesis, University of the Western Cape.
- Molina, A. & Poole, C. 2004. A comparative study using two methods to produce zeolites from fly ash. *Minerals Engineering*, 17, 167-173.
- Mondragon, F., Rincon, F., Sierra, L., Escobar, J., Ramirez, J. & Fernandez, J. 1990. New perspectives for coal ash utilization: synthesis of zeolitic materials. *Fuel*, 69, 263-266.
- Moreno, N., Querol, X., Ayora, C., Alastuey, A., Fernández-Pereira, C. & Janssen-Jurkovicová, M. 2001. Potential environmental applications of pure zeolitic material synthesized from fly ash. *Journal of environmental engineering*, 127, 994.
- Moreno, N., Querol, X., Plana, F., Andres, J. M., Janssen, M. & Nugteren, H. 2002. Pure zeolite synthesis from silica extracted from coal fly ashes. *Journal of Chemical Technology and Biotechnology*, 77, 274-279.
- Moutsatsou, A., Stamatakis, E., Hatzitzotzia, K. & Protonotarios, V. 2006. The utilization of Ca-rich and Ca–Si-rich fly ashes in zeolites production. *Fuel*, 86, 657-663.
- Murayama, N., Yamamoto, H. & Shibata, J. 2002. Mechanism of zeolite synthesis from coal fly ash by alkali hydrothermal reaction. *International Journal of Mineral Processing*, 64, 1-17.
- Musyoka, N. M. 2009. *Hydrothermal synthesis and optimisation of zeolite Na-P1 from South African coal fly ash*. MSc Thesis, University of the Western Cape.

- Musyoka, N. M., Petrik, L. F., Gitari, W. M., Balfour, G. & Hums, E. 2012. Optimization of hydrothermal synthesis of pure phase zeolite Na-P1 from South African coal fly ashes. *Journal of Environmental Science and Health, Part A*, 47, 337-350.
- Musyoka, N. M., Petrik, L. F. & Hums, E. 2011. Ultrasonic assisted synthesis of zeolite A from coal fly ash using mine waters (acid mine drainage and circumneutral mine water) as a substitute for ultrapure water. In: RÜDE, F. W. (ed.) *International Mine Water Association 2011*. Aachen, Germany.
- Nagy, J. B., Bodart, P., Hannus, I. & Kiricsi, I. 1998. *Synthesis, Characterization and Use of Zeolitic Microporous Materials*, Szeged, Hungary, Deca Gen Ltd.
- Occelli, M. L. & Robson, H. E. 1989. *Zeolite Synthesis*, Washington, DC, American Chemical Society.
- Ojha, K., Pradhan, N. C. & Samanta, A. N. 2004. Zeolite from fly ash: synthesis and characterisation. *Material Science*, 27, 555-564.
- Pacheco-Torgal, F., Castro-Gomes, J. & Jalali, S. 2008. Alkali-activated binders: A review:: Part 1. Historical background, terminology, reaction mechanisms and hydration products. *Construction and Building Materials*, 22, 1305-1314.
- Palomo, A., Alonso, S., Fernandez-Jimenez, A., Sobrados, I. & Sanz, J. 2004. Alkali activation of fly ashes: NMR study of the reaction products. *Journal of American Ceramic Society*, 87, 1141-1145.
- Panias, D., Giannopoulou, I. P. & Perraki, T. 2007. Effect of synthesis parameters on the mechanical properties of fly ash-based geopolymer. *Colloids and Surfaces A: Physicochemical Engineering Aspects*, 301, 246-254.
- Pfenninger, A. 1999. Manufacture and Use of Zeolites for Adsorption Process. *Molecular Sieves*, 2, 164-197.
- Querol, X., Alastuey, A., Fernández-Turiel, J. & López-Soler, A. 1995. Synthesis of zeolites by alkaline activation of ferro-aluminous fly ash. *Fuel*, 74, 1226-1231.
- Querol, X., Moreno, N., Alastuey, A., Juan, R., Andres, J. M., Lopez-Soler, A., Ayora, C., Medinaceli, A. & Valero, A. 2007. Synthesis of high ion exchange zeolites from coal fly ash. *Geologica Acta*, 5, 49-57.

- Querol, X., Moreno, N., Umana, J. C., Alastuey, A., Hernandez, E., Lopez-Soler, A. & Plana, F. 2002. Synthesis of zeolites from coal fly ash: an overview. *International Journal of Coal Geology*, 50, 413-423.
- Querol, X., Plana, F., Alastuey, A. & López-Soler, A. 1996. Synthesis of Na-zeolites from fly ash. *Fuel*, 76, 793-799.
- Querol, X., Umana, J. C., Plana, F., Alastuey, A., Lopez-Soler, A., Medinaceli, A., Valero, A., Domingo, M. J. & Garcia-Rojo, E. 2001. Synthesis of Zeolites from Fly Ash in a Pilot Plant Scale. Examples of Potential Environmental Applications. *Fuel*, 80, 857-865.
- Rayalu, S., Meshram, S. U. & Hasan, M. Z. 2000. Highly crystalline faujasite zeolites from fly ash. *Journal of Hazardous Materials*, 77, 123-131.
- Rayalu, S. S., Udhoji, J. S., Munshi, K. N. & Hasan, M. Z. 2001. Highly crystalline zeolite A from fly ash of bituminous and lignite coal combustion. *Journal of Hazardous Materials*, B88, 107-1201.
- Rees, C. A., Provis, J. L., Lukey, G. C. & Van Deventer, J. S. J. 2007. Attenuated total reflectance fourier transform infrared analysis of fly ash geopolymer gel aging. *Langmuir*, 23, 8170-8179.
- Reyes, C. a. R. 2008. *Synthesis of zeolites from geological materials and industrial wastes for potential application in environmental problems*. PhD, University of Wolverhampton.
- Ríos, C. A., Williams, C. D. & Roberts, C. L. 2009. A comparative study of two methods for the synthesis of fly ash-based sodium and potassium type zeolites. *Fuel*, 88, 1403-1416.
- Scheetz, B. E. & Earle, R. 1998. Utilization of fly ash. *Current Opinion in Solid State & Materials Science*, 3, 510-520.
- Shigemoto, N. 1996. 96/03377 - Characterization of Na-X, Na-A, and coal fly ash zeolites and their amorphous precursors by IR, MAS NMR and XPS. *Fuel and Energy Abstracts*, 37, 231.
- Shigemoto, N., Hayashi, H. & Miyaura, K. 1993. Selective formation of Na-X zeolite from coal fly ash by fusion with sodium hydroxide prior to hydrothermal reaction. *Journal of materials science*, 28, 4781-4786.

References

- Singer, A. & Berggaut, V. 1995. Cation exchange properties of hydrothermally treated coal fly ash. *Environmental science & technology*, 29, 1748-1753.
- Snoeyink, V. L. & Jenkins, D. 1980. *Water chemistry*, John Wiley.
- Somerset, V., Petrik, L. & Iwouha, E. 2005. Alkaline hydrothermal conversion of fly ash filtrates into zeolites 2: Utilization in wastewater treatment. *Journal of Environmental Science and Health*, 40, 1627-1636.
- Somerset, V. S., Petrik, L. F., White, R. A., Klink, M. J., Key, D. & Iwouha, E. I. 2005. Alkaline hydrothermal zeolites synthesized from high SiO₂ and Al₂O₃ co-disposal fly ash filtrates. *Fuel*, 84, 2324-2329.
- Sonqishe, T., Balfour, G., Iwouha, E. & Petrik, L. 2009. Treatment of Brines Using Commercial Zeolites and Zeolites Synthesized from Fly Ash Derivative. *International Mine Water Conference*. Pretoria.
- Szostak, R. 1989. *Molecular Sieves: Principles of synthesis and Identification*, London, Blackie Academic and Professional.
- Taylor, A. E. 2007. *Microwave synthesis and occlusion reactions of zeolites*. PhD Thesis, The University of Birmingham.
- Taylor, H. F. W. 1998. *Cement Chemistry 2nd Edition*, London, Thomas Telford.
- Tsai, W. T., Hsien, K. J. & Hsu, H. C. 2009. Preparation and characterization of a novel zeolite using hydrothermal synthesis in a stirred reactor. *Journal of Sol-Gel Science and Technology*, 49, 261-267.
- Uhlmann, W., Büttcher, H., Totsche, O. & Steinberg, C. 2004. Buffering of acidic mine lakes: the relevance of surface exchange and solid-bound sulphate. *Mine Water and the Environment*, 23, 20-27.
- Vadapalli, V. R. K., Klink, M. J., Etchebers, O., Petrik, L. F., Gitari, W., White, R. A., Key, D. & Iwouha, E. 2008. Neutralization of acid mine drainage using fly ash, and strength development of the resulting solid residues. *South African Journal of Science*, 104, 317-322.
- Vadapalli, V. R. K., Petrik, L. F., Fester, V., Slatter, P. & Sery, G. 2007. Effect of fly ash particle size on its capacity to neutralize acid mine drainage and influence on the rheological behavior of the residual solids *World of Coal Ash (WOCA)*. Northern Kentucky, USA

References

- Vassilev, S. V. & Vassileva, C. G. 2007. A new approach for the classification of coal fly ashes based on their origin, composition, properties, and behaviour. *Fuel*, 86, 1490-1512.
- Wang, C. F., Li, J. S., Wang, L. J. & Sun, X. Y. 2008. Influence of NaOH concentrations on synthesis of pure-form zeolite A from fly ash using two-stage method. *journal of hazardous materials*, 155, 58-64.
- Wang, S. & Wu, H. 2006. Environmental-benign utilisation of fly ash as low-cost adsorbents. *Journal of Hazardous Materials*, 136, 482-501.
- Weitkamp, J. & Puppe, L. 1999. *Catalysis and zeolites: fundamentals and applications*, German, Springer.